博 士 論 文

論文題目：Calcification responses of coral reef calcifiers to global marine environmental changes

（地球的規模の海洋環境の変化に対するサンゴ礁石灰化生物の応答に関する研究）

氏名：氷 上　　愛

Contents

Chapter 2 is based on: Hikami, M., H. Ushie, T. Irie, K. Fujita, A. Kuroyanagi, K. Sakai, Y. Nojiri, A. Suzuki, and H. Kawahata (2011), Contrasting calcification responses to ocean acidification between two reef foraminifers harboring different algal symbionts, Geophys. Res. Lett., 38, L19601, doi: 10.1029/2011GL048501.

Chapter 4 is based on: Kato, A., M. Hikami, N. H. Kumagai, A. Suzuki, Y. Nojiri, and K. Sakai (2013), Negative effects of ocean acidification on two crustose coralline species using genetically homogeneous samples, Mar. Environ. Res., 94, 1-6, doi: 10.1016/j.marenvres.2013.10.010.

Chapter 1

Preface

1. 1. Introduction

The atmospheric CO_2 partial pressure (PCO_2), one of the three major atmospheric components, has been increasing at about 0.4% per year with the seasonal variations representing the reduction in carbon dioxide by photosynthesis during the growing season in the northern hemisphere (e.g., Kleypas et al., 2006). This increasing trend can be attributed to the major contribution by the combustion of fossil fuels, which is about 2 to 5 times the effect of deforestation. Increase in PCO_2 induces an enhanced greenhouse effect, causing global warming of 4°C by the year 2100 (Intergovernmental Panel on Climate Change (IPCC), 2007). Another outcome of atmospheric CO_2 increase is acidification of the ocean. Surface ocean pH has decreased 0.1 pH units (equivalent to a 30% increase in H+ ions) since preindustrial times, and it is suggested that pH will further drop by 0.3 units by the end of this century (Representative Concentration Pathway [RCP] 8.5; IPCC, 2013). The pH change rate is 30 to 100 times faster than in the geological past (Zeebe and Ridgwell, 2011; Hönisch et al., 2012). Ocean acidification has been recognized as a severe threat to marine calcifiers such as corals, foraminifers, and calcareous algae (e.g., Feely et al., 2004) because their calcification rates are certainly reduced in the acidified seawater (Figure 1-1).

Although ocean uptake of CO_2 helps to modulate future climate change, the associated hydrolysis of CO_2 after its dissolution to the seawater is modifying dissolved carbonate system (e.g., Kleypas et al., 2006; Fabry et al., 2008). The sensitivity and degree of responses vary among species in response to the ocean acidification (Fabry et al., 2008). The total dissolved CO_2 concentration increases with pCO_2, and carbonate ion (CO_3^{2-}) declines with the decreasing pH, thus reducing the calcium carbonate

saturation state (Orr et al., 2005). The decrease in CO_3^{2-} may have a negative impact on calcification of major calcifiers even within the range of the pCO_2 predicted to occur over this century (Kleypas et al., 2006). On the other hand, some report that increase of pCO_2 may have a positive influence on some taxa of coccolithophores and uchins through an enhancement of symbiotic photosynthesis at higher-pCO_2 environments (e.g., Kroeker et al., 2013; Wittmann and Pörtner, 2013). Net calcification can be affected in either way and the overall response to ocean acidification is quite important to understand.

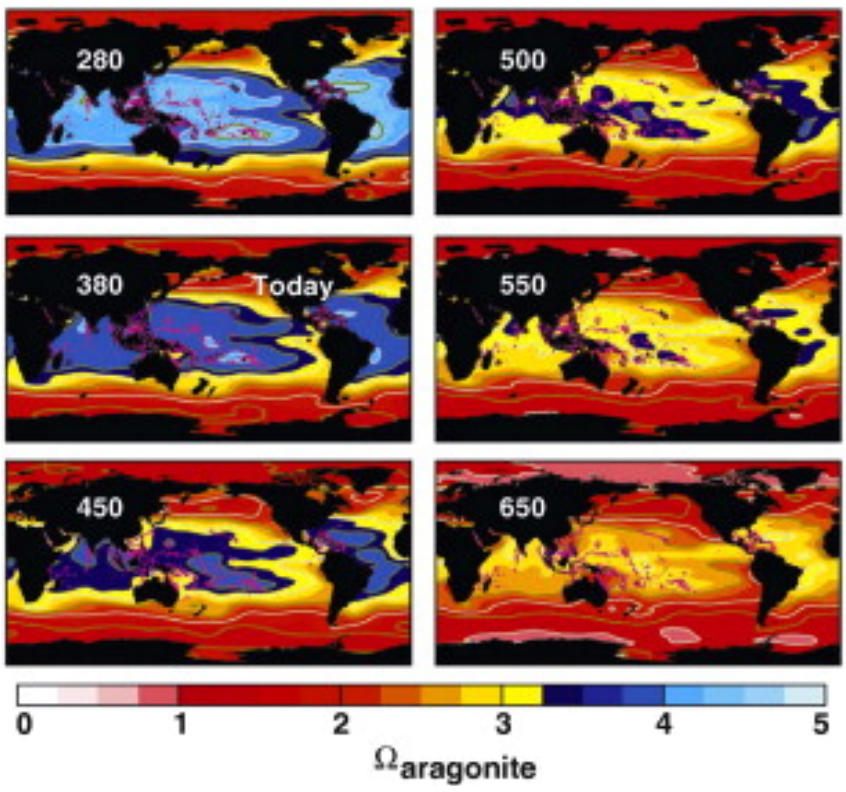

Figure 1-1. Predicted global saturation of $\Omega_{aragonite}$ under different PCO_2 (Hoegh-Guldberg et al., 2007)

1.2. Background of ocean carbon cycle in response to ocean acidification

The marine carbonate system is the largest carbon pool in the atmosphere, biosphere, and ocean (e.g., Kleypas et al., 2006). Currently oceanic reservoir has been absorbing anthropogenic CO_2. This response is controlled by (1) the kinetic property (transport and exchange processes of CO_2 between atmosphere and ocean) and (2) a thermodynamic property (the uptake capacity of sea-water for extra CO_2). As this chapter is focused on the carbonate stability in response to ocean acidification, I start to refer to the carbonate production.

1.2.1. Basic chemical reaction: relevant to the stability of carbonate minerals

Calcium carbonate shows poor solubility in pure water. The equilibrium of its solution is given by the equation (with dissolved calcium carbonate on the right):

$$CaCO_3 \rightleftarrows Ca^{2}+ + CO_3^{2-}$$

$$K_{sp} = 3.7 \times 10^{-9} \text{ to } 8.7 \times 10^{-9} \text{ at 25 °C, depending on carbonate minerals} \qquad (1)$$

In case of calcite, only 47 mg/L is soluble at current atmospheric PCO_2.

Ca concentration in seawater is relatively constant because of its variation within 1% in the world ocean. Therefore the stability of carbonate is depending on the CO_3^{2-}. However, this is more complication with equilibrium of HCO_3^- (bicarbonate ion).

$$HCO_3^- \rightleftarrows H^+ + CO_3^{2-}$$

$$[H^+][CO_3^{2-}]/[HCO_3^-] = K_2 = 10^{-10.3}\ [5.61\times10^{-11}] \text{ at 25 °C} \qquad (2)$$

$$H_2CO_3 \rightleftarrows H^+ + HCO_3^-$$

$$[H^+][HCO_3^-]/[H_2CO_3] = K_1 = 10^{-6.3}\ [2.5\times10^{-4}] \text{ at 25 °C} \qquad (3)$$

Also the following equilibrium can be established in any carbonate-containing solution:

$[H^+][OH^-] = K_w = 10^{-14}$ at 25 °C (4)

Once it has dissolved, a small proportion of the CO_2 reacts with water to form carbonic acid:

$H_2O + CO_2$ (dissolved) ⇄ H_2CO_3

$[H_2O][CO_2]/[H_2CO_3] = K_h = 10^{-2.76}$ $[1.70\times10^{-3}]$ at 25 °C (5)

$[CO_2(aq)] = 650\ [H_2CO_3]$ (6)

The common term of "dissolved carbon dioxide" consists mostly of the hydrated oxide CO_2(aq) together with a small amount of carbonic acid.

Dissolved CO_2 is in equilibrium with atmospheric carbon dioxide but CO_2 is only slightly soluble in water.

The solubility follows Henry's law: $[CO_2] = K_H PCO_2$

K_H=29.76 atm/(mol/L) at 25°C (7)

Carbon dioxide is slightly soluble in water. The pCO_2 in the surface ocean has been increasing versus PCO_2. Also its solubility decreases with temperature: 0.077 mol/Litre at 0°C, 0.066 mol/Litre at 4°C, 0.054 mol/Litre at 10°C, and 0.039 mol/Litre at 20°C. Therefore this means that the surface ocean in high latitudes will absorb more CO_2 than in the tropical and sub-tropical ocean because of lower temperature and will receive severe influence in future (e.g., Kleypas et al., 2006; Fabry et al., 2008).

1.2.2. Saturation state of carbonate minerals

The saturation state of seawater for certain carbonate mineral is described as Ω (Equation 1), from the thermodynamic point of view.

$\Omega = [Ca^{2+}]\ [CO_3^{2-}]/K_{sp}$

Here Ω is the product of the activities (concentrations) of the reacting ions that form the carbonate mineral, divided by the product of the concentrations of those ions when the mineral is at equilibrium (K_{sp}). K_{sp} value is dependent on temperature and pressure (seawater depth). It is much larger in deep sea than in surface ocean. Therefore below the saturation horizon, the inorganic carbonate mineral dissolves, when Ω is a value less than 1, while it does not readily dissolved above Ω of greater than 1. Although many calcifiers are dwelling above the saturation horizon, even below the depth, some organisms including benthic foraminiferas will take calcareous tests. Since the carbonate compensation depth (CCD) is defined as the water depth where the sedimentation of carbonate is exceeded by its dissolution, carbonate minerals will dissolve (not be preserved) under undersaturated condition.

Since Ca concentration in seawater is relatively constant because of its variation within 1% in the world ocean, the decrease in [CO_3^{2-}] reduces Ω. Increasing CO_2 levels and the resulting lower pH of seawater decreases the Ω. The decrease in Ω is often believed to be one of the main factors for decreased calcification in marine calcifiers (e.g., Kleypas et al., 2006; Fabry et al., 2008).

Biogenic carbonate minerals occur in three common polymorphs (crystalline forms): calcite, aragonite, and Mg-calcite. Modern surface seawater is saturated with respect to these three minerals. Of these, calcite is the most stable carbonate mineral, the second is aragonite, and high Mg-calcite is the least (e.g., Kleypas et al., 2006). Therefore high-Mg calcite is very easy to dissolve as ocean acidification proceeds. Also since aragonite is much more soluble than calcite, the aragonite saturation horizon is always shallower than the calcite saturation horizon. These features indicate that calcifiers which produce high-Mg calcite and aragonite would be more vulnerable to

response in ocean acidification than those with calcite tests.

1.2.3. Spatial difference on ocean acidification

Carbonate saturation state is higher in the tropical regions where coral reefs form than that in Arctic or Antarctic areas because more CO_2 is dissolved in colder water at high latitudes (Hoegh-Guldberg et al., 2007; Figure 1-1). Modeling results have also predicted that surface water in the Southern Ocean will be partly undersaturated with respect to aragonite by 2050 (Hoegh-Guldberg et al., 2007). All of the Southern Ocean south of 60°S and a part of the subarctic Pacific Ocean will become undersaturated by 2100 (Hoegh-Guldberg et al., 2007). Therefore calcifiers such as pteropods with aragonite tests will encounter a severer condition (Orr et al., 2005). On the other hand, the decreasing speed in $[CO_3^{2-}]$ from the pre-industrial period to the present is higher in the tropics (29 μmol/kg) than in the Southern Ocean (18 μmol/kg) due to global warming. Thus, the influence of ocean acidification is expected to be prominent also in tropical regions (e.g., Hoegh-Guldberg et al., 2007). However, the effect of acidified seawater on coral is still controversial because the increase of pCO_2 in the seawater causes the increase of HCO_3^-, which is used for photosynthesis in algal symbionts of corals although it is generally explained that the decrease of carbonate ion contributes to slowing coral calcification (e.g., Kleypas et al., 2006).

1.2.4. Biogenic carbonate production in association with photosynthesis

The coral reef carbon cycle is mainly driven by two biological processes: organic carbon metabolism (photosynthetic fixation and respiration / degradation) and inorganic carbon metabolism (precipitation and dissolution of calcium carbonate) (e.g., Kleypas et

al., 2006). The contribution of planktonic primary production to reef metabolism was negligible (Kinsey 1985). Planktonic primary production was estimated to be only 0.15% of the benthic gross production in particular for French Polynesian reef (Delesalle et al. 1993).

Photosynthesis (CO_2 invasion):

$$HCO_3^- + H_2O \rightarrow CO_2 + OH^- + H_2O \rightarrow CH_2O + OH^- + O_2 \quad (8)$$

Calcification (CO_2 evasion):

$$Ca^{2+} + 2\ HCO_3^- + OH^- \rightarrow Ca^{2+} + CO_3^{2-} + H^+ + OH^-$$

$$\rightarrow CaCO_3 + H_2O + CO_2 \uparrow \quad (9)$$

Respiration / degradation (CO_2 evasion):

$$CH_2O + O_2 \rightarrow CO_2 \uparrow + H_2O \quad (10)$$

Dissolution of carbonate (CO_2 invasion):

$$CaCO_3 + H_2O + CO_2 \rightarrow Ca^{2+} + 2\ HCO_3^- \quad (11)$$

Therefore photosynthesis triggers the production of OH^-, resulting in the production of carbonate.

1.3. Response of calcifiers in the ocean

1.3.1. Response of the production of calcifiers in Coastal Ocean (Coral Reefs and Other Benthic Calcifying Systems)

Coral reefs are one of the representative coastal ecosystems. It is composed of the major benthic calcifying organisms such as corals, calcifying macroalgae, benthic foraminifera, molluscs, and echinoderms. Calcification rates of reef-building corals and algae could decline by 10−50% under doubled CO_2 conditions (Gattuso et al.,

1998). Culture experiments of reef - dwelling benthic foraminifer *Marginopora* (*Amphisorus*) *kudakajimensis* shows the reduction of shell weight and diameter at lower pH (Kuroyanagi et al., 2009). Molluscan calcification showed a quarter decrease at acidified condition (Bijma et al., 1999; Spero et al., 1997; Gazeau et al., 2007). Specimens of *Mytilus galloprovincialis* that were exposed to pH = 7.3 for 3 months demonstrated a significant reduction in growth. Two species of sea urchin (*Hemicentrotus pulcherrimus* and *Echinometra mathaei*) were exposed for six months to CO_2 levels elevated by 200 ppmv over normal levels, which resulted in smaller size and body weight. In spite of biogeochemical and ecological importance of reef-calcifying organisms other than corals, they have been much less studied to date (Kuffner et al., 2008; Doney et al., 2009).

1.3.2. Response of the production of calcifiers in Open Ocean (Foraminifera, Coccolithophores, and Pteropods)

On a global basis, it is generally assumed that planktonic foraminifer and coccoliths constitute each comparable major flux (approximately 40%) of the total $CaCO_3$ flux (Kleypas et al., 2006). On the other hand, pteropods constitute 10−15% of the total $CaCO_3$ flux (Fabry and Deuser, 1991). Calcite is a major carbonate of foraminifer and coccoliths while the aragonitic shells of pteropods are important components of carbonate vertical flux in the open ocean. In most ocean areas, pteropod aragonite easily dissolves in the water column or soon after reaching the seafloor because of deep sea is undersaturated with respect to aragonite (see chapter 1.2.2.).

By the end of 21st century, the partial pressure of atmospheric CO_2 (PCO_2) is

estimated to go up to 500−1000 matm under various IPCC SRES scenarios (Solomon et al., 2007). These changes are expected to decrease seawater pH by an additional 0.3−0.4 units and the carbonate ion concentration by 50% (Orr et al., 2005). Such alteration of seawater chemistry can influence the calcification of marine calcifiers (Fabry et al., 2008). Various studies have revealed potentially dramatic responses in a variety of calcareous organisms to the range of PCO_2 values projected to occur over this century (e.g., Kleypas et al., 2006; Fabry et al., 2008). Planktonic foraminifer calcification is reduced by 8−14% at acidified ocean. On the other hand, *Emiliania huxleyi* and *Gephyrocapsa oceanica* are cosmopolitan species of calcifiers that can produce large blooms visible even in satellite imagery (Brown and Yoder, 1994). Their calcification have shown decreased, increased, or unchanged in response to increased pCO_2 (Fabry, 2008). It may be attributed to phytoplankton, which tends to increase the production under increased pCO_2.

1.3.3. The other response of calcifiers

1.3.3.1. Shift from calcareous to soft tissues in response to the acidification

1.3.3.1.1. Shift from calcareous to agglutinated foraminifera in acidified condition

Foraminifera as well as calcareous nanofossils are organisms of central importance in geology and biology (e.g., Kleypas et al., 2006). Foraminifera typically produce a test, or shell, which are usually composed of calcium carbonate ($CaCO_3$) or agglutinated sediment particles. Foraminifera has been affected by changing climate and ocean acidification (Kleypas et al., 2006). Since calcium carbonate is susceptible to dissolution in reduced carbonate saturation level, the calcium

carbonate of the shells is generally soluble in water in acidic (decreased pH) conditions and the extreme pressure especially at the deeper depths below the carbonate compensation depth.

In hydrothermal vents and mounds of the Okinawa Trough, bottom water temperature and salinity anomalies are commonly small except in the immediate vicinity of active hydrothermal chimneys. In the bottom and interstitial waters that are more acidic than the surrounding ambient bottom water, the proportion of the agglutinated foraminifera to total benthic foraminifera (A/T) was generally high (>40%). This value decreases in a very predictable manner with increasing distance from a hydrothermal vent. This observation indicates that the distinct ecological advantage that agglutinated foraminifera enjoy in waters where acidity becomes stronger (Akimoto et al., 1990). Similar results of the dominance by agglutinated species due to acidification were reported in an active volcanic caldera (Finger and Lapps, 1981).

1.3.3.1.2. Organic-cemented agglutinated foraminifera in deep-sea

In case of deep-sea, pressure is also another important factor to control carbonate saturation level, which controls calcification rate and carbonate dissolution. Saturation level of [CO_3^{2-}] decreases rapidly versus water depth if Ca concentration is constant (Kleypas et al., 2006). The values are 1.9 and 3.2 times of that of surface water at a water depth of 3,000m and 6,000 m, respectively, at temperature of 2°C and salinity of 35. Organic-cemented agglutinated walls of benthic foraminifera can be deposited in any water regardless of corrosivity with respect to carbonate. The majority of species live satisfactory only above the CCD although some live between the lysocline and CCD (Murray, 2008). Abundant small organisms (meiofauna) inhabiting sediments at

the Challenger Deep (10,900 m water depth), the deepest ocean, were found. Especially many living specimens of soft-walled foraminifera were identified in the sediment samples (Todo et al., 2005). Molecular evidence suggests that similar taxa are modern representatives of the basal foraminiferal evolutionary radiation that probably occurred in the Precambrian (Neoproterozoic) (Todo et al., 2005).

1.3.3.1.3. Organic-cemented agglutinated fauna at the P/E transition

Severe ocean acidification is considered to have occurred at the Paleocene-Eocene (P/E) transition at Ocean Drilling Program (ODP) Site 1220. The apparent change in the dominance of calcareous to agglutinated benthic fauna such as *S. ramosa*, *Rhabdammina* sp. and *Ammoglobigerina* sp. at the P/E transition at Site 1220 is particularly noteworthy and indicates the effect of increased acidic condition in the deep sea. The agglutinated species e.g., *Glomospira charoides*, *Karrerulina horrida, Rzehakina epigone, Ammodiscus* spp. and *Gaudryina pyramidata*, which is considered to be restricted to deep-sea paleo-environments, constitute an important proportion of the benthic foraminiferal assemblages in the southern Tethys (Zili and Zaghbib−Turki, 2010). These lines of evidence indicate that the agglutinated species contributed much across the P/E transition.

The other two important characteristics about the occurrence of planktonic and benthic foraminifera are presented at the same site: (1) The limited presence of tests of planktonic foraminifera in the sediments of the P/E transition in site 1220 core indicates that they were produced in the surface ocean. (2) The observation that planktonic foraminifera tests were largely dissolved but some were resistant against the dissolution on the seafloor. Anomalous shift in foraminiferal test

size across the P/E transition could result from pH reduction although Kaiho et al., (2006) atributed it to deficient dissolved oxygen. Since calcareous nannofossils and planktonic foraminifera were living at more oligotrophic surface ocean across the P/T transition (Raffi et al., 2005; Tantawy, 2006; Petrizzo, 2007), it is concluded that most of the calcareous tests were produced in the surface ocean and dissolved in the water column and in the sediments.

On the other hand, the absence of the more resistant calcareous benthic foraminifera indicates that calcareous benthic foraminifera suffered much and hardly lived on the seafloor at the P/E transition at Site 1220. It is quite interesting in light of the fact that calcareous benthic foraminifera are absent in the same sediments, even though tests of benthic foraminifera are generally much more resistant to corrosive seawater (reduced pH) than those of planktonic foraminifera. I do not necessarily imply that the carbonate ion concentration of the deep waters at the time was undersaturated with respect to minerals, calcite or aragonite. In fact the preservation of planktonic foraminiferal tests, even in small amounts, would argue that the deep waters were not undersaturated. I suggest, however, that the degree of supersaturation was sufficiently low that the calcification of benthic foraminifera was severely retarded or limited and this is likely the cause of their extinction. The same feature of non-calcareous agglutinated foraminifera increase dramatically, probably related to intense but no complete dissolution of carbonate across the P/E transition in Egypt, Italy and Spain (Alegret and Ortiz, 2006; Zili et al., 2009; Giusberti et al., 2009).

Therefore, ocean acidification at deep-sea with reduced carbonate saturation level would be the most plausible cause for the drastic change from calcareous to agglutinated benthic foraminiferal fauna at the P/E transition. It is supported by

the observation that benthic foraminifera from marginal and epicontinanal basins show lesser extinctions and/or temporary assemblage change (Alegret and Ortiz, 2006).

1.3.3.1.4. Community shift from hard to soft corals in acidified water

This feature is also observed in coral community. Experimental studies on ocean acidiffcation have reported negative impacts of high pCO_2 on several hard coral species (Kleypas et al., 2006; Ries et al., 2010) although some exceptions show that some corals are not impacted by high pCO_2 (Rodolfo-Metalpa et al., 2010). Both hard and soft coral communities in volcanically acidified, semi-enclosed waters off Iwotorishima Island, Japan, are specially distributed as a function of pCO_2 levels (Inoue et al., 2013). Hard corals are restricted to non-acidified low-pCO_2 (225 μatm) zones while dense populations of the soft coral *Sarcophyton elegans* dominate medium-pCO_2 (831 μatm) zones. The highest- pCO_2 (1,465 μatm) zone has neither hard nor soft corals. Based upon culture experiments, high-pCO_2 conditions provided enhancing photosynthesis rates to Sarcophyton elegans with negative net calcification. These results suggest that coral reef communities may shift from reef-building hard corals to non-reef-building soft corals under much higher pCO_2 levels (550−970 μatm) by the end of this century (Inoue et al., 2013).

1.3.3.2. Opposite response by different types of symbiotic algae to symbiont foraminifera

The calcification of corals, coralline algae, and large benthic foraminifers mainly supports carbonate production of coral reefs in tropical and sub-tropical regions. High-Mg calcite shows generally higher solubility in seawater than low-Mg

calcite or aragonite and the least stable carbonate minerals in lower pH (Morse et al., 2006). This mineral is the main constituent carbonate mineral of reef-dwelling foraminifers and coralline algae. Thus their tests are transported by waves and currents and contribute to the formation and retention of sand beaches and coastal landforms (Hohenegger, 2006; Fujita et al., 2009). Also some benthic foraminifer dwelling at coral reefs has algal symbionts.

In case of calcifier with symbiotic algae including coral and foraminifer, the effect of acidified seawater remains controversial (Jury et al., 2010). An increase in pCO_2 results in a decrease of carbonate ion, which is generally expected to contribute to slowing of coral calcification (Hoegh-Guldberg et al., 2007; Kleypas et al., 2006), but this also results in an increase of the concentration of HCO_3^-, which is used by coral algal endosymbionts for photosynthesis (Marubini et al., 2008; Jury et al., 2010). Thus, the effect of acidified seawater on calcifier's physiological aspects is complicated owing to the effect of these endosymbionts.

1.3.3.2.1. Corals

Culture experiments of a massive coral, *Porites australiensis*, a common species in the Ryukyu Archipelago of Japan, represented the calcification and symbiotic algae (zooxanthellae density, chlorophyll content per single algal cell, fluorescence yield (Fv/Fm)). Iguchi et al. (2011) found that acidified seawater significantly decreased the calcification and fluorescence yield without any influence on zooxanthellae density and chlorophyll content per single algal cell. Contrary to these findings, Acropora species showed an increase in chlorophyll content per cell, in both acidified seawater conditions (600-790 ppm, 1160-1500 ppm)

(Crawley et al., 2009). Significant correlation between calcification and fluorescence yield was observed, showing a strong relationship between calcification and algal photosynthesis. This means that acidified seawater may impair the photosynthetic activity of *P. australiensis* and decreases calcification and that the degree of dependence on photosynthesis by symbiotic algae for calcification may be different among coral species (Iguchi et al., 2011).

1.3.3.2.2. Benthic foraminifera

In the carbonate system in seawater, as CO_2 dissolves into seawater, carbonate ion (CO_3^{2-}) in seawater decreases and at the same time bicarbonate ion (HCO_3^-), CO_2 and total dissolved carbonate (ΣCO_2) increase. The former change may have negative effect on the calcification of foraminifers by reducing the calcium carbonate saturation state (Ω) of the seawater, whereas the CO_2 increase may positively influence through enhancement of symbiont photosynthesis. Thus two algal symbiont-bearing, reef-dwelling foraminifers, *Amphisorus kudakajimensis* and *Calcarina gaudichaudii*, were cultured by using a high-precision pCO_2-controlling and monitoring system called the AICAL system (a high-precision pCO_2 control system; Fujita et al., 2011). They harbor different algal symbionts. *Amphisorus kudakajimensis* and *Calcarina gaudichaudii* hosts dinoflagellates as their symbiont algae and diatom endosymbionts (Lee, 1998). By using clonal individuals for culture experiments, genetic influences can be eliminated. The five treatment levels used, 245, 375, 588, 763, and 907 μatm, represented pre-industrial (Low pCO_2), present-day (Control), and three near-future (High pCO_2 1 – 3) pCO_2 conditions, respectively. Interestingly, net calcification

of *A. kudakajimensis* was reduced under higher pCO_2, whereas calcification of *C. gaudichaudii* generally increased with increased pCO_2.

Comparison of these results with those of a culture experiment under a constant CO_3^{2-} concentration suggested that the negative response may be due to the decrease in CO_3^{2-} in the seawater, and the positive response to the increase in CO_2. The results imply that these different influences of seawater chemistry may be attributable to the different types of symbiotic algae hosted by *Amphisorus* and *Calcarina*. Culture and mesocosm bloom experiments demonstrate that high-CO_2 seawater makes positive response to diatom growth (Engel et al., 2008; Wu et al., 2010). On the other hand, dinoflagellates use HCO_3^- as their carbon source so that carbon fixation rate may be unaffected by CO_2 concentration (Rost et al., 2006). In addition, various coral species have dinoflagellates as their symbiotic algae and its calcification rates decrease with increasing pCO_2 (Doney et al., 2009). However, the symbiont interaction between calcifiers and symbionts remained unknown and further experiments should be required (Figure 1-2).

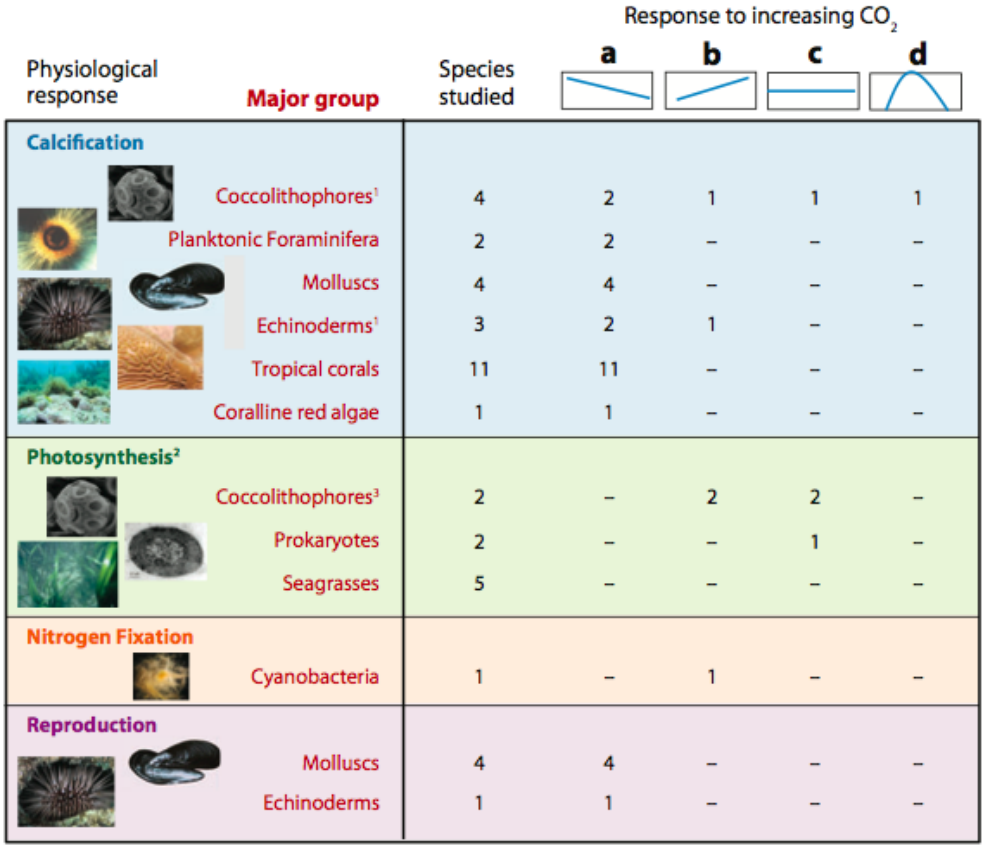

Physiological response	Major group	Species studied	Response to increasing CO_2 a	b	c	d
Calcification						
	Coccolithophores[1]	4	2	1	1	1
	Planktonic Foraminifera	2	2	–	–	–
	Molluscs	4	4	–	–	–
	Echinoderms[1]	3	2	1	–	–
	Tropical corals	11	11	–	–	–
	Coralline red algae	1	1	–	–	–
Photosynthesis[2]						
	Coccolithophores[3]	2	–	2	2	–
	Prokaryotes	2	–	–	1	–
	Seagrasses	5	–	–	–	–
Nitrogen Fixation						
	Cyanobacteria	1	–	1	–	–
Reproduction						
	Molluscs	4	4	–	–	–
	Echinoderms	1	1	–	–	–

Figure 1-2. Different responses to increasing CO_2 (Doney et al., 2009).

Chapter 2

Contrasting calcification responses to ocean acidification between two coral reef benthic foraminifers harboring different algal symbionts

2.1. Introduction

Nearly one-third of all anthropogenic CO_2 produced since the beginning of industrialization has been absorbed by the ocean (Sabine et al., 2004; Sabine and Feely, 2007). This has caused a decrease in seawater pH of 0.1 (Raven et al., 2005) and altered the carbonate chemistry of surface seawater. Together, these changes are referred to as ocean acidification. By the end of 21st century, the partial pressure of atmospheric CO_2 (pCO_2) is predicted to reach 500–1000 μatm under various IPCC SRES scenarios (Solomon et al., 2007). These changes are expected to decrease seawater pH by an additional 0.3–0.4 units and the carbonate ion concentration by 50% (Orr et al., 2005). Such alteration of seawater chemistry can influence the calcification of marine calcifiers. Various studies have revealed potentially dramatic responses in a variety of calcareous organisms to the range of pCO_2 values projected to occur over this century. For example, an 8–14% reduction of planktonic foraminifer calcification and a 25% decrease of molluscan calcification (Bijma et al., 1999; Spero et al., 1997; Gazeau et al., 2007). The sensitivity of the response varies both among and within species, and some taxa of coccolithophores and sea urchins even show enhanced calcification in environments with higher pCO_2 (Iglesias-Rodriguez et al., 2008; Doney et al., 2009; Ries et al., 2009). In particular, different populations of *Emiliania huxleyi* have shown decreased, increased, or unchanged calcification in response to higher pCO_2 (Fabry, 2008).

According to Hoegh-Guldberg et al. (2007), aragonite saturation will drop below the threshold for major changes to coral communities within this century, which will result in less diverse reef communities and carbonate reef structures that fail to be maintained. Carbonate mineral production in coral reefs is largely supported by the calcification of corals, coralline algae, and large benthic foraminifers. Among these,

reef-dwelling foraminifers and coralline algae mainly produce carbonate shells composed of high-Mg calcite, which has generally higher solubility in seawater than low-Mg calcite or aragonite (Morse et al., 2006). Therefore, these organisms with high-magnesium calcite shells may be the "first responders" among reef calcifying organisms to the decreasing saturation state of seawater caused by ocean acidification.

Large benthic foraminifera are important producers of carbonate in tropical and subtropical shallow-water areas. Also, they are important producers of organic matter (Fujita and Fujimura, 2008). Large, reef-dwelling benthic foraminifers (defined as mature individuals >1 mm in diameter) are shelled protists that are host to algal endosymbionts (Lee, 1998; Hallock, 1999), which allows rapid growth (50-100 times that of most temperate species). So I sometime refer to them as symbiont-bearing reef foraminifera. The empty tests of foraminifers, released by reproduction or death, are entrained at the reef crest by waves and transported by currents, and contribute to the formation and retention of sand beaches and coastal landforms (Hohenegger, 2006; Fujita et al., 2009). Previous studies for carbon budget of foraminifera observed widely different mechanisms for uptake of inorganic and for calcification between the perforate and imperforate groups of foraminifera (ter Kuile and Ezez, 1991). Therefore, in order to evaluate the difference between them, three different species (*Calcarina gaudichaudii* (perforate), *Amphisorus kudakajimensis* and *Amphisorus hemprichii* (imperforate)) were cultured under the same conditions in this study.

Reef-calcifying organisms other than corals are also both biogeochemically and ecologically important, but they have been much less studied to date (Kuffner et al., 2008; Doney et al., 2009). Kuroyanagi et al. (2009) cultured the reef-dwelling benthic foraminifer *Marginopora* (*Amphisorus*) *kudakajimensis* in pH-controlled seawater and

showed that lower pH decreased both the shell weight and diameter. However, in their experiment they controlled the seawater pH by adding a strong acid or base, which also alters the alkalinity and does not precisely reproduce actual ocean acidification conditions. During calcification, foraminifers are able to elevate the pH at the site of calcification (vesicles or seawater vacuoles) by one unit above seawater pH (Erez, 2003; Bentov et al., 2009; de Nooijer et al., 2009). In acidified seawater, foraminifers would require more energy to elevate the intracellular pH, leading to a decrease in calcification. Previous culturing results have indicated that shell weights of both planktonic and benthic foraminifers reduce with decreasing [CO_3^{2-}] or pH (Bijma et al., 1999; Bijma et al., 2002; Dissard et al., 2010; Lombard et al., 2010).

During ocean acidification, carbonate ion (CO_3^{2-}) in seawater is decreased and at the same time bicarbonate ion (HCO_3^-) and CO_2 are increased. The former change may negatively influence the calcification of foraminifers by reducing the calcium carbonate saturation state (**Ω**) of the seawater, whereas the latter changes may have a positive effect through enhancement of symbiont photosynthesis. Thus, ocean acidification may affect net calcification of foraminifers in either direction. Sensitivity differences to each of these changes may determine the overall response of a particular species to ocean acidification. Therefore, to accurately estimate the impacts of ocean acidification, the effect of each change should be examined separately.

In this study, I focused on a varying responses to ocean acidification between species of algal symbiont-bearing, reef-dwelling foraminifers by conducting a series of culture experiments. I used a high-precision pCO_2 control system to evaluate the effects of ongoing ocean acidification on foraminiferal calcification under possible near-future pCO_2 conditions. To evaluate the impact of HCO_3^- and CO_3^{2-} concentration changes in

seawater on net calcification of foraminifers separately, I also conducted a culture experiment in which seawater was chemically manipulated to vary the HCO_3^- concentration under a constant CO_3^{2-} concentration.

2.2. Materials and methods

I selected two genera (three species) of large, algal symbiont-bearing benthic foraminifers commonly found on coral reefs in the northwest Pacific. *Amphisorus kudakajimensis* Gudmundsson, 1994 and the closely related species *Amphisorus hemprichii* Ehrenberg, 1839 are imperforate and have porcelaneous shell (Fig. 2-1). Typically, these species are found on macroalgae in the reef moat (Hohenegger, 1994). *Calcarina gaudichaudii* d'Orbigny in Ehrenberg, 1840, is perforate and has a hyaline appearance shell. It typically lives on algal turf on the reef crest (Hohenegger, 1994). They are host to endosymbionts, dinoflagellates and diatom as their symbiont algae, respectively (Lee, 1998). In addition, these three species have been observed to reproduce asexually during spring and summer (Sakai and Nishihira, 1981; Hohenegger, 2006). Thus, asexually reproduced clone individuals can be used for culture experiments to exclude the effect of genetic variability on the experimental results. For more detailed information on the taxonomy, biology, and ecology of these species, see Röttger and Krüger (1990) and Hohenegger (1994).

Mature living foraminifer individuals were collected from Okinawa, Japan, in early May 2010; *A. kudakajimensis* and *A. hemprichii* were collected from Aka Island (26°39′ N, 127°51′ E) and *C. gaudichaudii* from Ikei Island (26°39′ N, 127°99′ E). Collected individuals were maintained separately in small Petri dishes filled with natural seawater at room temperature (approximately 25 °C) under a natural light:dark

cycle near a window (light intensity, ~100 μmol m-2 s-1). Because *C. gaudichaudii* are commonly found in high energy reef flat environments (Hohenegger, 1994), the species were maintained under continuous water motion produced by using a continuous-action shaker (approximately 30 rpm; in vitro Shaker, Wave-PR, TAITEC Inc., Saitama, Japan). In contrast, *A. hemprichii* individuals were maintained under stagnant conditions on a flat shelf, because they are commonly found in relatively calm reef-moat environments (Hohenegger, 1994). These individuals were not fed during maintenance, and the culture medium was changed weekly. After a few weeks, the mature individuals reproduced asexually, each producing 500–1000 clonal (i.e., genetically identical) individuals (Figure 2-1). Juveniles of the clone populations were kept under the same conditions as the adults for 4 to 6 weeks until the experiments were started. I cultured three separate clone populations of each species. By using clonal individuals for culture experiments, genetic influences can be eliminated. Moreover, since the initial size and weight of clone individuals are practically identical, weight differences of clone populations between treatments can be assumed to directly reflect differences in calcification during the experimental period. Therefore in the present paper I focus on the variation of shell weight, not shell size, between treatments.

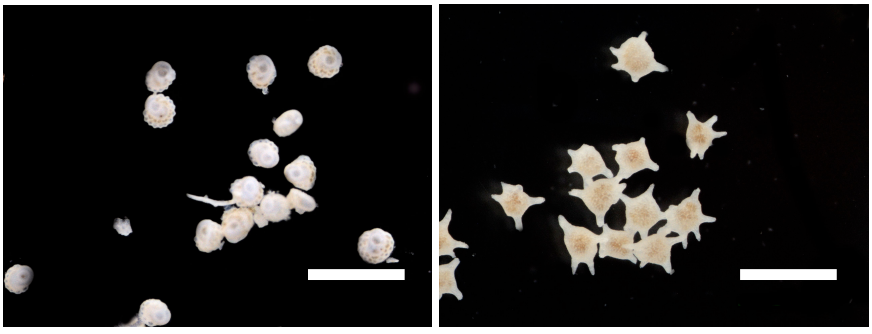

Figure 2-1 Clone individuals for the experiment actually. Scale bar: 1mm.

2.2.1. Ocean acidification (OA) experiment

I cultured *A. kudakajimensis* and *C. gaudichaudii* individuals in seawater under five different pCO_2 conditions. Highly precise and stable pCO_2 conditions (pCO_2 levels were maintained mostly within 5% throughout the experimental period) were achieved by using a high-precision pCO_2 control system called the AICAL system (Fujita et al., 2011). In this system, filtered seawater (pore size 1 μm) is exposed to a gas mixture of CO_2 and dilution air pCO_2 of seawater flowing out from a bubbling tank was measured directly and maintained at the desired level by continuously regulating the ratio of CO_2 in the gas mixture (Figures 2-2 and 2-3). The five treatment levels used, 245, 375, 588, 763, and 907 μatm, represented pre-industrial (Low pCO_2), present-day (Control), and three near-future (High pCO_2 1–3) pCO_2 conditions, respectively (Table 1).

Ten to fifteen individuals of each clone population were sealed in an acrylic pipe cage constructed from 180 μm mesh nylon sheets and submerged in a 12-L aquarium filled with pCO_2-controlled seawater. For each pCO_2 treatment, two aquariums were prepared so that reproducibility could be assessed. Seawater was continuously supplied to the aquariums at the rate of 150 mL per minute. Cultured individuals were maintained for about 4 weeks in an indoor flow-through system at the same constant water temperature and light intensity under a 12 h:12 h light:dark cycle. They were not fed during the experimental period. After the experiment, foraminiferal shells were dried and their weights were measured separately using a Thermo Cahn C-35 microbalance, which can measure weights down to 0.1 μg with a precision (reproducibility) of less than 1.0 μg. The contribution of organic matter to the dry weight in this procedure is less than 3% (Fujita and Fujimura, 2008) with negligible differences among treatment conditions.

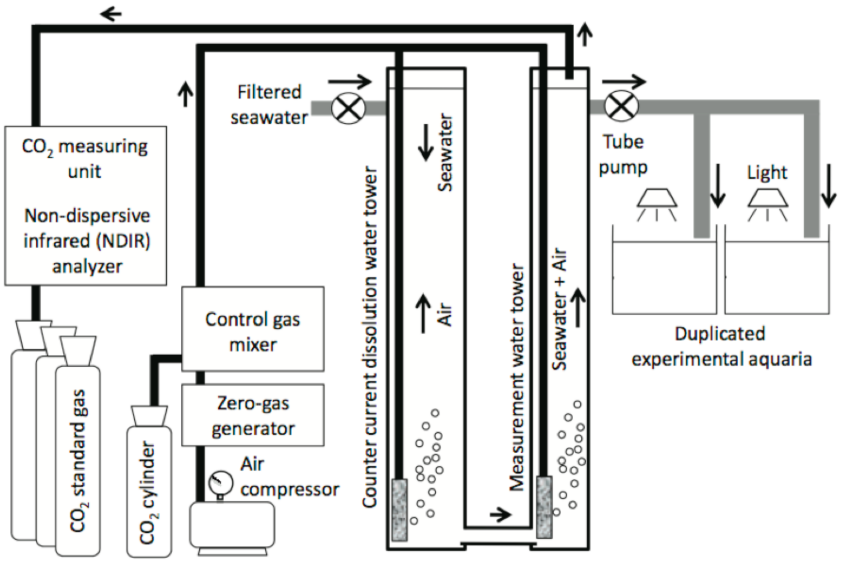

Figure 2-2. Schematic diagram of cultural set up.

Figure 2-3. The AICAL system.

2.2.2. Constant carbonate (CC) experiment

To separately evaluate the impact on calcification of HCO_3^- and CO_3^{2-} concentration changes in seawater, I conducted a culture experiment with *A. hemprichii* and *C. gaudichaudii* using seawater chemically manipulated to vary the HCO_3^- concentration while maintaining a constant CO_3^{2-} concentration. The seawater carbonate chemistry was manipulated by the following two steps. First, I altered the total

alkalinity (TA) of the seawater by adding Na_2CO_3 or HCl, and then I manipulated the dissolved inorganic carbon (DIC) content by bubbling either CO_2 gas, air, or CO_2-free air, selected as appropriate for the required direction of DIC change. The seawater chemistry was modified just before the seawater was to be used in a culture experiment. The carbonate chemistry in the five treatments in this experiment was designed to represent a similar range of HCO_3^- concentrations to those in the OA experiment while maintaining a constant CO_3^{2-} concentration similar to that of the control treatment in the OA experiment (Table 2-1).

About 10 individuals of a clonal population were sealed in a 120-mL glass vial filled with chemically manipulated seawater. I prepared duplicate sets of three clone populations for each species. The culturing seawater was replaced every week, and the glass vials were tightly sealed with minimum headspace to prevent any CO_2 gas exchange between the seawater and the atmosphere. The duration of cultivation was 4 weeks for *A. hemprichii* and 5 weeks for *C. gaudichaudii*.

2.2.3. Statistical analysis

A preliminary graphical plot of measured shell weight showed a long-tailed distribution, suggesting that shell length rather than weight is normally distributed. Therefore, before the statistical analysis, I calculated the square root of the measured shell weights for *Amphisorus* spp. and the cube root for *C. gaudichaudii*, in accordance with the species-specific geometric direction of skeletal growth (*Amphisorus* spp. have disc-shaped shells, and *Calcarina* shells are spherical with spikes), which results in their having different surface-to-volume ratios (Irie and Adams, 2007; Kuroyanagi et al., 2009). The transformed shell weight was analyzed by ANOVA in which pCO_2, clone,

replicate tank nested within pCO_2, and all possible interactions were considered fixed effects. ANOVA was followed by Tukey's HSD tests to find significant differences in the focal factors among levels ($\alpha = 0.05$). I used JMP statistical software (version 7.0.1. SAS Institute Inc.) for all statistical analyses.

Table 2-1. Carbonate chemistry speciation for each treatment of the Ocean Acidification (OA) and Constant Carbonate (CC) experiments*

Treatment	pH at 25 °C	TA	DIC	pCO_2	HCO_3^-	CO_3^{2-}	CO_2	Ωcal	Ωarg
Ocean Acidification (OA) Experiment (~27.1 °C, salinity 34.1)									
Low pCO_2	8.232	2224	1821	245	1536	278	7	6.8	4.5
Control	8.085	2224	1914	375	1686	218	10	5.3	3.5
High pCO_2 - 1	7.924	2224	2002	588	1823	163	16	4.0	2.6
High pCO_2 - 2	7.826	2224	2047	763	1891	135	21	3.3	2.2
High pCO_2 - 3	7.761	2224	2075	907	1932	119	24	2.9	1.9
Constant Carbonate (CC) Experiment (~26.9 °C, salinity 34.5)									
Low HCO_3^-	8.081	2165	1855	354	1630	216	10	5.2	3.5
Control	8.057	2271	1965	398	1737	218	11	5.3	3.5
High HCO_3^- - 1	8.031	2371	2071	448	1841	217	12	5.3	3.5
High HCO_3^- - 2	8.014	2447	2151	486	1920	218	13	5.3	3.5
High HCO_3^- - 3	8.003	2491	2197	511	1966	217	14	5.3	3.5

*Total alkalinity (TA) and pCO_2 data in the OA experiment and TA and pH (total hydrogen ion scale) in the CC experiment are the means over the experimental period. Other values were calculated from these values using CO2SYS software (Pierrot et al., 2006), the temperature and salinity given in the table, and the apparent dissociation constants for carbonic acid of Mehrbach et al. (1973), refit by Dickson and Millero (1987). Units of concentration are μmol kg^{-1} and those of pCO_2 are μatm.

2.3. Results

2.3.1. OA experiment

The main effects of pCO_2 on shell weight were independent of clone or rearing tank in both species (Table 2-2, 2-3, and 2-4). Higher seawater pCO_2 led to smaller mean shell weight in *A. kudakajimensis* (Figure 2-4). Conversely, in *C. gaudichaudii* seawater pCO_2 and shell weight were positively related (Figure 2-4). Difference in clonal origin was also statistically significant, reflecting the differences in the initial weights of the clone populations (Tables 2-5 and 2-6). In contrast, the significant effect observed between replicate tanks might reflect a difference in environmental conditions unrelated to pCO_2 (Tables 2-5 and 2-6). As temperature (monitored, not shown) and seawater composition other than carbonate chemistry were identical in all tanks, the difference might be attributable to insufficient randomization of light conditions, but I cannot ascertain the reason from the available data. However, I was able to reduce the influence of the difference on the result by combining the results of replicate tanks. It would also be possible to reduce this effect by increasing the sample size.

Table 2-2. Shell weight means for five varied pCO_2 treatment calculated from total raw data of three clone populations of each species, *Amphisorus kudakajimensis* and *Calcarina gaudichaudii*.

	pCO_2 treatment	Mean (μg)	Max. (μg)	Min. (μg)	SE[a]	N[b]
Amphisorus kudakajimensis	Low	41.9	66.3	20.9	1.51	61
	Control	41.3	65.4	16.9	1.40	62
	High - 1	38.6	61.3	9.5	1.40	61
	High - 2	37.1	63.9	20.6	1.20	61
	High - 3	35.4	58.8	13.9	1.36	62
Calcarina gaudichaudii	Low	22.0	52.8	3.6	1.17	88
	Control	21.0	43.4	4.6	1.06	87
	High - 1	22.8	47.1	5.5	1.04	90
	High - 2	25.4	48.3	5.9	1.15	83
	High - 3	26.3	89.1	5.5	1.51	87

[a]SE: Standard Error
[b]N: Number of cultured individuals

Table 2-3. Shell weight value of *Amphisorus kudakajimensis* (OA experiment).

Tank	group	pCO2(ppm)	weight (μg)	weight-squar(μg)
A	α	300	45.7	6.760
A	α	300	51.7	7.190
A	α	300	58.4	7.642
A	α	300	39.1	6.253
A	α	300	49	7.000
A	α	300	52.1	7.218
A	α	300	48	6.928
A	α	300	61.5	7.842
A	α	300	53.9	7.342
A	α	300	38.3	6.189
A	α	300	51.3	7.162
A	α	400	52.6	7.253
A	α	400	51.1	7.148
A	α	400	47.9	6.921
A	α	400	41.6	6.450
A	α	400	32.1	5.666
A	α	400	51.5	7.176
A	α	400	63.6	7.975
A	α	400	39.6	6.293
A	α	400	36	6.000
A	α	400	30.9	5.559
A	α	400	55.4	7.443
A	α	600	49	7.000
A	α	600	33.4	5.779
A	α	600	51.4	7.169
A	α	600	41.3	6.427
A	α	600	46.5	6.819
A	α	600	38.4	6.197
A	α	600	48.1	6.935
A	α	600	46.3	6.804
A	α	600	44.3	6.656
A	α	600	31.6	5.621
A	α	600	33.8	5.814
A	α	800	52.7	7.259
A	α	800	40.9	6.395
A	α	800	32.4	5.692
A	α	800	33.5	5.788
A	α	800	45.2	6.723
A	α	800	49.4	7.029
A	α	800	52.3	7.232
A	α	800	37.3	6.107
A	α	800	40.9	6.395
A	α	800	35.2	5.933
A	α	800	52.3	7.232
A	α	1000	32.6	5.710
A	α	1000	41.3	6.427
A	α	1000	41.9	6.473
A	α	1000	40.6	6.372
A	α	1000	41	6.403
A	α	1000	37.5	6.124
A	α	1000	27.1	5.206
A	α	1000	38.1	6.173
A	α	1000	35.5	5.958
A	α	1000	46.6	6.826
A	α	1000	53.6	7.321
B	α	300	44.9	6.701
B	α	300	40.7	6.380
B	α	300	44	6.633
B	α	300	43.7	6.611
B	α	300	47.3	6.877
B	α	300	66.3	8.142
B	α	300	58.1	7.622
B	α	300	48.3	6.950
B	α	300	54	7.348
B	α	300	41.1	6.411
B	α	400	43	6.557
B	α	400	46.9	6.848
B	α	400	48.1	6.935
B	α	400	43.3	6.580
B	α	400	43.9	6.626
B	α	400	44.4	6.663
B	α	400	63.2	7.950
B	α	400	43.4	6.588
B	α	400	36.1	6.008
B	α	400	45.1	6.716
B	α	400	36.7	6.058
B	α	600	48.3	6.950
B	α	600	37.5	6.124
B	α	600	43.4	6.588

Table 2-3. continued.

B	α	600	42.9	6.550
B	α	600	48.2	6.943
B	α	600	61.3	7.829
B	α	600	49.6	7.043
B	α	600	53.2	7.294
B	α	600	51.3	7.162
B	α	600	48.5	6.964
B	α	800	35.1	5.925
B	α	800	35	5.916
B	α	800	34.9	5.908
B	α	800	37.4	6.116
B	α	800	37.4	6.116
B	α	800	48.1	6.935
B	α	800	30.4	5.514
B	α	800	32.7	5.718
B	α	800	44.9	6.701
B	α	800	44.9	6.701
B	α	800	40.4	6.356
B	α	1000	46.9	6.848
B	α	1000	39.5	6.285
B	α	1000	45	6.708
B	α	1000	58.8	7.668
B	α	1000	45	6.708
B	α	1000	52.8	7.266
B	α	1000	37.6	6.132
B	α	1000	51.1	7.148
B	α	1000	42.3	6.504
B	α	1000	42.4	6.512
B	α	1000	38.8	6.229
A	β	300	61	7.810
A	β	300	53.1	7.287
A	β	300	42.3	6.504
A	β	300	37.3	6.107
A	β	300	39.3	6.269
A	β	300	40.9	6.395
A	β	300	33.6	5.797
A	β	300	50.1	7.078
A	β	300	49.9	7.064
A	β	300	54.5	7.382
A	β	400	52.8	7.266
A	β	400	47	6.856
A	β	400	26.9	5.187
A	β	400	64.6	8.037
A	β	400	40	6.325
A	β	400	44.1	6.641
A	β	400	49.6	7.043
A	β	400	41.4	6.434
A	β	400	34.9	5.908
A	β	400	42.1	6.488
A	β	600	38	6.164
A	β	600	35.3	5.941
A	β	600	47.1	6.863
A	β	600	35.9	5.992
A	β	600	31.4	5.604
A	β	600	61	7.810
A	β	600	45.6	6.753
A	β	600	42.7	6.535
A	β	600	25.8	5.079
A	β	600	31.5	5.612
A	β	800	49.8	7.057
A	β	800	47.4	6.885
A	β	800	43.4	6.588
A	β	800	52	7.211
A	β	800	46.8	6.841
A	β	800	63.9	7.994
A	β	800	34.1	5.840
A	β	800	33.1	5.753
A	β	800	43.7	6.611
A	β	1000	33.6	5.797
A	β	1000	41.6	6.450
A	β	1000	29.7	5.450
A	β	1000	40.1	6.332
A	β	1000	40.9	6.395
A	β	1000	41	6.403
A	β	1000	32.4	5.692
A	β	1000	40.7	6.380
A	β	1000	29.8	5.459
A	β	1000	46.7	6.834
B	β	300	46.3	6.804
B	β	300	33.4	5.779
B	β	300	50.8	7.127

Table 2-3. continued

B	β	300	39.6	6.293
B	β	300	51.7	7.190
B	β	300	39.4	6.277
B	β	300	42.7	6.535
B	β	300	49	7.000
B	β	300	48.9	6.993
B	β	300	37.4	6.116
B	β	400	40.3	6.348
B	β	400	45	6.708
B	β	400	45.7	6.760
B	β	400	46.6	6.826
B	β	400	57.3	7.570
B	β	400	65.4	8.087
B	β	400	50.1	7.078
B	β	400	41	6.403
B	β	400	48.7	6.979
B	β	400	44	6.633
B	β	600	35	5.916
B	β	600	57.5	7.583
B	β	600	55	7.416
B	β	600	30	5.477
B	β	600	38.1	6.173
B	β	600	46.8	6.841
B	β	600	44.7	6.686
B	β	600	48.1	6.935
B	β	600	32.7	5.718
B	β	600	35.5	5.958
B	β	800	42.6	6.527
B	β	800	40.7	6.380
B	β	800	37.5	6.124
B	β	800	40.3	6.348
B	β	800	33.6	5.797
B	β	800	44	6.633
B	β	800	29.7	5.450
B	β	800	40.7	6.380
B	β	800	37	6.083
B	β	800	47	6.856
B	β	1000	33.4	5.779
B	β	1000	32	5.657
B	β	1000	47.7	6.907
B	β	1000	32.1	5.666
B	β	1000	40.3	6.348
B	β	1000	42.7	6.535
B	β	1000	43.4	6.588
B	β	1000	34.4	5.865
B	β	1000	46.7	6.834
B	β	1000	56.6	7.523
A	γ	300	40.3	6.348
A	γ	300	27.9	5.282
A	γ	300	36.1	6.008
A	γ	300	23.3	4.827
A	γ	300	28.1	5.301
A	γ	300	56	7.483
A	γ	300	33.9	5.822
A	γ	300	26.2	5.119
A	γ	300	22.7	4.764
A	γ	300	57	7.550
A	γ	400	44.9	6.701
A	γ	400	37.1	6.091
A	γ	400	34.5	5.874
A	γ	400	46.8	6.841
A	γ	400	33.9	5.822
A	γ	400	32.2	5.675
A	γ	400	34.2	5.848
A	γ	400	28	5.292
A	γ	400	30.5	5.523
A	γ	400	25.7	5.070
A	γ	600	23.8	4.879
A	γ	600	37.4	6.116
A	γ	600	23.4	4.837
A	γ	600	24.9	4.990
A	γ	600	32.1	5.666
A	γ	600	28.9	5.376
A	γ	600	42.6	6.527
A	γ	600	30.7	5.541
A	γ	600	22.4	4.733
A	γ	600	36.1	6.008
A	γ	800	26.3	5.128
A	γ	800	37	6.083

Table 2-3. Continued.

A	γ	800	27.9	5.282
A	γ	800	25.5	5.050
A	γ	800	38.4	6.197
A	γ	800	29.1	5.394
A	γ	800	23.1	4.806
A	γ	800	22.6	4.754
A	γ	800	25.1	5.010
A	γ	800	39	6.245
A	γ	1000	26.2	5.119
A	γ	1000	18.7	4.324
A	γ	1000	21.5	4.637
A	γ	1000	22.9	4.785
A	γ	1000	27.4	5.235
A	γ	1000	13.9	3.728
A	γ	1000	21.3	4.615
A	γ	1000	21	4.583
A	γ	1000	18.8	4.336
A	γ	1000	23.4	4.837
B	γ	300	29.2	5.404
B	γ	300	30.9	5.559
B	γ	300	31.7	5.630
B	γ	300	28.2	5.310
B	γ	300	30.6	5.532
B	γ	300	21.8	4.669
B	γ	300	27.7	5.263
B	γ	300	20.9	4.572
B	γ	300	21.9	4.680
B	γ	300	25.1	5.010
B	γ	400	16.9	4.111
B	γ	400	25.9	5.089
B	γ	400	19.6	4.427
B	γ	400	27.1	5.206
B	γ	400	32.1	5.666
B	γ	400	41.6	6.450
B	γ	400	38.8	6.229
B	γ	400	32.4	5.692
B	γ	400	28.3	5.320
B	γ	400	24.7	4.970
B	γ	600	28.9	5.376
B	γ	600	9.5	3.082
B	γ	600	31.6	5.621
B	γ	600	36	6.000
B	γ	600	38.1	6.173
B	γ	600	30.9	5.559
B	γ	600	21.9	4.680
B	γ	600	25.4	5.040
B	γ	600	25.1	5.010
B	γ	600	36.1	6.008
B	γ	800	32.5	5.701
B	γ	800	27.4	5.235
B	γ	800	28.9	5.376
B	γ	800	23.9	4.889
B	γ	800	22.2	4.712
B	γ	800	27	5.196
B	γ	800	28.7	5.357
B	γ	800	32.3	5.683
B	γ	800	20.6	4.539
B	γ	800	22.7	4.764
B	γ	1000	26	5.099
B	γ	1000	24.9	4.990
B	γ	1000	28	5.292
B	γ	1000	30.5	5.523
B	γ	1000	26.6	5.158
B	γ	1000	25.2	5.020
B	γ	1000	25.8	5.079
B	γ	1000	31.3	5.595
B	γ	1000	20.6	4.539
B	γ	1000	19.9	4.461

Table 2-4. Shell weight value of *Calcarina gaudichaudii* (OA experiment).

Tank	group	pCO2 (ppm)	weight (μg)	one-third root weight (μng)
A	α	300	12.8	2.3
A	α	300	10.4	2.2
A	α	300	9.0	2.1
A	α	300	10.6	2.2
A	α	300	6.3	1.8
A	α	300	22.5	2.8
A	α	300	8.2	2.0
A	α	300	5.9	1.8
A	α	300	13.4	2.4
A	α	300	5.5	1.8
A	α	300	9.9	2.1
A	α	300	10.3	2.2
A	α	300	7.0	1.9
A	α	400	10.7	2.2
A	α	400	16.4	2.5
A	α	400	4.8	1.7
A	α	400	17.1	2.6
A	α	400	9.8	2.1
A	α	400	5.0	1.7
A	α	400	6.4	1.9
A	α	400	8.9	2.1
A	α	400	9.0	2.1
A	α	400	13.1	2.4
A	α	400	10.1	2.2
A	α	400	9.3	2.1
A	α	400	8.8	2.1
A	α	400	1.6	1.2
A	α	600	11.5	2.3
A	α	600	9.0	2.1
A	α	600	10.0	2.2
A	α	600	6.8	1.9
A	α	600	11.6	2.3
A	α	600	14.4	2.4
A	α	600	10.7	2.2
A	α	600	11.0	2.2
A	α	600	23.0	2.8
A	α	600	14.7	2.4
A	α	600	7.5	2.0
A	α	600	13.9	2.4
A	α	600	12.2	2.3
A	α	600	9.9	2.1
A	α	600	10.0	2.2
A	α	800	10.5	2.2
A	α	800	12.9	2.3
A	α	800	13.6	2.4
A	α	800	7.3	1.9
A	α	800	9.4	2.1
A	α	800	12.7	2.3
A	α	800	11.9	2.3
A	α	800	12.4	2.3
A	α	800	11.1	2.2
A	α	800	8.8	2.1
A	α	1000	7.2	1.9
A	α	1000	19.4	2.7
A	α	1000	14.9	2.5
A	α	1000	15.2	2.5
A	α	1000	14.2	2.4
A	α	1000	16.5	2.5
A	α	1000	19.7	2.7
A	α	1000	13.9	2.4
A	α	1000	13.1	2.4
A	α	1000	10.1	2.2
A	α	1000	11.9	2.3
A	α	1000	12.4	2.3
A	α	1000	10.1	2.2
B	α	300	7.8	2.0
B	α	300	7.8	2.0
B	α	300	7.1	1.9
B	α	300	10.1	2.2
B	α	300	13.0	2.4
B	α	300	9.0	2.1
B	α	300	8.8	2.1
B	α	300	8.6	2.0
B	α	300	4.6	1.7
B	α	300	7.0	1.9
B	α	300	6.0	1.8
B	α	300	7.1	1.9
B	α	300	3.6	1.5
B	α	300	16.3	2.5

Table 2-4. Continued.

B	α	300	8.6	2.0
B	α	400	12.2	2.3
B	α	400	10.0	2.2
B	α	400	10.8	2.2
B	α	400	17.0	2.6
B	α	400	9.6	2.1
B	α	400	6.1	1.8
B	α	400	8.3	2.0
B	α	400	8.4	2.0
B	α	400	4.6	1.7
B	α	400	10.4	2.2
B	α	400	8.7	2.1
B	α	400	7.5	2.0
B	α	400	6.9	1.9
B	α	400	17.1	2.6
B	α	400	11.7	2.3
B	α	600	6.5	1.9
B	α	600	6.5	1.9
B	α	600	15.7	2.5
B	α	600	17.6	2.6
B	α	600	15.4	2.5
B	α	600	5.5	1.8
B	α	600	14.6	2.4
B	α	600	14.8	2.5
B	α	600	7.2	1.9
B	α	600	13.3	2.4
B	α	600	6.3	1.8
B	α	600	12.6	2.3
B	α	600	10.0	2.2
B	α	600	11.0	2.2
B	α	600	8.1	2.0
B	α	800	16.6	2.6
B	α	800	7.8	2.0
B	α	800	5.9	1.8
B	α	800	16.5	2.5
B	α	800	13.6	2.4
B	α	800	16.8	2.6
B	α	800	10.0	2.2
B	α	800	18.3	2.6
B	α	800	17.4	2.6
B	α	800	14.6	2.4
B	α	800	11.6	2.3
B	α	800	7.8	2.0
B	α	800	15.9	2.5
B	α	1000	14.3	2.4
B	α	1000	7.5	2.0
B	α	1000	11.2	2.2
B	α	1000	18.6	2.6
B	α	1000	32.3	3.2
B	α	1000	7.3	1.9
B	α	1000	11.8	2.3
B	α	1000	7.5	2.0
B	α	1000	6.7	1.9
B	α	1000	5.5	1.8
B	α	1000	10.7	2.2
B	α	1000	7.0	1.9
B	α	1000	16.4	2.5
B	α	1000	7.9	2.0
A	β	300	51.1	3.7
A	β	300	29.4	3.1
A	β	300	27.5	3.0
A	β	300	32.8	3.2
A	β	300	20.3	2.7
A	β	300	28.4	3.1
A	β	300	29.3	3.1
A	β	300	38.5	3.4
A	β	300	27.2	3.0
A	β	300	27.9	3.0
A	β	300	23.2	2.9
A	β	300	20.8	2.8
A	β	300	34.9	3.3
A	β	300	18.6	2.6
A	β	300	27.3	3.0
A	β	400	31.4	3.2
A	β	400	33.0	3.2
A	β	400	43.4	3.5
A	β	400	36.3	3.3
A	β	400	29.7	3.1
A	β	400	30.7	3.1
A	β	400	26.6	3.0
A	β	400	28.3	3.0

Table 2-4. Continued.

A	β	400	25.4	2.9
A	β	400	26.2	3.0
A	β	400	26.7	3.0
A	β	400	22.0	2.8
A	β	400	32.7	3.2
A	β	400	32.0	3.2
A	β	600	34.8	3.3
A	β	600	20.5	2.7
A	β	600	35.1	3.3
A	β	600	19.2	2.7
A	β	600	28.0	3.0
A	β	600	22.5	2.8
A	β	600	22.6	2.8
A	β	600	19.0	2.7
A	β	600	35.3	3.3
A	β	600	25.6	2.9
A	β	600	26.9	3.0
A	β	600	31.3	3.2
A	β	600	27.2	3.0
A	β	600	23.9	2.9
A	β	600	24.3	2.9
A	β	800	22.5	2.8
A	β	800	21.7	2.8
A	β	800	22.8	2.8
A	β	800	34.0	3.2
A	β	800	32.1	3.2
A	β	800	38.8	3.4
A	β	800	36.9	3.3
A	β	800	32.0	3.2
A	β	800	26.1	3.0
A	β	800	23.0	2.8
A	β	800	25.6	2.9
A	β	800	29.5	3.1
A	β	800	29.4	3.1
A	β	800	34.9	3.3
A	β	800	20.1	2.7
A	β	1000	31.1	3.1
A	β	1000	23.4	2.9
A	β	1000	33.3	3.2
A	β	1000	48.3	3.6
A	β	1000	32.5	3.2
A	β	1000	22.3	2.8
A	β	1000	32.8	3.2
A	β	1000	89.1	4.5
A	β	1000	27.2	3.0
A	β	1000	18.6	2.6
A	β	1000	44.6	3.5
A	β	1000	35.0	3.3
A	β	1000	33.5	3.2
A	β	1000	29.8	3.1
A	β	1000	32.1	3.2
B	β	300	26.7	3.0
B	β	300	29.8	3.1
B	β	300	24.4	2.9
B	β	300	52.8	3.8
B	β	300	26.1	3.0
B	β	300	30.7	3.1
B	β	300	29.9	3.1
B	β	300	34.9	3.3
B	β	300	29.1	3.1
B	β	300	33.8	3.2
B	β	300	25.5	2.9
B	β	300	35.3	3.3
B	β	300	29.8	3.1
B	β	300	22.5	2.8
B	β	300	18.9	2.7
B	β	400	28.9	3.1
B	β	400	37.4	3.3
B	β	400	31.9	3.2
B	β	400	33.7	3.2
B	β	400	34.1	3.2
B	β	400	23.2	2.9
B	β	400	34.6	3.3
B	β	400	23.1	2.8
B	β	400	17.6	2.6
B	β	400	28.0	3.0
B	β	400	32.0	3.2
B	β	400	21.1	2.8
B	β	400	21.2	2.8

Table 2-4. Continued.

B	β	400	43.2	3.5
B	β	600	25.1	2.9
B	β	600	32.2	3.2
B	β	600	26.8	3.0
B	β	600	25.3	2.9
B	β	600	33.0	3.2
B	β	600	23.8	2.9
B	β	600	36.4	3.3
B	β	600	30.6	3.1
B	β	600	24.9	2.9
B	β	600	30.9	3.1
B	β	600	26.3	3.0
B	β	600	23.4	2.9
B	β	600	27.5	3.0
B	β	600	33.9	3.2
B	β	600	27.1	3.0
B	β	800	32.3	3.2
B	β	800	36.4	3.3
B	β	800	31.5	3.2
B	β	800	25.2	2.9
B	β	800	44.2	3.5
B	β	800	26.3	3.0
B	β	800	35.0	3.3
B	β	800	30.7	3.1
B	β	800	37.5	3.3
B	β	800	34.3	3.2
B	β	800	28.5	3.1
B	β	800	28.9	3.1
B	β	800	41.0	3.4
B	β	800	28.6	3.1
B	β	800	34.9	3.3
B	β	1000	19.8	2.7
B	β	1000	22.1	2.8
B	β	1000	43.9	3.5
B	β	1000	41.9	3.5
B	β	1000	38.7	3.4
B	β	1000	50.1	3.7
B	β	1000	35.6	3.3
B	β	1000	24.3	2.9
B	β	1000	30.7	3.1
B	β	1000	24.3	2.9
B	β	1000	16.3	2.5
B	β	1000	26.0	3.0
B	β	1000	26.7	3.0
B	β	1000	20.9	2.8
B	β	1000	36.4	3.3
A	γ	300	40.6	3.4
A	γ	300	20.4	2.7
A	γ	300	23.7	2.9
A	γ	300	37.5	3.3
A	γ	300	29.7	3.1
A	γ	300	19.8	2.7
A	γ	300	19.0	2.7
A	γ	300	19.0	2.7
A	γ	300	19.8	2.7
A	γ	300	37.4	3.3
A	γ	300	35.1	3.3
A	γ	300	11.0	2.2
A	γ	300	30.1	3.1
A	γ	300	24.1	2.9
A	γ	300	23.3	2.9
A	γ	400	23.2	2.9
A	γ	400	35.8	3.3
A	γ	400	14.0	2.4
A	γ	400	33.1	3.2
A	γ	400	21.1	2.8
A	γ	400	24.6	2.9
A	γ	400	17.4	2.6
A	γ	400	23.4	2.9
A	γ	400	29.2	3.1
A	γ	400	23.2	2.9
A	γ	400	19.7	2.7
A	γ	400	19.5	2.7
A	γ	400	26.7	3.0
A	γ	400	25.7	3.0
A	γ	400	19.0	2.7
A	γ	600	23.5	2.9
A	γ	600	31.1	3.1
A	γ	600	38.3	3.4
A	γ	600	39.3	3.4
A	γ	600	26.7	3.0

Table 2-5. ANOVA results on shell weight of *Amphisorus kudakajimensis* in ocean acidification experiment with pCO_2, clone, and tank as fixed-effect factors.

Factor	*df*	*SS*[b]	*F*	*P*
pCO_2	4	12.3	8.4	**$<10^{-5}$**
Clone	2	109.9	150.3	**$<10^{-44}$**
Tank [pCO_2]	5	6.3	3.5	**$<10^{-2}$**
pCO_2 × Clone	8	3.9	1.3	0.23
Tank × Clone [pCO_2]	10	4.6	1.3	0.26
Error	277	101.2		

[a]Bold type signifies $P<0.05$.

[b]SS: Sum of squares.

Table 2-6. ANOVA results on shell weight of *Calcarina gaudichaudii* in ocean acidification experiment with pCO_2, clone, and tank as fixed-effect factors.

Factor	*df*	*SS*[b]	*F*	*P*
pCO_2	4	2.2	7.8	**$<10^{-5}$**
Clone	2	69.8	491.7	**$<10^{-108}$**
Tank [pCO_2]	5	1.4	3. 9	**$<10^{-2}$**
pCO_2 × Clone	8	1.0	1. 7	0.10
Tank × Clone [pCO_2]	10	1.2	1.6	0.09
Error	405	28.7		

[a]Bold type signifies $P<0.05$.

[b]SS: Sum of squares.

2.3.2. CC experiment

No statistically significant trend in shell weight was found among the five treatments in either *A. hemprichii* or *C. gaudichaudii* (Figure 2-4 and Tables 2-7, 2-8, and 2-9), but *A. hemprichii* exhibited a significant interaction between pCO_2 and clone, suggesting that the reaction norm is variable among clones. However, Tukey's HSD test revealed no impact of pCO_2 level on shell weight in two of the three clonal groups, and the pH effect was not unidirectional in the other group (growth rates in the Low and High-3 treatments were higher than in the other treatments) (Table 2-10). Similarly, neither the pCO_2 × clone nor the tank × clone interaction was statistically negligible in *C. gaudichaudii*, but the Tukey's HSD test result suggested that shell weight was independent of pCO_2 condition in five of the six tank × clone combinations (in the sixth combination, the test detected significantly slower growth in High-1 than in the other treatments) (Table 2-11).

Table 2-7. Shell weight means for five varied HCO_3^- treatment with constant CO_3^{2-} concentration (~217 μmol/ kg) calculated from total raw data of three clone populations of each species, *Amphisorus hemprichii* and *Calcarina gaudichaudii*.

	HCO_3^- treatment	Mean (μg)	Max. (μg)	Min. (μg)	SE	N
Amphisorus hemprichii	Low	71.6	117.8	17.2	3.22	59
	Control	56.9	103.9	15.6	2.70	59
	High - 1	55.0	90.6	17.4	2.76	56
	High - 2	60.6	119.6	14.9	3.13	59
	High - 3	64.9	115.7	14.9	2.83	59
Calcarina gaudichaudii	Low	37.7	72.6	13.0	1.92	58
	Control	35.6	65.5	11.7	1.81	57
	High - 1	31.3	61.5	14.1	1.68	55
	High - 2	34.9	56.6	19.6	1.31	56
	High - 3	36.6	66.9	19.4	1.62	53

Table 2-8. Shell weight value of *Amphisorus hemprichii* (CC experiment).

Tank	group	pCO2 (ppm)	weight (μg)	weight−squar (μng)
A	α	300	92.8	9.6
A	α	300	116.8	10.8
A	α	300	98.5	9.9
A	α	300	63.0	7.9
A	α	300	81.1	9.0
A	α	300	92.2	9.6
A	α	300	62.8	7.9
A	α	300	83.2	9.1
A	α	300	113.8	10.7
A	α	400	67.5	8.2
A	α	400	98.0	9.9
A	α	400	75.3	8.7
A	α	400	46.5	6.8
A	α	400	86.0	9.3
A	α	400	78.8	8.9
A	α	400	91.5	9.6
A	α	400	32.5	5.7
A	α	400	57.1	7.6
A	α	400	65.8	8.1
A	α	600	80.4	9.0
A	α	600	56.4	7.5
A	α	600	65.4	8.1
A	α	600	68.9	8.3
A	α	600	67.6	8.2
A	α	600	58.5	7.6
A	α	600	58.0	7.6
A	α	600	65.8	8.1
A	α	600	90.6	9.5
A	α	600	78.5	8.9
A	α	800	79.8	8.9
A	α	800	68.4	8.3
A	α	800	66.1	8.1
A	α	800	91.0	9.5
A	α	800	49.7	7.0
A	α	800	55.9	7.5
A	α	800	31.0	5.6
A	α	800	99.0	9.9
A	α	800	66.2	8.1
A	α	1000	104.1	10.2
A	α	1000	81.2	9.0
A	α	1000	61.0	7.8
A	α	1000	92.5	9.6
A	α	1000	115.7	10.8
A	α	1000	59.3	7.7
A	α	1000	103.0	10.1
A	α	1000	108.5	10.4
A	α	1000	86.9	9.3
A	α	1000	72.3	8.5
B	α	300	75.3	8.7
B	α	300	117.8	10.9
B	α	300	115.0	10.7
B	α	300	76.1	8.7
B	α	300	62.9	7.9
B	α	300	80.2	9.0
B	α	300	93.5	9.7
B	α	300	93.2	9.7
B	α	300	85.7	9.3
B	α	300	75.4	8.7
B	α	400	73.8	8.6
B	α	400	80.3	9.0
B	α	400	80.8	9.0
B	α	400	83.1	9.1
B	α	400	82.1	9.1
B	α	400	82.2	9.1
B	α	400	83.0	9.1
B	α	400	103.9	10.2
B	α	400	67.5	8.2
B	α	400	96.1	9.8
B	α	600	81.1	9.0
B	α	600	67.9	8.2
B	α	600	81.4	9.0
B	α	600	69.5	8.3
B	α	600	71.6	8.5
B	α	600	66.3	8.1
B	α	600	69.3	8.3
B	α	600	67.0	8.2
B	α	600	54.3	7.4
B	α	600	78.0	8.8
B	α	800	69.1	8.3

Table 2-8. Continued.

B	α	800	91.6	9.6
B	α	800	101.5	10.1
B	α	800	73.1	8.5
B	α	800	33.5	5.8
B	α	800	87.9	9.4
B	α	800	119.6	10.9
B	α	800	95.4	9.8
B	α	800	83.6	9.1
B	α	800	86.5	9.3
B	α	1000	79.3	8.9
B	α	1000	78.3	8.8
B	α	1000	88.8	9.4
B	α	1000	65.2	8.1
B	α	1000	77.6	8.8
B	α	1000	33.6	5.8
B	α	1000	69.1	8.3
B	α	1000	91.7	9.6
B	α	1000	74.0	8.6
B	α	1000	60.9	7.8
A	β	300	76.9	8.8
A	β	300	91.2	9.5
A	β	300	111.0	10.5
A	β	300	50.3	7.1
A	β	300	49.6	7.0
A	β	300	44.2	6.6
A	β	300	90.8	9.5
A	β	300	63.9	8.0
A	β	300	34.2	5.8
A	β	300	57.6	7.6
A	β	400	36.9	6.1
A	β	400	52.3	7.2
A	β	400	63.5	8.0
A	β	400	45.4	6.7
A	β	400	61.6	7.8
A	β	400	75.5	8.7
A	β	400	70.1	8.4
A	β	400	52.4	7.2
A	β	400	46.5	6.8
A	β	600	68.8	8.3
A	β	600	48.1	6.9
A	β	600	56.4	7.5
A	β	600	82.1	9.1
A	β	600	81.3	9.0
A	β	600	23.9	4.9
A	β	600	37.6	6.1
A	β	600	67.7	8.2
A	β	800	45.0	6.7
A	β	800	70.4	8.4
A	β	800	72.0	8.5
A	β	800	58.5	7.6
A	β	800	47.7	6.9
A	β	800	71.0	8.4
A	β	800	55.4	7.4
A	β	800	75.1	8.7
A	β	800	82.2	9.1
A	β	800	61.2	7.8
A	β	1000	63.8	8.0
A	β	1000	54.7	7.4
A	β	1000	44.4	6.7
A	β	1000	42.2	6.5
A	β	1000	75.2	8.7
A	β	1000	41.1	6.4
A	β	1000	66.9	8.2
A	β	1000	73.2	8.6
A	β	1000	45.1	6.7
A	β	1000	32.9	5.7
B	β	300	71.6	8.5
B	β	300	105.0	10.2
B	β	300	83.3	9.1
B	β	300	72.3	8.5
B	β	300	92.5	9.6
B	β	300	57.6	7.6
B	β	300	92.9	9.6
B	β	300	61.5	7.8
B	β	300	70.1	8.4
B	β	300	22.9	4.8
B	β	400	47.6	6.9
B	β	400	53.8	7.3
B	β	400	70.4	8.4
B	β	400	50.7	7.1
B	β	400	60.8	7.8

Table 2-8. Continued.

B	β	400	56.0	7.5
B	β	400	69.1	8.3
B	β	400	59.0	7.7
B	β	400	56.5	7.5
B	β	400	45.4	6.7
B	β	600	48.3	6.9
B	β	600	50.0	7.1
B	β	600	55.8	7.5
B	β	600	76.2	8.7
B	β	600	70.0	8.4
B	β	600	78.6	8.9
B	β	600	51.1	7.1
B	β	600	51.0	7.1
B	β	600	63.1	7.9
B	β	600	56.7	7.5
B	β	800	61.3	7.8
B	β	800	59.3	7.7
B	β	800	59.0	7.7
B	β	800	105.6	10.3
B	β	800	56.9	7.5
B	β	800	72.6	8.5
B	β	800	66.4	8.1
B	β	800	69.7	8.3
B	β	800	72.4	8.5
B	β	800	40.3	6.3
B	β	1000	80.3	9.0
B	β	1000	74.5	8.6
B	β	1000	54.3	7.4
B	β	1000	35.5	6.0
B	β	1000	64.2	8.0
B	β	1000	69.1	8.3
B	β	1000	68.2	8.3
B	β	1000	29.0	5.4
B	β	1000	53.7	7.3
A	γ	300	80.1	8.9
A	γ	300	54.2	7.4
A	γ	300	66.6	8.2
A	γ	300	32.8	5.7
A	γ	300	51.7	7.2
A	γ	300	43.4	6.6
A	γ	300	66.9	8.2
A	γ	300	34.8	5.9
A	γ	300	36.0	6.0
A	γ	300	70.3	8.4
A	γ	400	22.0	4.7
A	γ	400	35.3	5.9
A	γ	400	39.0	6.2
A	γ	400	36.2	6.0
A	γ	400	20.6	4.5
A	γ	400	43.9	6.6
A	γ	400	36.1	6.0
A	γ	400	15.6	3.9
A	γ	400	67.6	8.2
A	γ	400	32.9	5.7
A	γ	600	37.2	6.1
A	γ	600	35.6	6.0
A	γ	600	41.3	6.4
A	γ	600	22.8	4.8
A	γ	600	36.1	6.0
A	γ	600	24.0	4.9
A	γ	600	33.7	5.8
A	γ	600	42.9	6.5
A	γ	600	34.9	5.9
A	γ	800	43.6	6.6
A	γ	800	34.6	5.9
A	γ	800	59.8	7.7
A	γ	800	26.4	5.1
A	γ	800	45.3	6.7
A	γ	800	20.1	4.5
A	γ	800	27.7	5.3
A	γ	800	81.5	9.0
A	γ	800	45.7	6.8
A	γ	800	31.3	5.6
A	γ	1000	80.2	9.0
A	γ	1000	76.2	8.7
A	γ	1000	59.5	7.7
A	γ	1000	88.3	9.4
A	γ	1000	25.7	5.1
A	γ	1000	63.5	8.0

Table 2-8. Continued.

A	γ	1000	43.3	6.6
A	γ	1000	42.1	6.5
A	γ	1000	14.9	3.9
A	γ	1000	43.8	6.6
B	γ	300	48.4	7.0
B	γ	300	88.7	9.4
B	γ	300	70.6	8.4
B	γ	300	60.5	7.8
B	γ	300	70.0	8.4
B	γ	300	66.0	8.1
B	γ	300	65.1	8.1
B	γ	300	61.1	7.8
B	γ	300	60.9	7.8
B	γ	300	17.2	4.1
B	γ	400	28.3	5.3
B	γ	400	36.9	6.1
B	γ	400	37.1	6.1
B	γ	400	50.8	7.1
B	γ	400	39.6	6.3
B	γ	400	26.4	5.1
B	γ	400	41.5	6.4
B	γ	400	59.2	7.7
B	γ	400	35.7	6.0
B	γ	400	48.9	7.0
B	γ	600	21.1	4.6
B	γ	600	42.5	6.5
B	γ	600	30.1	5.5
B	γ	600	17.4	4.2
B	γ	600	57.1	7.6
B	γ	600	29.3	5.4
B	γ	600	29.1	5.4
B	γ	600	35.0	5.9
B	γ	600	45.1	6.7
B	γ	800	32.5	5.7
B	γ	800	32.5	5.7
B	γ	800	38.0	6.2
B	γ	800	37.6	6.1
B	γ	800	60.0	7.7
B	γ	800	14.9	3.9
B	γ	800	19.3	4.4
B	γ	800	59.5	7.7
B	γ	800	57.8	7.6
B	γ	800	54.0	7.3
B	γ	1000	88.9	9.4
B	γ	1000	58.4	7.6
B	γ	1000	88.4	9.4
B	γ	1000	88.5	9.4
B	γ	1000	42.4	6.5
B	γ	1000	77.2	8.8
B	γ	1000	68.6	8.3
B	γ	1000	60.8	7.8
B	γ	1000	17.0	4.1
B	γ	1000	29.3	5.4

Table 2-9. Shell weight value of *Calcarina gaudichaudii* (CC experiment).

Tank	group	pCO2 (ppm)	weight (μg)	weight-cubic (μng)
A	α	300	56.9	3.8
A	α	300	52.0	3.7
A	α	300	58.3	3.9
A	α	300	70.8	4.1
A	α	300	58.8	3.9
A	α	300	71.6	4.2
A	α	300	52.0	3.7
A	α	300	72.6	4.2
A	α	300	40.1	3.4
A	α	300	55.3	3.8
A	α	400	64.0	4.0
A	α	400	35.6	3.3
A	α	400	65.5	4.0
A	α	400	56.3	3.8
A	α	400	56.8	3.8
A	α	400	41.1	3.5
A	α	400	43.7	3.5
A	α	400	42.8	3.5
A	α	600	45.3	3.6
A	α	600	53.4	3.8
A	α	600	61.5	3.9
A	α	600	56.3	3.8
A	α	600	50.6	3.7
A	α	600	44.9	3.6
A	α	600	46.9	3.6
A	α	600	45.8	3.6
A	α	600	45.6	3.6
A	α	600	53.6	3.8
A	α	800	46.4	3.6
A	α	800	50.4	3.7
A	α	800	49.9	3.7
A	α	800	47.2	3.6
A	α	800	56.6	3.8
A	α	800	53.8	3.8
A	α	800	40.5	3.4
A	α	800	36.2	3.3
A	α	800	37.6	3.4
A	α	800	43.7	3.5
A	α	1000	50.9	3.7
A	α	1000	40.7	3.4
A	α	1000	64.0	4.0
A	α	1000	51.5	3.7
A	α	1000	47.5	3.6
A	α	1000	47.7	3.6
A	α	1000	32.9	3.2
A	α	1000	66.9	4.1
A	α	1000	41.0	3.4
B	α	300	49.2	3.7
B	α	300	34.8	3.3
B	α	300	57.4	3.9
B	α	300	40.9	3.4
B	α	300	49.6	3.7
B	α	300	50.6	3.7
B	α	300	37.8	3.4
B	α	300	46.9	3.6
B	α	300	40.3	3.4
B	α	300	49.3	3.7
B	α	400	51.3	3.7
B	α	400	46.9	3.6
B	α	400	49.8	3.7
B	α	400	49.3	3.7
B	α	400	54.5	3.8
B	α	400	65.5	4.0
B	α	400	50.8	3.7
B	α	400	53.5	3.8
B	α	400	41.4	3.5
B	α	400	54.5	3.8
B	α	600	34.8	3.3
B	α	600	57.2	3.9
B	α	600	41.4	3.5
B	α	600	32.7	3.2
B	α	600	42.7	3.5
B	α	600	43.1	3.5
B	α	600	33.5	3.2
B	α	600	25.3	2.9
B	α	600	25.4	2.9
B	α	800	32.4	3.2
B	α	800	45.4	3.6
B	α	800	45.7	3.6

Table 2-9. Continued.

B	α	800	31.4	3.2
B	α	800	46.3	3.6
B	α	800	36.4	3.3
B	α	800	39.6	3.4
B	α	800	33.0	3.2
B	α	800	43.9	3.5
B	α	800	40.9	3.4
B	α	1000	43.0	3.5
B	α	1000	37.8	3.4
B	α	1000	52.8	3.8
B	α	1000	33.9	3.2
B	α	1000	36.3	3.3
B	α	1000	52.9	3.8
B	α	1000	29.1	3.1
B	α	1000	52.5	3.7
B	α	1000	45.5	3.6
B	α	1000	63.0	4.0
A	β	300	16.1	2.5
A	β	300	27.2	3.0
A	β	300	25.6	2.9
A	β	300	36.6	3.3
A	β	300	17.4	2.6
A	β	300	33.0	3.2
A	β	300	19.2	2.7
A	β	300	16.4	2.5
A	β	400	22.7	2.8
A	β	400	17.1	2.6
A	β	400	29.5	3.1
A	β	400	20.1	2.7
A	β	400	24.4	2.9
A	β	400	23.2	2.9
A	β	400	20.4	2.7
A	β	400	30.3	3.1
A	β	400	23.0	2.8
A	β	400	17.2	2.6
A	β	600	17.7	2.6
A	β	600	25.1	2.9
A	β	600	19.7	2.7
A	β	600	21.2	2.8
A	β	600	17.0	2.6
A	β	600	14.5	2.4
A	β	600	14.1	2.4
A	β	600	14.6	2.4
A	β	800	23.7	2.9
A	β	800	25.0	2.9
A	β	800	20.7	2.7
A	β	800	26.3	3.0
A	β	800	21.9	2.8
A	β	800	27.6	3.0
A	β	800	22.8	2.8
A	β	800	22.9	2.8
A	β	800	24.3	2.9
A	β	800	24.4	2.9
A	β	1000	20.2	2.7
A	β	1000	24.1	2.9
A	β	1000	20.0	2.7
A	β	1000	22.1	2.8
A	β	1000	27.0	3.0
A	β	1000	38.6	3.4
A	β	1000	21.0	2.8
B	β	300	23.0	2.8
B	β	300	29.7	3.1
B	β	300	29.8	3.1
B	β	300	23.0	2.8
B	β	300	40.1	3.4
B	β	300	61.6	3.9
B	β	300	37.8	3.4
B	β	300	30.3	3.1
B	β	300	28.9	3.1
B	β	300	13.0	2.4
B	β	400	29.0	3.1
B	β	400	27.6	3.0
B	β	400	19.9	2.7
B	β	400	11.7	2.3
B	β	400	22.3	2.8
B	β	400	32.1	3.2
B	β	400	17.0	2.6
B	β	400	24.0	2.9
B	β	400	20.6	2.7
B	β	600	26.7	3.0
B	β	600	27.5	3.0

Table 2-9. Continued.

B	β	600	19.1	2.7
B	β	600	22.4	2.8
B	β	600	27.5	3.0
B	β	600	29.2	3.1
B	β	600	18.3	2.6
B	β	600	19.3	2.7
B	β	600	20.9	2.8
B	β	800	21.6	2.8
B	β	800	25.8	3.0
B	β	800	25.5	2.9
B	β	800	24.5	2.9
B	β	800	19.6	2.7
B	β	800	25.2	2.9
B	β	800	24.1	2.9
B	β	1000	42.4	3.5
B	β	1000	25.8	3.0
B	β	1000	30.6	3.1
B	β	1000	41.1	3.5
B	β	1000	37.8	3.4
B	β	1000	35.0	3.3
B	β	1000	25.9	3.0
B	β	1000	21.5	2.8
A	γ	300	26.1	3.0
A	γ	300	32.2	3.2
A	γ	300	29.5	3.1
A	γ	300	43.9	3.5
A	γ	300	25.6	2.9
A	γ	300	26.9	3.0
A	γ	300	45.0	3.6
A	γ	300	32.5	3.2
A	γ	300	32.7	3.2
A	γ	300	45.3	3.6
A	γ	400	24.0	2.9
A	γ	400	31.4	3.2
A	γ	400	38.0	3.4
A	γ	400	30.1	3.1
A	γ	400	36.9	3.3
A	γ	400	30.2	3.1
A	γ	400	35.0	3.3
A	γ	400	27.7	3.0
A	γ	400	29.9	3.1
A	γ	400	31.0	3.1
A	γ	600	23.4	2.9
A	γ	600	23.8	2.9
A	γ	600	24.1	2.9
A	γ	600	32.1	3.2
A	γ	600	24.8	2.9
A	γ	600	18.4	2.6
A	γ	600	20.7	2.7
A	γ	600	22.3	2.8
A	γ	600	26.5	3.0
A	γ	600	20.5	2.7
A	γ	800	39.1	3.4
A	γ	800	30.9	3.1
A	γ	800	34.5	3.3
A	γ	800	44.5	3.5
A	γ	800	40.7	3.4
A	γ	800	39.1	3.4
A	γ	800	38.7	3.4
A	γ	800	24.0	2.9
A	γ	800	29.6	3.1
A	γ	800	37.7	3.4
A	γ	1000	37.9	3.4
A	γ	1000	25.1	2.9
A	γ	1000	24.5	2.9
A	γ	1000	28.8	3.1
A	γ	1000	33.2	3.2
A	γ	1000	34.5	3.3
A	γ	1000	26.0	3.0
A	γ	1000	33.1	3.2
A	γ	1000	38.5	3.4
A	γ	1000	45.9	3.6
B	γ	300	25.2	2.9
B	γ	300	28.5	3.1
B	γ	300	31.5	3.2
B	γ	300	34.4	3.3
B	γ	300	19.7	2.7
B	γ	300	20.0	2.7
B	γ	300	35.5	3.3

Table 2-9. Continued.

B	γ	300	31.2	3.1
B	γ	300	23.2	2.9
B	γ	300	42.4	3.5
B	γ	400	23.5	2.9
B	γ	400	34.1	3.2
B	γ	400	38.4	3.4
B	γ	400	45.2	3.6
B	γ	400	48.6	3.6
B	γ	400	40.3	3.4
B	γ	400	34.3	3.2
B	γ	400	18.0	2.6
B	γ	400	40.0	3.4
B	γ	400	35.9	3.3
B	γ	600	39.6	3.4
B	γ	600	22.0	2.8
B	γ	600	26.7	3.0
B	γ	600	36.7	3.3
B	γ	600	38.3	3.4
B	γ	600	38.4	3.4
B	γ	600	31.5	3.2
B	γ	600	30.4	3.1
B	γ	600	25.7	3.0
B	γ	800	43.4	3.5
B	γ	800	37.6	3.4
B	γ	800	41.7	3.5
B	γ	800	50.8	3.7
B	γ	800	22.2	2.8
B	γ	800	38.2	3.4
B	γ	800	31.8	3.2
B	γ	800	29.3	3.1
B	γ	800	39.5	3.4
B	γ	1000	29.1	3.1
B	γ	1000	37.9	3.4
B	γ	1000	46.3	3.6
B	γ	1000	25.9	3.0
B	γ	1000	21.7	2.8
B	γ	1000	19.4	2.7
B	γ	1000	35.5	3.3
B	γ	1000	34.7	3.3
B	γ	1000	40.9	3.4

Table 2-10. ANOVA result on shell weight of *Amphisorus hemprichii* in constant carbonate experiment with pCO_2 clone, and tank as fixed-effect factors.

Factor	*df*	*SS*[b]	*F*	*P*
pCO_2	4	1.4	6.3	**$<10^{-4}$**
Clone	2	23.4	213.3	**$<10^{-53}$**
Tank [pCO_2]	5	0.2	0.8	0.56
pCO_2 × Clone	8	1.4	3.2	**$<10^{-2}$**
Tank × Clone [pCO_2]	10	2.6	4.8	**$<10^{-5}$**
Error	249	13.7		

[a]Bold type signifies $P<0.05$.

[b]SS: Sum of squares.

Table 2-11. ANOVA result on shell weight of *Calcarina gaudichaudii* in constant carbonate experiment with pCO_2, clone, and tank as fixed-effect factors.

Factor	*df*	*SS*[b]	*F*	*P*
pCO_2	4	44.3	8.3	**$<10^{-5}$**
Clone	2	231.4	87.1	**$<10^{-29}$**
Tank [pCO_2]	5	6.0	0.9	0.48
pCO_2 × Clone	8	24.3	2.3	**0.02**
Tank × Clone [pCO_2]	10	11.6	0.9	0.56
Error	262	348.0		

[a]Bold type signifies $P<0.05$.

[b]SS: Sum of squares.

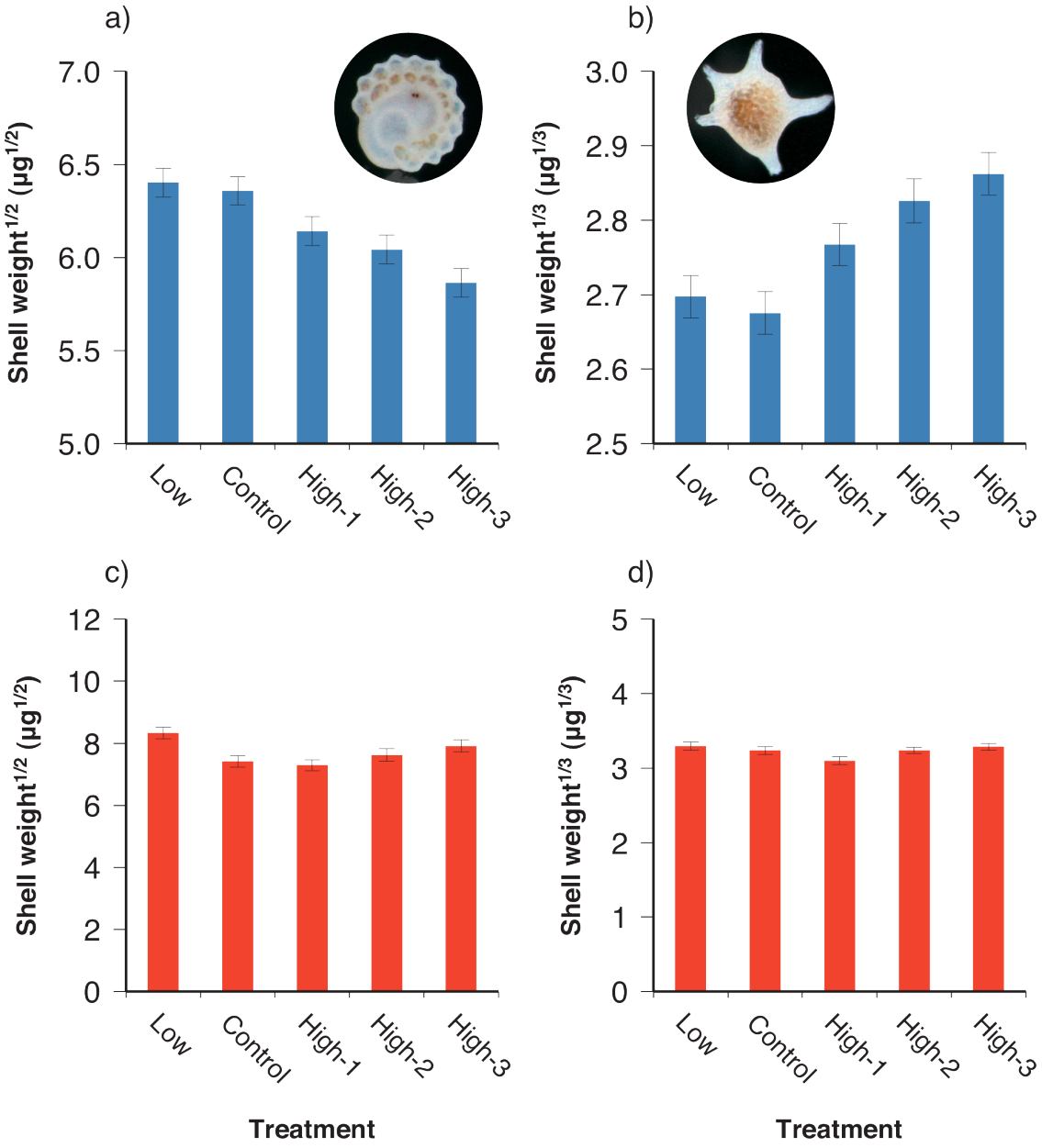

Fig 2-4. Least mean square (± standard error) adjusted for the rearing tank of a) the square root of the shell weight of *A. kudakajimensis* and b) the cube root of the shell weight of *C. gaudichaudii* after the ocean acidification experiment. Arithmetic mean (± standard error) of c) the square root of the shell weight of *A. hemprichii* and d) the cube root of the shell weight of *C. gaudichaudii* after the constant carbonate experiment.

2.4. Discussion

A decreasing trend of *A. kudakajimensis* skeletal weight with lower pH was previously reported by Kuroyanagi et al. (2009), who used the acid addition method. I thus confirmed the negative impact of ocean acidification on this species by performing a precise perturbation experiment using the gas-bubbling method, which more realistically simulates ocean acidification.

To shed light on the causes of the different calcification responses between *Amphisorus* (*A. kudakajimensis* and *A. hemprichii*) and *Calcarina* (*C. gaudichaudii*), I considered the combined results of the OA and CC experiments to evaluate which inorganic carbon species in seawater most affected calcification by foraminifers. As *Amphisorus* did not show any significant trend with higher pCO_2 or lower pH in the CC experiment, it is highly likely that the CO_3^{2-} concentration, and thus the saturation state of the seawater with respect to calcium carbonate (Ω), importantly influences calcification in *Amphisorus*.

Despite lower CO_3^{2-} and Ω, *Calcarina* showed an increase in net calcification with higher pCO_2 in the OA experiment, but like *Amphisorus*, no significant trend in the CC experiment. The two experiments were designed to have a similar bicarbonate ion concentration range (Figure 2-3), so the upward trend in the OA experiment can probably be attributed to the increase in CO_2, possibly through enhancement of symbiont photosynthesis, a phenomenon known as the CO_2-fertilizing effect (e.g., Ries et al., 2009). In the OA experiment pCO_2 increased by as much as 140% compared with the control, whereas in the CC experiment pCO_2 increased by only 30% (Table 2-1, Figure 2-5). The different responses of *Calcarina* between the two experiments may

have been due to this different pCO_2 gradient. A positive calcification response to ocean acidification has also been reported in coccolithophores (Iglesias-Rodriguez et al., 2008), which also calcify and photosynthesize simultaneously.

As one possible cause of these different sensitivities, I speculate that the type of symbiont influences the strength of the CO_2-fertilizing effect. *Calcarina* hosts diatoms as its symbiotic algae, whereas *Amphisorus* hosts dinoflagellates. Both a single-species culture experiment (Wu et al., 2010) and a mesocosm bloom experiment (Engel et al., 2008) have shown that high-CO_2 seawater is favorable to diatom growth. Moreover, Badger et al. (1998) pointed out that a rise in CO_2 may lead to enhanced phytoplankton growth owing to the low affinity of the carboxylating enzyme (Rubisco) for CO_2. Although it is difficult from my data to evaluate the importance of increased growth of the symbiont, it is possible that *Calcarina* acquires an increased amount of energy from its symbiotic diatoms under high pCO_2 conditions, leading to enhanced calcification. On the other hand, Rost et al. (2006) reported that dinoflagellates use HCO_3^- as their carbon source, so their rate of carbon fixation may remain unaffected by fluctuating CO_2 levels. Many laboratory studies of various coral species having dinoflagellates as their symbiotic algae have confirmed that coral calcification rates decrease with increasing pCO_2 (Doney et al., 2009); these results may indicate that the CO_2-fertilizing effect of dinoflagellates is weak, or that the dependence of *Amphisorus* on photosynthesis is low (Lee et al., 1991).

In conclusion, the results of my precisely CO_2-controlled culture experiment revealed that two genera of large benthic foraminifers, *Amphisorus* and *Calcarina*, showed contrasting net calcification responses, with *Calcarina* even showing enhanced calcification. Comparison of these results with those of a culture experiment under a

constant CO_3^{2-} concentration suggested that the negative response may be due to the decrease in CO_3^{2-} in the seawater, and the positive response to the increase in CO_2. I speculate that these different influences of seawater chemistry may be attributable to the different types of symbiotic algae hosted by *Amphisorus* and *Calcarina*.

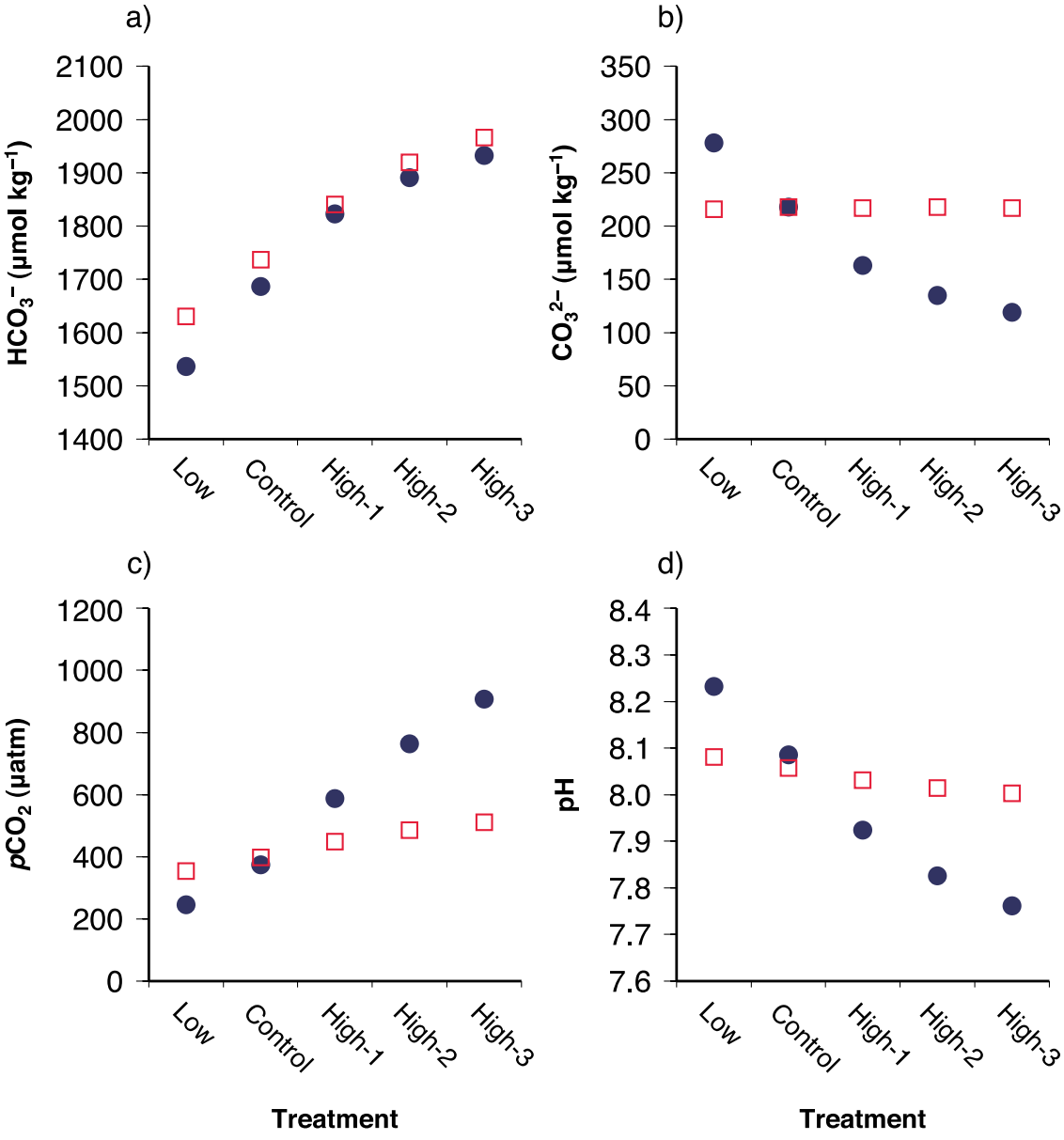

Figure 2-5. a) Bicarbonate and b) carbonate ion concentrations, c) pCO_2, and d) pH in the experimental seawater of each treatment in the ocean acidification (closed blue circles) and constant carbonate (open red squares) experiments.

2.5. Summary and Conclusion

In order to examine the effects of ocean acidification on foraminiferal calcification under possible near-future pCO_2 conditions, I cultured two algal symbiont-bearing, reef-dwelling foraminifers, *A. kudakajimensis* and *C. gaudichaudii*, in seawater under five different pCO_2 conditions, 245, 375, 588, 763 and 907 μatm, maintained with a precise pCO_2-controlling technique. My experimental results suggest that calcification responses of symbiont-bearing reef foraminifers to ongoing ocean acidification are not uniform trend. *A. kudakajimensis* tended to decrease mean shell weight with increasing seawater pCO_2. Conversely, mean shell weight of *C. gaudichaudii* generally increased as seawater pCO_2 elevated. Considering results of constant carbonate experiments showed no significant correlations between HCO_3^- and calcification, CO_3^{2-} concentration is possibly the most important factor among carbonate species for *Amphisorus* secreted imperforate shells, which host dinoflagellate. Therefore, calcification of *Amphisorus* is highly possible to be affected negatively according to ocean acidification for the next century. On the other hand, the different responses of *Calcarina* between the two experiments described that the most influence factor among seawater carbonate species for shell calcification of *Calcarina* is CO_2 concentration. Therefore the upward trend of *Calcarina* in the OA experiment can probably be attributed to the increase in CO_2, possibly through enhancement of symbiont photosynthesis.

Chapter 3

Effect of carbon isotope signature on larger benthic foraminiferal test: does it predict inter-species difference of tolerance to ocean acidification?

3.1. Introduction

Marine calcifiers face a credible threat from ocean acidification (e.g., Feely et al., 2004). Absorption of rising atmospheric CO_2 by the ocean has resulted in a decrease in the calcite saturation state of surface seawater (Ω_{cal}), making it more difficult to precipitate calcium carbonate in seawater. Some recent experimental studies have reported that marine calcifiers may show interspecific, or even intraspecific, differences in their calcification response to ocean acidification, although most studies have shown a consistent decline in calcification rates (Kroeker et al., 2013; Wittmann and Pörtner, 2013).

Experimental studies on large reef-dwelling benthic foraminifers, all performed in a high-precision pCO_2 control system using the same settings (AICAL system: Ohki et al., 2013; Kato et al., 2013), have shown that calcification rates of *Baculogypsina sphaerulata* and *Calcarina gaudichaudii*, which have hyaline test walls and are perforate species, increase with increasing seawater pCO_2, whereas those of *Amphisorus hemprichii* and *Amphisorus kudakajimensis*, which have porcelaneous test walls and are imperforate species, decrease (Hikami et al., 2011). The cause of this contrasting calcification response to ocean acidification between these two species groups is not attributable to methodological differences. Instead, the results suggest that the calcification response to high pCO_2 seawater differs among species, depending on the crystal structure of their tests (Fujita et al., 2011; Hikami et al., 2011). Another difference between these two groups is that *A. hemprichii* is host to dinoflagellate endosymbionts, whereas *B. sphaerulata* and *C. gaudichaudii* are host to diatom endosymbionts (Lee, 1998, 2006). As one possible cause of this different response to ocean acidification, I have speculated that there is a stronger CO_2 fertilizing effect in

perforate species harboring diatoms as their symbiont than in imperforate species (Hikami et al., 2011).

A CO_2 fertilizing effect of diatom species has been reported in a single-species culture experiment (Wu et al., 2010) and in a mesocosm bloom experiment (Engel et al., 2008); the results of both experiments showed that high pCO_2 seawater is favorable to diatom growth. In addition, Iglesias-Rodriguez et al. (2008) found a CO_2-fertilizing effect in the coccolithophore *Emiliania huxleyi*; the cell-specific calcification rate at a seawater pCO_2 of 750 μatm was double that at a pCO_2 of 300 μatm. Ries et al. (2009) also described a fertilization effect of photosynthesis on calcification in coralline red and calcareous green algae and in temperate corals harboring photosynthesizing symbionts. Thus, increased CO_2 levels in seawater may increase calcification rates by increasing the rate of photosynthesis.

Although the relationship between calcification and photosynthesis is complex in symbiotic systems, I can utilize the carbon isotope signature of carbonate skeletons to explore carbon metabolism. In a pioneering work, Erez (1978) first applied this approach to large reef-dwelling foraminifers, and then others extended it to planktonic foraminifers with and without symbionts in offshore environments (e.g., Wefer and Berger, 1980; Spero and DeNiro, 1987; Spero, 1992). The basic idea proposed by Erez (1978) has been confirmed by a series of reports on the isotope compositions of tests of relatively large reef-dwelling foraminifers from different tropical localities (e.g., Wefer et al., 1981; Langer, 1995; Saraswati et al., 2004). A similar approach has also been successfully applied to the investigation of carbon metabolism in symbiotic coral systems (Suzuki et al., 2003; Omata et al., 2008).

To investigate possible factors leading to different calcification responses to ocean

acidification, I analyzed the stable oxygen and carbon isotope compositions of tests from imperforate (*A. hemprichii*) and perforate (*B. sphaerulata* and *C. gaudichaudii*) foraminifer species cultured at five different pCO_2 levels for 12 weeks.

3.2. Materials and Methods

3.2.1. Foraminifera Incubation Experiment

I selected three species of large, algal symbiont-bearing benthic foraminifers, *Amphisorus hemprichii* Ehrenberg, *Baculogypsina sphaerulata* (Parker and Jones), and *Calcarina gaudichaudii* d'Orbigny in Ehrenberg, commonly found on reef flats in the northwest Pacific (e.g., Hohenegger, 1994), and they were collected from the subtidal zone (approximately 0.5 m in depth during low tide) of a reef flat northwest of Sesoko Island (26°39′ N, 127°51′ E), Okinawa, Japan (Figure 3-1). I cultured these foraminifers in five different seawater pCO_2 treatments (approximately 260, 360, 580, 770, and 970 μatm, corresponding to the estimated preindustrial pCO_2, the present value, and three IPCC SRES predicted values for 100 years hence, respectively (Meehl and Stocker, 2007), for 12 weeks at a constant water temperature (27.5 ± 0.1°C). All foraminifer individuals were clones produced asexually by a mature individual. Several of the cultured foraminifers from each treatment were randomly selected for stable isotope analysis. Further details of the collection and culture methods have been reported by Fujita et al. (2011).

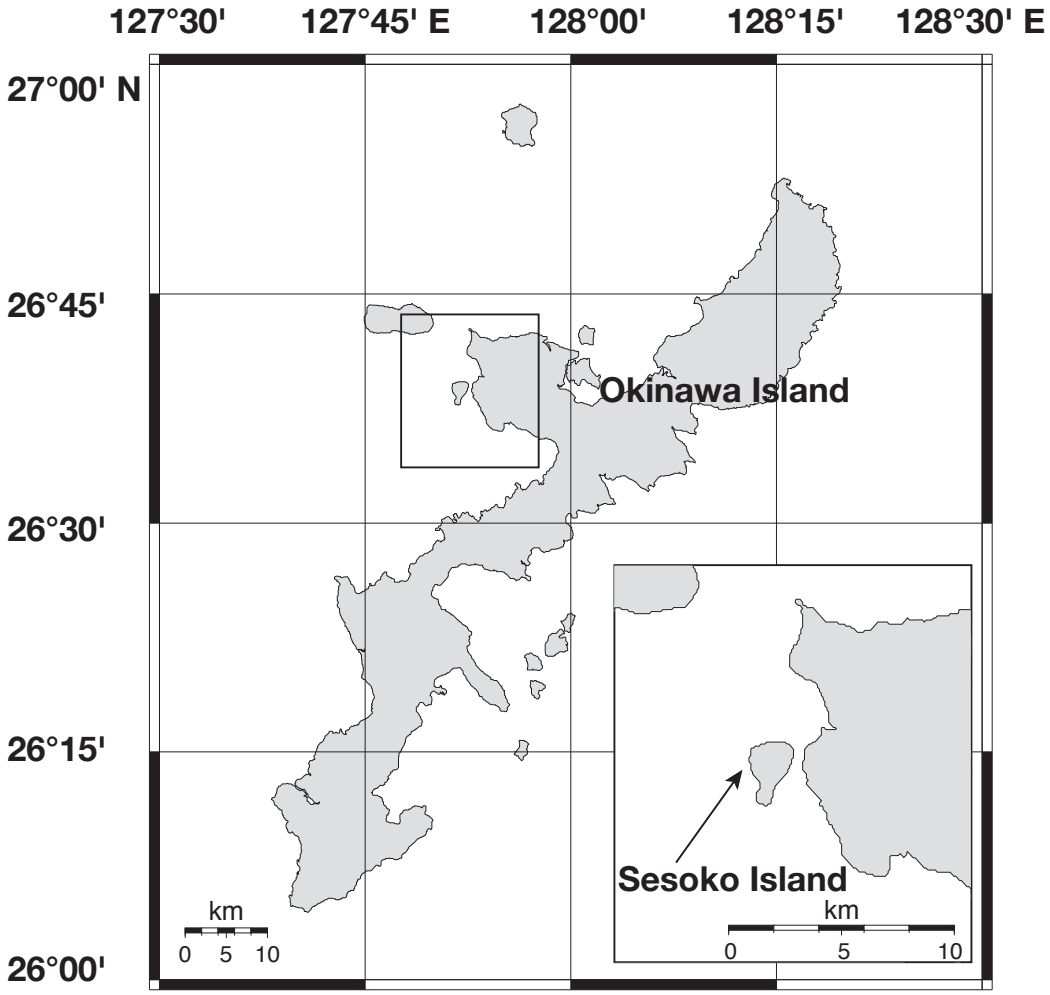

Figure 3-1. Location of sampling site (northwest of Sesoko Island).

3.2.2 Stable Isotopic Analysis of Foraminiferal Tests and Seawater

I used a continuous-flow isotope ratio mass spectrometry analytical system (Ishimura et al., 2004, 2008) at the Geological Survey of Japan (AIST, Tsukuba, Japan) to determine $\delta^{18}O$ and $\delta^{13}C$ values of single individual foraminifers. Isotopic data are reported as permil (‰) deviations relative to the Vienna Peedee Belemnite (V-PDB) standard. The NBS-19 international carbonate standard (U.S. National Bureau of Standards) was used for calibration of the V-PDB scale. The internal precision was < ±0.10‰ and < ±0.16‰ (1 SD) for $\delta^{18}O$ and $\delta^{13}C$, respectively.

The oxygen isotope ratio of water ($\delta^{18}O_w$) and the carbon isotope ratio of dissolved inorganic carbon ($\delta^{13}C_{DIC}$), together with the salinity, of discretely collected water samples were also measured. The $\delta^{18}O_W$ values are reported relative to V-SMOW (Vienna Standard Mean Ocean Water), and the $\delta^{13}C_{DIC}$ values are reported relative to V-PDB. The fractionation factors ε for carbonate species and calcite were taken from Mook (1986) and Erez and Luz (1983). The $\delta^{13}C$ values of carbonate species, along with variation in pH, were calculated following Wolf-Gladlow and Zeebe (2008). I used a $CaCO_3$–HCO_3^- $\delta^{13}C$ offset of about 1‰, taken from Romanek et al. (1992).

I used JMP statistical software (SAS Institute Inc.) for all statistical analyses. Statistically significant differences among the experimental treatments were determined by one-way factorial ANOVA followed by Tukey's HSD test. Significance (type I error level) was set at $\alpha = 0.05$. All data were assessed for normality and homogeneity.

3.3. Results and Discussion

3.3.1. Oxygen isotopic ratios of foraminiferal tests in Acidified Seawater

Temperature and seawater carbonate system parameters of each treatment,

including $\delta^{18}O_W$ and $\delta^{13}C_{DIC}$ of the ambient water in the experimental tanks, are shown in Table 3-1 and the isotopic composition of individual foraminiferal tests are shown in Table 3-2. In general, the oxygen isotope compositions of the foraminiferal tests ($\delta^{18}O_{shell}$) fell within a relatively small range, between –2.0‰ and 0.5‰, with no significant correlation with pCO_2 (Figure 3-2a), but more detailed examination found species-specific differences. $\delta^{18}O_{shell}$ of the heaviest species, *A. hemprichii,* varied from –0.80‰ to –1.73‰, with a mean of –1.16‰; $\delta^{18}O_{shell}$ data of *C. gaudichaudii* were scattered, varying from –0.90‰ to –2.10‰, with a mean of –1.46‰; and $\delta^{18}O_{shell}$ of the lightest species, *B. sphaerulata*, ranged from –1.25‰ to –2.66‰, with a mean of –1.84‰. These differences among species were significant after I controlled for the minor contribution of $\delta^{18}O_W$ variation among the treatments (Figure 3-3b).

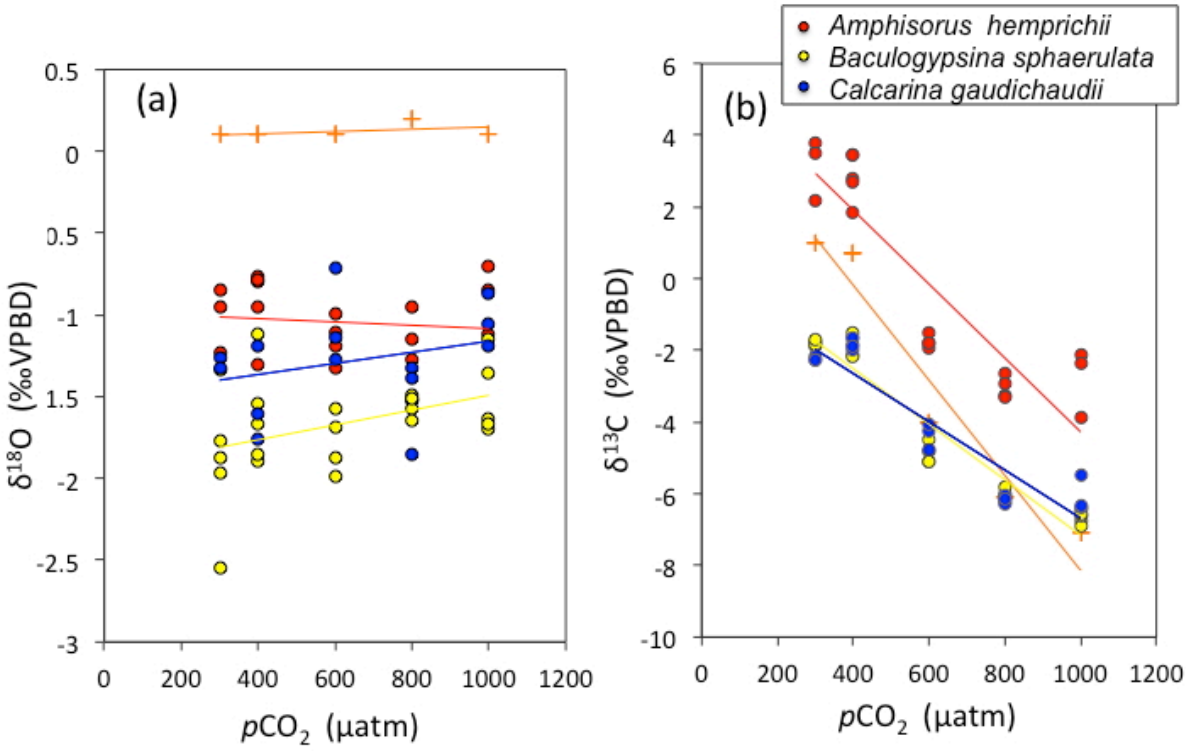

Figure 3-2 Oxygen isotope (a) and carbon isotope (b) ratios of three foraminifera test and cultured under five pCO_2 treatments (260, 360, 580, 770, and 970 µatm). Crosses in panel a and b represent oxygen isotope ratios of the ambient water ($\delta^{18}O_W$) and carbon isotope ratio of seawater DIC ($\delta^{13}O_{DIC}$), respectively.

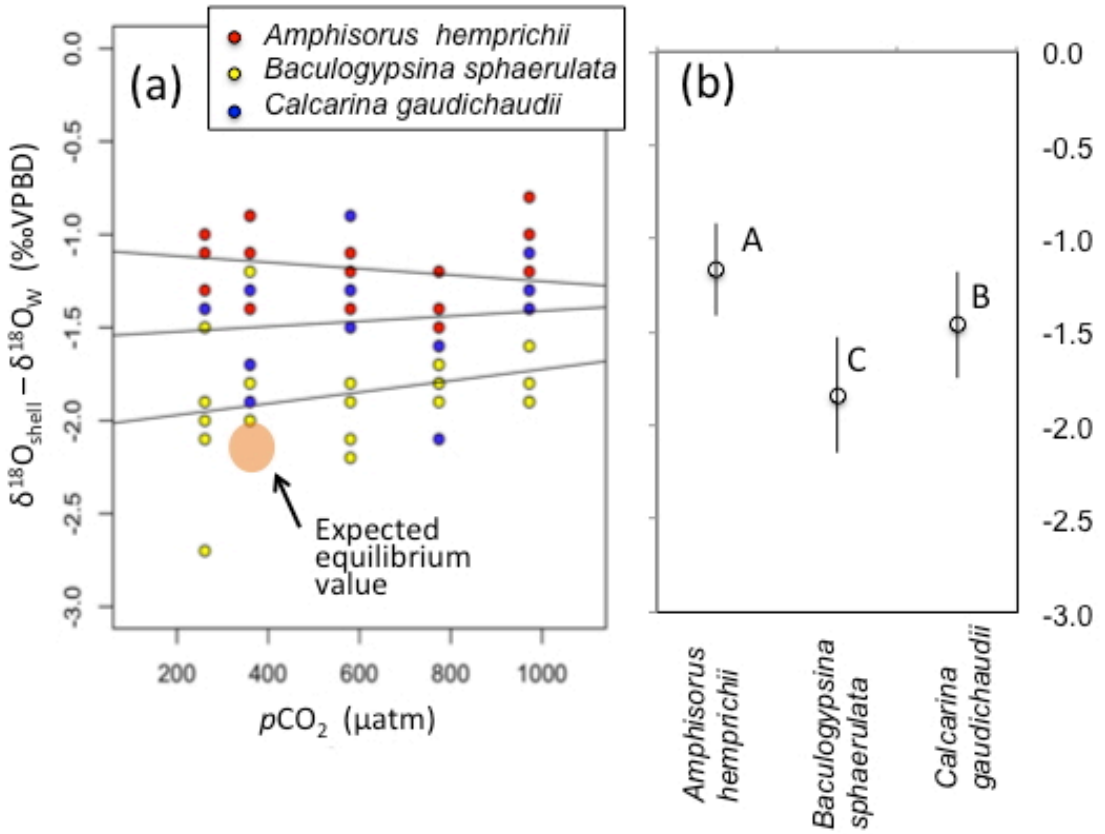

Figure 3-3 (a) Differences in the oxygen isotope ratio between tests ($\delta^{18}O_{shell}$) and ambient waters ($\delta^{18}O_W$) of three larger reef-dwelling foraminiferal species cultured under five different pCO_2 treatments (260, 360, 580, 770, and 970 µatm). The expected equilibrium value was calculated from the $\delta^{18}O_W$ of the control tank and an equation proposed by McConnoughe*y* (1989). (b) Means (± 1 SD) of pooled $\delta^{18}O_{shell}$ values of each of the three species tested. Different letters indicate a significant difference.

Table 3-1. Temperature and seawater carbonate system parameters of each treatment and $\delta^{13}C_{DIC}$ of ambient water in the experimental tanks.

Treatment	Temperature [°C]	pH_T at 25°C	pCO_2 [μatm]	DIC [μmol kg_{-1}]	Ωcal	$\delta^{13}C_{DIC}$ [‰]	$\delta^{18}O_w$ [‰]
Pre-industrial	27.5	8.170	261±29	1796	6.39	1.0	0.13
Present	27.4	8.072	360±19	1865	5.32	0.7	0.13
Future 1	27.5	7.926	580±30	1958	3.91	−4.0	0.18
Future 2	27.5	7.826	774±56	2007	3.18	−6.1	0.24
Future 3	27.6	7.756	972±43	2043	2.69	−7.1	0.20

Table 3-2 Carbon and oxygen isotopic compositions of foraminiferal tests cultured in each treatment. The first numeral of the sample number is the plate number, and the second numeral (after the hyphen) is the polyp number.

Sample no.	Species	pCO_2 [μatm]	weight [μg]	$\delta^{13}C_{shell}$ [‰]	$\delta^{18}O_{shell}$ [‰]	$\delta^{13}C_{shell} - \delta^{13}C_{DIC}$ [‰]	$\delta^{18}O_{shell} - \delta^{18}O_w$ [‰]
#A-1	*Amphisorus hemprichii*	261	45.0	2.16	−0.95	1.2	−1.1
#A-2	*Amphisorus hemprichii*	261	44.1	3.78	−1.24	2.8	−1.3
#A-3	*Amphisorus hemprichii*	261	44.7	3.49	−0.85	2.5	−1.0
#A-4	*Amphisorus hemprichii*	360	36.9	1.83	−1.31	1.1	−1.4
#A-5	*Amphisorus hemprichii*	360	35.2	2.81	−0.79	2.1	−0.9
#A-6	*Amphisorus hemprichii*	360	42.6	3.43	−0.76	2.7	−0.9
#A-7	*Amphisorus hemprichii*	360	39.9	3.45	−0.78	2.8	−0.9
#A-8	*Amphisorus hemprichii*	360	43.2	2.69	−0.95	2.0	−1.1
#A-9	*Amphisorus hemprichii*	580	42.6	−1.94	−1.32	2.1	−1.4
#A-10	*Amphisorus hemprichii*	580	39.9	−1.80	−1.19	2.2	−1.3
#A-11	*Amphisorus hemprichii*	580	34.4	−1.49	−1.10	2.5	−1.2
#A-12	*Amphisorus hemprichii*	580	50.2	−1.80	−0.99	2.2	−1.1
#A-13	*Amphisorus hemprichii*	774	24.0	−2.65	−1.15	3.5	−1.4
#A-14	*Amphisorus hemprichii*	774	29.9	−2.93	−1.28	3.2	−1.5
#A-15	*Amphisorus hemprichii*	774	24.1	−3.25	−1.53	2.9	−1.7
#A-16	*Amphisorus hemprichii*	774	34.9	−3.29	−0.95	2.8	−1.2
#A-17	*Amphisorus hemprichii*	972	33.4	−2.13	−0.70	5.0	−0.8
#A-18	*Amphisorus hemprichii*	972	35.6	−3.89	−0.85	3.2	−1.0
#A-19	*Amphisorus hemprichii*	972	37.6	−2.38	−1.11	4.7	−1.2
#C-1	*Calcarina gaudichaudii*	261	46.6	−2.18	−1.27	−2.2	−1.4
#C-2	*Calcarina gaudichaudii*	261	41.6	−2.27	−1.33	−2.3	−1.4
#C-3	*Calcarina gaudichaudii*	360	36.2	−1.63	−1.76	−1.6	−1.9
#C-4	*Calcarina gaudichaudii*	360	36.4	−1.97	−1.19	−2.0	−1.3
#C-5	*Calcarina gaudichaudii*	360	35.5	−1.87	−1.61	−1.9	−1.7
#C-6	*Calcarina gaudichaudii*	580	31.2	−4.24	−1.14	−4.2	−1.3
#C-7	*Calcarina gaudichaudii*	580	30.2	−4.04	−0.71	−4.0	−0.9
#C-8	*Calcarina gaudichaudii*	580	30.2	−4.76	−1.28	−4.8	−1.5
#C-9	*Calcarina gaudichaudii*	774	39.0	−6.03	−1.86	−6.0	−2.1
#C-10	*Calcarina gaudichaudii*	774	44.7	−6.27	−1.33	−6.3	−1.6
#C-11	*Calcarina gaudichaudii*	774	37.6	−6.17	−1.39	−6.2	−1.6
#C-12	*Calcarina gaudichaudii*	972	13.0	−6.36	−1.06	−6.4	−1.3
#C-13	*Calcarina gaudichaudii*	972	27.3	−5.48	−0.86	−5.5	−1.1
#C-14	*Calcarina gaudichaudii*	972	26.4	−6.35	−1.19	−6.4	−1.4
#B-1	*Baculogypsina sphaerulata*	261	18.2	−1.78	−1.87	−1.8	−2.0
#B-2	*Baculogypsina sphaerulata*	261	16.2	−1.88	−1.34	−1.9	−1.5
#B-3	*Baculogypsina sphaerulata*	261	17.0	−1.76	−1.97	−1.8	−2.1
#B-4	*Baculogypsina sphaerulata*	261	16.2	−1.84	−2.54	−1.8	−2.7
#B-5	*Baculogypsina sphaerulata*	261	16.5	−1.68	−1.77	−1.7	−1.9
#B-6	*Baculogypsina sphaerulata*	360	14.9	−2.12	−1.55	−2.1	−1.7
#B-7	*Baculogypsina sphaerulata*	360	16.4	−1.84	−1.90	−1.8	−2.0
#B-8	*Baculogypsina sphaerulata*	360	12.9	−2.18	−1.12	−2.2	−1.2
#B-9	*Baculogypsina sphaerulata*	360	14.7	−1.64	−1.66	−1.6	−1.8
#B-10	*Baculogypsina sphaerulata*	360	14.1	−1.52	−1.86	−1.5	−2.0
#B-11	*Baculogypsina sphaerulata*	580	19.3	−4.84	−1.58	−4.8	−1.8
#B-12	*Baculogypsina sphaerulata*	580	22.1	−5.08	−1.87	−5.1	−2.1
#B-13	*Baculogypsina sphaerulata*	580	22.3	−5.11	−1.69	−5.1	−1.9
#B-14	*Baculogypsina sphaerulata*	580	23.7	−4.51	−1.99	−4.5	−2.2
#B-15	*Baculogypsina sphaerulata*	774	21.5	−6.00	−1.49	−6.0	−1.7
#B-16	*Baculogypsina sphaerulata*	774	21.2	−6.23	−1.53	−6.2	−1.8
#B-17	*Baculogypsina sphaerulata*	774	18.8	−6.16	−1.57	−6.2	−1.8
#B-18	*Baculogypsina sphaerulata*	774	19.9	−5.81	−1.51	−5.8	−1.8
#B-19	*Baculogypsina sphaerulata*	774	18.4	−6.11	−1.64	−6.1	−1.9
#B-20	*Baculogypsina sphaerulata*	972	11.4	−6.74	−1.70	−6.7	−1.9
#B-21	*Baculogypsina sphaerulata*	972	15.6	−6.41	−1.15	−6.4	−1.3
#B-22	*Baculogypsina sphaerulata*	972	12.1	−6.91	−1.64	−6.9	−1.8
#B-23	*Baculogypsina sphaerulata*	972	11.2	−6.60	−1.66	−6.6	−1.9
#B-24	*Baculogypsina sphaerulata*	972	11.5	−6.56	−1.35	−6.6	−1.6

Temperature and δ^{18}Ow, which depends on salinity, are the major parameters that determine $\delta^{18}O$ values in foraminiferal tests (e.g., Urey, 1947; Emiliani, 1966; Shackleton, 1967). In this study, however, water temperature was held constant during the experimental period, and I corrected for the contribution from $\delta^{18}O_W$; thus, these parameters were excluded as possible causes of the observed variation in $\delta^{18}O$ of the foraminiferal tests. Tarutani et al. (1969) reported that $\delta^{18}O$ in Mg-calcite varied depending on the concentration of $MgCO_3$. They suggested that in Mg-calcite, $\delta^{18}O$ increased relative to that of pure calcite by 0.06‰ for each mol% $MgCO_3$ substituted in the crystal structure. All three species of this study have tests composed of Mg-calcite. Saraswati et al. (2004) reported that $MgCO_3$ concentrations in the tests of mature *A. hemprichii*, *B. sphaerulata*, and *C. gaudichaudii* individuals from a reef flat at Akajima, Okinawa, were 11.1, 10.9, and 9.7 mol %, respectively. Therefore, the $\delta^{18}O$ variation among these species may reflect, at least partly, the Mg content of their calcite tests.

Symbiont photosynthesis is expected to influence $\delta^{18}O$ values in tests of both planktonic and larger reef-dwelling symbiotic foraminifers. However, the observed $\delta^{18}O_{shell}$ values in this study were all close to equilibrium values, suggesting that the contribution of photosynthesis was minor. This result is consistent with the findings of previous studies on larger reef-dwelling foraminifers (Wefer et al., 1981; Langer, 1995; Saraswati et al., 2004).

Spero et al. (1997) reported that $\delta^{18}O$ of planktonic foraminifer tests decreases with increasing $[CO_3^{2-}]$ (CO_3^{2-} concentration in seawater). This carbonate-concentration effect suggests a possible influence of ocean acidification on $\delta^{18}O$ of test carbonate. In this study, however, I found no significant correlation between $\delta^{18}O$ and seawater pCO_2 or $\delta^{18}O$ and $[CO_3^{2-}]$ in any species (Figures 3-2a, 3-3a). Thus, within the narrow range

of [CO_3^{2-}] (111–264 μmol kg^{-1}) corresponding to predicted near-future levels of ocean acidification, I could not detect an influence of the carbonate ion effect on $\delta^{18}O$.

3.3.2. Carbon Isotopic Ratios of Foraminiferal Tests in Acidified Seawater

The carbon isotopic compositions of planktonic and benthic foraminiferal tests reflect, at least in principle, the $\delta^{13}C_{DIC}$ of the seawater, although they are also controlled by physiological processes such as respiration and symbiont photosynthesis (e.g., Spero, 1992). In tropical reef-dwelling foraminifers, Wefer et al. (1981) found a difference in the $\delta^{13}C$ shift from equilibrated precipitation between the foraminifer suborders Rottaliida and Miliolida: rottaliid species showed a larger $\delta^{13}C$ shift toward lighter values than miliolid species. This finding was subsequently confirmed by Langer (1995) and Saraswati et al. (2004). The tendency in the modern treatment (pCO_2 = 380 μatm) of my experiment was also consistent with this finding: $\delta^{13}C$ values of the rottaliid species *C. gaudichaudii* and *B. sphaerulata* were 2–3‰ more depleted than those of *A. hemprichii*, a miliolid species (Figure 3-2b). Further, *A. hemprichii* tests precipitated almost in equilibrium with the ambient $\delta^{13}C_{DIC}$ of the seawater, whereas $\delta^{13}C$ of tests of the two rottaliid species was lighter by as much as –4‰ relative to $\delta^{13}C_{DIC}$ of the seawater in the modern treatment (Figure 3-4a).

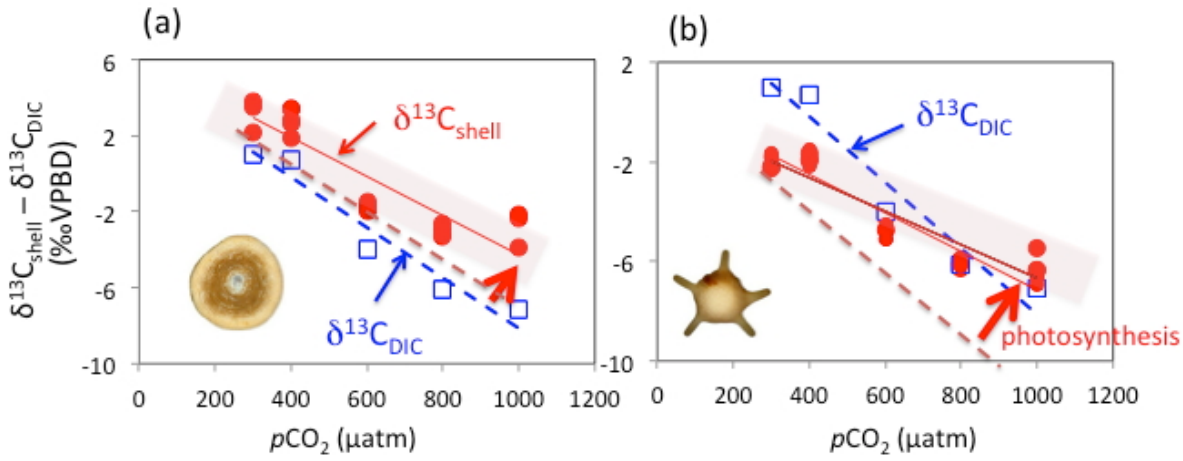

Figure 3-4 Relationship between the difference $\delta^{13}C_{shell} - \delta^{13}C_{DIC}$ and pCO_2 in (a) imperforate species and (b) perforate species. Mean carbon isotopic values ± 1 SD are shown for each species. Circles, *Amphisorus hemprichii*; triangles, *Calcarina gaudichaudii*; squares, *Baculogypsina sphaerulata*. The $\delta^{13}C_{shell} - \delta^{13}C_{DIC}$ of foraminiferal tests increased with as pCO_2 increased in all species, suggesting a CO_2 fertilization effect.

In my experiments, it was possible to examine $\delta^{13}C_{shell}$ variation over a wide range of pCO_2 (up to ~1000 µatm) because I could adjust pCO_2 and Ω_{cal} in each experimental tank by adding CO_2 gas from a commercially available liquefied CO_2 cylinder. $\delta^{13}C_{DIC}$ showed a considerable variation among the five treatments, ranging from –7.1‰ to 1.0‰ (Figure 3-2b, Table 3-1). This steep gradient of $\delta^{13}C_{DIC}$ across the five experimental tanks provided a unique opportunity to examine the carbon metabolism of complex foraminifer–symbiont systems. In the future treatments (pCO_2 = 580 µatm and above) of my experiment, the $\delta^{13}C_{shell}$ values in all three species increased as pCO_2 increased, showing that the $\delta^{13}C_{shell}$ values well reflected the $\delta^{13}C_{DIC}$ variations of the seawater (Figure 3-2b).

However, the slopes of the regression lines of $\delta^{13}C_{shell}$ and $\delta^{13}C_{DIC}$ against pCO_2 show notable differences: In all three species, the regression slope of $\delta^{13}C_{shell}$ is smaller than that of $\delta^{13}C_{DIC}$ on pCO_2, indicating that as pCO_2 increased, carbon isotope fractionation between seawater DIC and test carbonate also increased in all species (Figure 3-4). This ^{13}C enrichment of carbonate tests relative to $\delta^{13}C_{DIC}$ may be due to enhanced photosynthesis at higher pCO_2 (a CO_2 fertilization effect). In the CO_2 fertilization effect, a high seawater pCO_2 promotes photosynthetic activity and causes $\delta^{13}C_{shell}$ to increase by accelerating the preferential uptake of light carbon (^{12}C) by the symbiont, thus enriching the calcifying environment in ^{13}C (Spero and DeNiro, 1987).

The relationship between the difference $\delta^{13}C_{shell}$ minus $\delta^{13}C_{DIC}$ and seawater pCO_2 (Figure 3-5) revealed another contrast between the rottaliid and miliolid species. In the rottaliid species with diatoms as their symbiont (*C. gaudichaudii* and *B. sphaerulata*), ^{13}C enrichment of the test with increasing pCO_2 was accelerated compared with that in the miliolid species *A. hemprichii* with dinoflagellate endosymbionts. Hilami et al.

(2011) hypothesized that the different response to ocean acidification between these two foraminiferal suborders could be explained by that fact that perforate species harbor a diatom symbiont, which strengthens the CO_2 fertilization effect. Interestingly, this hypothesis is clearly supported by the carbon isotope evidence of the carbonate tests of perforate and imperforate species in this study.

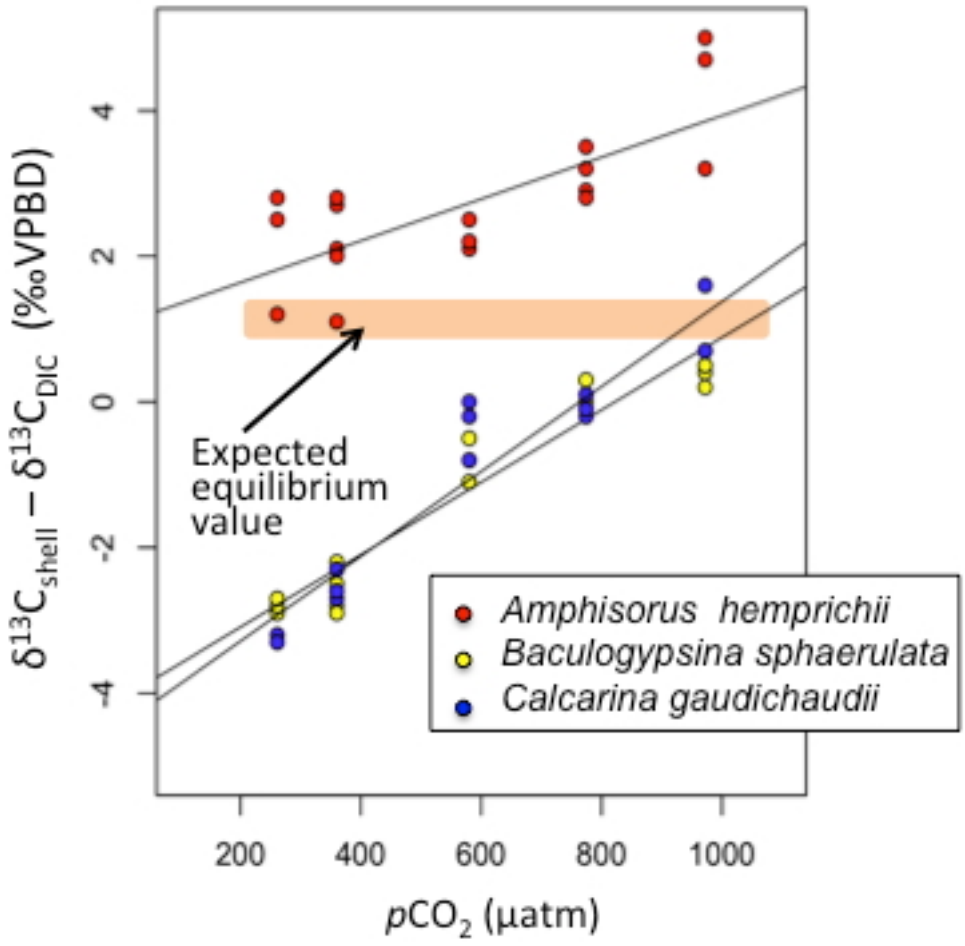

Figure 3-5. Relationships between $\delta^{13}C_{shell} - \delta^{13}C_{DIC}$ and pCO_2 in *A. hemprichii*, *B. sphaerulata*, and *C. gaudichaudii* cultured in five pCO_2 treatments. The expected equilibrium value was calculated from the $\delta^{13}C_{DIC}$ of the control tank and an equation proposed by Erez and Luz (1983).

3.3.3. Species-specific Tolerance to Ocean Acidification and Carbon Isotope Signature

In section 3.2, I pointed out two major differences in carbon metabolism between rottaliid and miliolid foraminifers, based on their $\delta^{13}C_{shell}$ values (Table 3-3): 1) a difference in the magnitude of the $\delta^{13}C$ shift at the modern pCO_2 level, and 2) a difference in the intensity of the CO_2 fertilization effect at higher pCO_2 levels. I have already discussed how the CO_2 fertilization effect might shape their tolerance to ocean acidification. Thus, I address here the magnitude of the $\delta^{13}C$ shift at the modern pCO_2 level, in particular the metabolic mechanisms of the two suborders, and I explore their possible connection to the observed species-specific tolerance to ocean acidification.

Table 3-3 Summary of the characteristics of two suborders of symbiotic reef-dwelling foraminifers. Data on the photosynthetic rate and the presence or absence of an internal carbon pool are from ter Kuile and Erez (1987), and data on tolerance to ocean acidification (OA) are from Hikami et al. (2011) and Fujita et al. (2011).

Suborder	Rottaliid	Miliolid
Representative species	*Calcarina gaudichaudii* *Baculogypsina sphaerulata*	*Marginopora kudakajimaensis* *Amphisorus hemprichii*
Test form	Perforate	Imperforate/porcelaneous
Endosymbiont	Diatom	Dinoflagellate
Internal carbon pool	Present	Absent
Photosynthetic rate	Large	Small
Carbon isotope offset (negative)	<2.5‰ to 3.0‰	>2.0‰ to 3.0‰
Tolerance to OA	Robust	Sensitive

$\delta^{13}C_{shell}$ of the cultured individuals of the perforate rottaliid species *B. sphaerulata* and *C. gaudichaudii* was at least 3‰ smaller than the equilibrium value of calcite (Figure 3-5). This negative offset probably reflects utilization of metabolic CO_2 for calcification. ter Kuile and Erez (1987) hypothesized that the perforate rottaliid species *Amphistegina lobifera* has an internal inorganic carbon pool for calcification. In follow-up studies, ter Kuile and Erez (1988, 1991) and ter Kuile et al. (1989a, 1989b) extended this hypothesis. They found that the internal pool contained not only dissolved carbon species derived directly from the ambient seawater but also dissolved carbon species that had been photoassimilated (^{13}C-depleted) by the symbionts and respired by the host. Therefore, they hypothesized that the $\delta^{13}C$ values of tests of perforate rottaliid species should be smaller.

In the present study, I found $\delta^{13}C_{shell}$ of *A. hemprichii* and $\delta^{13}C_{DIC}$ were in almost the same range, indicating equilibrated precipitation of tests of miliolid species (Figure 3-5). This result is well explained by the hypothesis of ter Kuile and Erez (1987) that miliolid species with imperforate tests have no internal carbon pool. ter Kuile (1991) reported that in imperforate species, the pH in vesicles, where calcite needles are precipitated, freely changes as the external pH changes.

The presence or absence of an internal carbon pool may be a key to whether a foraminifer can tolerate ocean acidification. I hypothesize that the calcification sites of miliolid species with imperforate tests are more permeable, and that calcification in those species is therefore more sensitive to seawater pH, compared with calcification in perforate rottaliid species. As a result, the decline of Ω_{cal} in ambient seawater due to ocean acidification might affect the calcification site of miliolid species and lead directly to decreased calcification. Fujita and Fujimura (2008) reported that in

imperforate species, but not in perforate species, biological dissolution might occur in the dark, because the pH of the surrounding seawater decreases at night owing to the release of CO_2 by host and symbiont respiration. The pH of the inorganic carbon pool in perforate species is not affected by the external pH because of a pH-regulating mechanism in the membrane of the pool (ter Kuile et al., 1991). Furthermore, a field survey of natural CO_2 seeps in the Mediterranean Sea showed that at a low-pH site (pH_T = ~7.78), miliolid species (imperforate) were absent whereas rottaliid species (perforate) were present (Dias et al., 2010). These lines of evidence all support a contrasting tolerance of rottaliid and miliolid species to ocean acidification.

3.4. Summary and Conclusions

In my previous culture experiment with reef-dwelling symbiotic benthic foraminifers, *Amphisorus hemprichii* (a miliolid species with imperforate tests) and *Baculogypsina sphaerulata* (a rottaliid species with perforate tests) showed increased and decreased calcification, respectively, at higher pCO_2 levels. In this study, I found that test $\delta^{13}C$ at the present-day pCO_2 level indicated that test precipitation in the imperforate species (*A. hemprichii*) almost in isotopic equilibrium with seawater DIC, whereas $\delta^{13}C$ of tests of perforate species (*B. sphaerulata*, *Calcarina gaudichaudii*) showed an evident negative shift, probably caused by more incorporation of ^{13}C-depleted metabolic carbon into their tests compared with the imperforate species. I hypothesize that calcification sites of imperforate species are more permeable, and thus that calcification in those species is more sensitive to seawater pH than calcification in perforate species. The carbon isotope signature of tests thus has the potential to reveal interspecies differences in the ocean acidification tolerance of symbiotic foraminifers.

Chapter 4

Impact of ocean acidification on two crustose coralline species

4.1. Introduction

Coralline algae (the orders Corallinales and Sporolithales in the subclass Corallinophycidae) are one of largest calcifying macroalgal group. Approximately 1600 nongeniculate species (more or less crustose forms, so-called crustose coralline algae or CCA) and 400 geniculate species (articulated forms with uncalcified segments) have been reported worldwide (Johansen 1981, Woelkerling 1988). Coralline algae are important components of benthic marine communities; they contribute to formation of coral reef structures and provide habitats for other organisms at the cold temperate to tropical shores, and also play roles as settlement or morphogenetic inducers for marine invertebrates around the world (e.g. Nelson 2009).

Recently coralline algae have been heavily investigated due to the potential impact of ocean acidification, which represents a reduction of pH and carbonate saturation caused by rising anthropogenic carbon dioxide (Koch et al. 2013). Many studies reported negative effects of elevated *p*CO2 on growth of coralline algae (e.g. Anthony et al. 2008, Hoffman et al. 2011, Diaz-Pulido et al. 2012). A decline in CCA abundance may affect recruitment of invertebrates and reef accretion and cementation (Anthony et al. 2008, Kleypas and Yates 2009). A cause of the negative effects is related to the solubility of coralline skeleton. Coralline algae contain calcium carbonate ($CaCO_3$) in 80 to 90% of the biomass (Bilan and Usov 2001) and deposit high magnesium calcite, in which Mg occupies ranging from 12.3 to 18.9 mol% $MgCO_3$ (Smith et al. 2012). Mg calcite with Mg substitution greater than about 12 mol% $MgCO_3$ is more soluble than aragonite (Andersson et al. 2008), which is precipitated by other calcifying macroalgae and corals (Okazaki et al. 1986, Lee and Carpenter 2001). Therefore, coralline algae are potentially vulnerable to ocean acidification compared to many other organisms.

Besides negative effects of elevated pCO_2 on coralline algae, however, there have been also reports of positive to no significant effects. In laboratory-based studies, increased photosynthetic rate was reported for *Hydrolithon* sp. (Semesi et al. 2009) and increased net calcification for *Neogoniolithon* sp. (Ries et al. 2009). Even in the field, at volcanic CO2 vent sites, only *Hydrolithon cruciatum* (Bressan) Y. M. Chamberlain was more abundant despite significant reduction in abundance of other coralline algae (Porzio et al. 2011). Photosynthesis and calcification is important physiological processes for growth of coralline algae, and use dissolved inorganic carbon (DIC: CO2, HCO3-, CO32-), of which speciation and subsequently the seawater carbonate system will be altered under ocean acidification. Therefore, effects of the acidification depend on the ability of species to modulate which carbon is utilized for the photosynthesis and subsequent growth along with their environments (Harley et al. 2012). For example, many macroalgae grown at the intertidal zone or rockpool can utilize bicarbonate by converting it to CO_2 for photosynthesis using carbon concentrating mechanisms (CCMs, Raven et al. 2012), whereas species at the subtidal or shaded intertidal zone rely on CO2 diffusion (Marconi et al. 2011). Nonetheless species with CCMs increase their use of CO_2 under the acidification condition, which may provide the advantage to them by reducing the energetic costs of using CCMs (Cornwell et al. 2012). However, there is few comparative study with more than one coralline species at the same treatments (e.g. Comeau et al. 2013b).

In relation to corals and coccolithophores, which also conduct photosynthesis and calcification for organism growth, the responses to acidified seawater are highly variable within species (Marubini et al. 2003, Fabry 2008, Langer et al. 2009, Iguchi et al. 2012), which likely has a genetic basis. Crustose coralline algae and other calcareous

red algae (e.g. Peyssonneliaceae) often harbor high levels of genetic variation within species or among closely related species, which have subtle or no significant morphological differences (Kato et al. 2011, 2013, Dixon and Saunders 2013). *Porolithon onkodes* (Heydrich) Foslie, which is known as a reef-building coralline species and is frequently used for experiments of acidification effects, is divided into at least two lineages even in the subtropical region of Japan (Kato et al. 2011). In this study, I have investigated species-level effects of acidification using genetically homogenous samples of two crustose coralline species, *Lithophyllum kotschyanum* Unger and *Hydrolithon samoense* (Foslie) Keats et Y. M. Chamberlain, which are commonly found in the shallow water in Pacific coral reefs. I have used a high-precision CO_2 partial pressure (pCO_2) control system to evaluate the effects of ongoing ocean acidification on growth rates and calcification under pre-Industrial Revolution, present and possible near-future pCO_2 conditions.

4.2. Materials and methods

4.2.1. Sample preparation

Two crustose species, *L. kotschyanum* and *H. samoense*, were collected at the upper sublittoral zones around Sesoko Island in Okinawa, Japan, in October 2010 (Fig. 4-1). Identification of these species followed descriptions presented in Yoshida and Baba (1998) and Harvey et al. (2006). Sixty fragments (less than 100mg) were cut from a single parent thallus and mounted to acrylic bolts with superglue to prevent exposure of the fracture surface of the fragments, and were treated as a clonal sample in order to eliminate genetic influences. The fragments were kept in a flow-through aquarium for 2 weeks under natural light conditions before the start of the experiment.

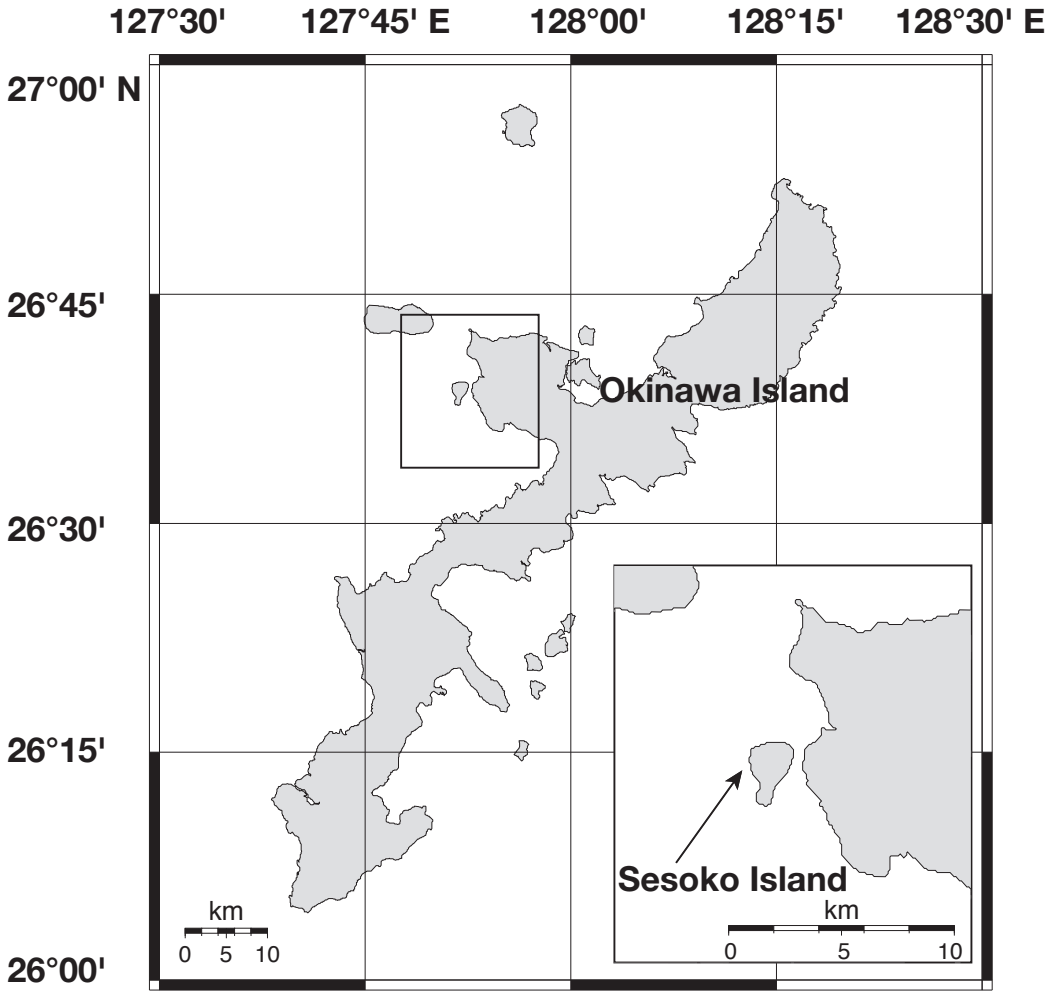

Figure 4-1. Location of sampling site (Sesoko Island).

4.2.2. Experimental set-up

L. kotschyanum and *H. samoense* samples were cultured at the Sesoko Station, University of the Ryukyus, Okinawa, Japan in seawater under three levels of pCO_2 (281 μatm representing conditions of the pre-Industrial Revolution; 418 μatm for the present; 1019 μatm for the end of this century) predicted by the Intergovernmental Panel on Climate Change (IPCC 2007) (Table 4-1). pCO_2-adjusted seawater was supplied to flow-through (150 ml min-1) aquaria systems (12 L) using a precise pCO_2 control

system (Fujita et al., 2011). Two replicate aquaria containing 10 samples of each species were used for each CO_2 treatment. The seawater temperature was maintained at 27˚C, with a 12:12 h light : dark photoperiod (40-60 μmol m2 s-1) under metal-halide lamps (Funnel2 150W, Kamihata, Japan) throughout all treatments. Seawater temperature, pH and light intensity were confirmed twice a week. Carbonate chemistry (pCO_2, HCO_3^-, CO_3^{2-}, CO_2) and carbonate saturation state ($\Omega_{calcite}$ and $\Omega_{aragonite}$) were calculated from total scale pH and total alkalinity at in situ temperature and salinity (34.1 μmol kg-1) using the CO2SYS software (Pierrot et al. 2006) and the carbonate dissociation constants of Mehrbach et al. (1973), refit by Dickson and Millero (1987) (Table 4-1).

Table 4-1. Summary of carbonate chemistry parameters and water temperature in the experimental treatments. Values are presented as averages. Numbers in parentheses are standard deviations.

Temperature (°C)	pH_T	TA (μmol kg^{-1})	pCO_2 (μatm)	HCO_3^- (μmol kg^{-1})	CO_3^{-2} (μmol kg^{-1})	CO_2 (μmol kg^{-1})	$\Omega_{calcite}$	$\Omega_{araonite}$
27.3 (0.2)	8.18 (0.06)	2224	281.1 (49.8)	1577.8 (60.8)	261.8 (24.4)	7.6 (1.3)	6.4 (0.4)	4.2 (0.4)
27.3 (0.1)	8.04 (0.03)	2224	418.3 (34.5)	1717.1 (30.2)	205.8 (12.1)	11.2 (0.9)	5.0 (0.3)	3.3 (0.2)
27.2 (0.2)	7.71 (0.06)	2224	1019.1 (153.8)	1952.7 (34.5)	110.5 (14.0)	27.4 (4.1)	2.7 (0.3)	1.8 (0.2)

4.2.3. Growth rate and calcification analysis

Growth rates of samples were determined by calculating the percentage increase of fresh weight during the experiment (8 weeks) relative to the initial weight. Fresh weights were measured with a microbalance (LIBROR AEM-5200, Shimadzu, Japan) after the samples were blotted dry with paper towels. To obtain an index of the change of calcification rate with change of pCO_2, I also examined walls of epithallial cells, which are the surface cells of the thallus and usually lack calcified outermost walls (Woelkerling, 1988). Calcified lateral walls of epithallial cells can therefore be easily recognized. Scanning electron microscope (SEM) observations of epithallial cells were made on five randomly selected samples for each pCO_2 and for each species. Samples were imaged with an SEM (JEOL, JSM-6390LV instrument) at the National Institute of Advanced Industrial Science and Technology (AIST), Japan, at an acceleration voltage of 15 kV. Samples were gold-coated to a thickness of 20 nm in preparation for SEM imaging. The cell wall as a fraction of the whole epithallial cell was quantified as follows; fifty random points were plotted on each of the SEM photos, and the points plotted on cell walls were counted. The ratio of the number of points on cell walls to the total points was used as a measure of the degree of calcification of cell walls in this study.

For determination of the Mg content of the calcareous algae, microsampling of the fragments from each thallus before the start of the experiment was conducted, and the resulting powders were then weighed (~100 μg each) prior to dissolution in 5 ml of 2% HNO_3. The Mg concentrations were measured by inductively coupled plasma atomic emission spectroscopy（IRIS Advantage, Thermo Electron Co., Ltd.）at the AIST. The precision, estimated by repeated measurements of the JCp-1 standard, was 0.17% (1

standard deviation) (Okai et al., 2002; Mishima et al., 2009).

4.2.4. Statistical analysis

For the analysis of the growth rate, I used a generalized linear model (GLM) with a normal error distribution and a log link function. It is appropriate for fitting skew data to a normal distribution, because no data alternation (e.g. logarithmic transformation) is used (Dobson, 2002). I used analysis of deviance on the GLM to test the changes in the growth rates of the two coralline species with increases in pCO_2, with two aquaria nested within pCO_2 levels. In the case of the ratio of the calcified cell wall, I used a generalized linear mixed effects model (GLMM) with a binomial error distribution and a logit link function (logistic regression model) adding a normally distributed random intercept term for each binomial count. This is a suitable approach for modeling a number of counts per total counts, when the sample size is under 20 (Warton and Hui, 2011). I then used analysis of deviance on the GLMM to evaluate whether there were differences in the changes of ratio in the calcification of cell walls with increases in pCO_2 between the two coralline species, where aquarium were partly nested within pCO_2 levels. The analyses of deviance were based on Type II Wald c^2 statistics. Furthermore, I calculated 95% credible intervals of the coefficients and regression curves based on the bootstrap samples. Model accuracy was assessed using deviance explained by the model that indicates the goodness of fit between the modeled values and the observed values, which substitute for R^2 (Dobson, 2002). The percent of deviance explained was calculated as the null deviance less the residual deviance as a proportion of the null deviance. Furthermore parameter estimates and 95% confidence intervals were calculated using a bootstrapping procedure with 10,000 permutations. All

analyses were conducted using the statistical software R 3.0.1 (R Development Core Team 2013). I used the function 'Anova' and 'Boot' in the package car and 'glm' in the package stats to carry out the GLM and bootstrap; I used 'glmer' and 'bootMer' in the package lme4 to implement the GLMM and bootstrap.

4.3. Results

ANCOVA including the differences of aquaria showed no significant effects on intercept and coefficients (Tables 4-2 and 4-4). For both *L. kotschyanum* and *H. samoense*, the growth rates decreased with increasing pCO_2 (Fig. 4-2 and Table 4-2), although intercept and coefficient of the regression lines were significantly different between the species. *L. kotschyanum* displayed four-times larger growth rate than *H. samoense* under all examined pCO_2 treatments, whereas the growth rate of *L. kotschyanum* declined sharply unlike that of *H. samoense* (Table 4-3). The analysis revealed that 59.9% of the growth rates data were explained by increasing pCO_2 and the difference of species (Adjusted R2 = 0.599). SEM images of the two species indicated that walls of epithallial cells (thallus surface cells) become thinner along with rising pCO_2 concentration (Fig. 4-3 and 4-4). In *L. kotschyanum*, calcification between epithallial cells was reduced and cracks (deep grooves) between epithallial cells were partly found under 1019 μatm, although boundaries (shallow grooves) between epithallial cells were visible under 281 and 418 μatm (Fig. 4-3). Whereas in *H. samoense*, boundaries or even cracks between epithallial cells were hardly found under any CO2 treatments (Fig. 4-3). Results of the analysis of deviance supported that calcification of epithallial cell walls reduced with pCO_2 concentration in both of the species (Fig. 4-3, Tables 4-4, 4-5, 4-6, and 4-7). Calcification of *H. samoense* was larger

than that of *L. kotschyanum* (difference in the intercept was significant), although decrease rate with pCO_2 concentration was not different between examined species. The analysis revealed that 30.6% of the growth rates data were explained by increasing pCO_2 and the difference of species (Deviance explained = 0.306).

Table 4-2. Results of analysis of deviance on the growth rate (wet weight after experiment / before experiment) as a function pCO_2 and examined species, with aquarium nested within pCO_2 level.

Parameter	c^2	df	*P*
pCO_2	44.1	1	<0.0001
Aquarium (pCO_2)	0.027	1	0.869
Species	125	1	<0.0001
Aquarium (Species)	1.26	1	0.262
pCO_2 × Species	12.6	1	<0.001
pCO_2 × Aquarium (Species)	0.068	1	0.794

Table 4-3. Parameter estimates and standard errors (SEs) of the generalized linear model with a normal error distribution and a log link function for explaining differences in growth ratio (after experiment / before experiment) due to pCO2 and examined species. Only significant parameters in the analysis of deviance (Table 4-2) were used for the model.

Parameter	Estimate	SE	*t*	*P*
Intercept of *L. kotschyanum*	1.78 x 10^{-1}	0.01	17.7	<0.0001
Coefficient of pCO_2	–1.17 x 10^{-4}	1.61 x 10^{-5}	–7.25	<0.0001
Difference for intercept of *H. samoense*	–1.27 x 10^{-1}	1.49 x 10^{-2}	–8.55	<0.0001
Difference for pCO_2 coefficient of *H. samoense*	8.48 x 10^{-5}	2.36 x 10^{-5}	3.60	<0.001

Table 4-4. Results of analysis of deviance on ratio of the calcified cell wall as a function pCO_2 level and examined species, where aquarium were partly nested within pCO_2 level.

Parameter	df	c^2	*P*
pCO_2	1	6.63	0.0101
Aquarium (pCO_2)	1	1.24	0.265
Species	1	5.65	0.0175
pCO_2 × Species	1	12.6	0.229

Table 4-5. Parameter estimates and standard errors (SEs) of generalized linear mixed effects model (GLMM) with a binomial error distribution and a logit link function for explaining the ratio of the calcified cell wall by pCO_2 and examined species. Only significant parameters in the analysis of deviance (Table 4) were used for the model.

Parameter	Estimate	SE	z	P
Intercept of *L. kotschyanum*	1.17	0.156	7.47	<0.0001
Coefficient of pCO_2	-5.30×10^{-4}	2.11×10^{-4}	–2.52	0.012
Difference for intercept of *H. samoense*	0.573	0.140	4.09	<0.0001

Table 4-6. Raw data of the weight and growth rate of *Lithophyllum kotschyanum*.

Tank #	Sample ID	Initial mean weight (mg)	Mean weight after 4 weeks (mg)	Growth weight from 1 to 4 weeks (mg)	Growth rate from 1 to 4 weeks (mg)	Growth weight from 5 to 8 weeks (mg)	Growth rate from 5 to 8 weeks (mg)	Mean weight after 8 weeks (mg)	Grow1h weight from 5 to 8 weeks (mg)	Growth rate from 1 to 8 weeks (mg)	SEM photo
1A	1	61.118	64.196	3.078	4.8%	0.328	0.5%	64.524	3.406	5.3%	
1A	2	56.423	57.377	0.954	1.7%	2.557	4.3%	59.934	3.511	5.9%	
1A	3	59.869	65.276	5.408	8.3%	−0.598	−0.9%	64.679	4.810	7.4%	
1A	4	56.097	62.731	6.634	10.6%	0.250	0.4%	62.981	6.884	10.9%	
1A	5	50.370	51.818	1.449	2.8%	0.649	1.2%	52.468	2.098	4.0%	
1A	6	63.176	65.242	2.067	3.2%	0.205	0.3%	65.447	2.272	3.5%	
1A	7	68.979	73.254	4.276	5.8%	2.807	3.7%	76.061	7.083	9.3%	
1A	8	58.559	62.258	3.699	5.9%	−2.379	−4.0%	59.879	1.320	2.2%	SEM
1A	9	38.883	39.153	0.270	0.7%	−0.550	−1.4%	38.602	−0.281	−0.7%	
1A	10	52.403	54.395	1.992	3.7%	0.519	0.9%	54.914	2.511	4.6%	
1B	51	72.473	74.815	2.341	3.1%	1.625	2.1%	76.439	3.966	5.2%	
1B	52	81.034	88.867	7.833	8.8%	−1.010	−1.1%	87.857	6.823	7.8%	
1B	53	71.483	78.335	6.851	8.7%	3.246	4.0%	81.581	10.098	12.4%	SEM
1B	54	69.555	76.511	6.955	9.1%	−1.549	−2.1%	74.962	5.407	7.2%	
1B	55	83.255	84.078	0.823	1.0%	1.106	1.3%	85.184	1.929	2.3%	
1B	56	47.009	48.289	1.280	2.7%	1.501	3.0%	49.789	2.781	5.6%	
1B	57	67.479	72.495	5.017	6.9%	0.913	1.2%	73.408	5.930	8.1%	
1B	58	74.515	80.364	5.849	7.3%	0.976	1.2%	81.340	6.825	8.4%	
1B	59	96.998	98.300	1.302	1.3%	−1.472	−1.5%	96.828	−0.170	−0.2%	
1B	60	61.457	64.591	3.135	4.9%	1.912	2.9%	66.503	5.047	7.6%	
4A	11	43.515	47.614	4.100	8.6%	3.187	6.3%	50.802	7.287	14.3%	
4A	12	49.075	57.895	8.821	15.2%	3.657	5.9%	61.552	12.478	20.3%	
4A	13	51.208	56.591	5.383	9.5%	2.436	4.1%	59.027	7.819	13.2%	
4A	14	53.476	57.394	3.918	6.8%	4.182	6.8%	61.576	8.100	13.2%	SEM
4A	15	51.120	57.472	6.352	11.1%	2.094	3.5%	59.566	8.446	14.2%	
4A	16	51.959	60.023	8.064	13.4%	0.218	0.4%	60.241	8.282	13.7%	
4A	17	58.287	61.702	3.415	5.5%	0.732	1.2%	62.434	4.148	6.6%	
4A	18	47.641	50.917	3.277	6.4%	1.345	2.6%	52.262	4.622	8.8%	
4A	19	42.085	48.620	6.535	13.4%	−1.232	−2.6%	47.388	5.303	11.2%	
4A	20	53.530	59.552	6.022	10.1%	4.089	6.4%	63.640	10.110	15.9%	
4B	41	51.088	56.671	5.583	9.9%	3.142	5.3%	59.814	8.725	14.6%	SEM
4B	42	44.971	51.968	6.997	13.5%	1.042	2.0%	53.010	8.039	15.2%	
4B	43	67.361	68.591	1.230	1.8%	−0.929	−1.4%	67.661	0.300	0.4%	
4B	44	63.137	67.311	4.174	6.2%	4.685	6.5%	71.996	8.859	12.3%	
4B	45	57.076	63.043	5.968	9.5%	5.821	8.5%	68.864	11.789	17.1%	
4B	46	64.887	71.760	6.873	9.6%	6.706	8.5%	78.466	13.580	17.3%	
4B	47	44.157	51.305	7.148	13.9%	1.709	3.2%	53.014	8.857	16.7%	
4B	48	69.688	77.257	7.569	9.8%	5.618	6.8%	82.875	13.187	15.9%	
4B	49	75.037	81.942	6.905	8.4%	1.017	1.2%	82.958	7.921	9.5%	
4B	50	68.547	77.309	8.763	11.3%	0.575	0.7%	77.884	9.338	12.0%	
5A	21	57.673	58.070	0.397	0.7%	4.425	7.1%	62.495	4.822	7.7%	
5A	22	59.629	65.212	5.583	8.6%	3.833	5.6%	69.045	9.416	13.6%	
5A	23	61.777	67.922	6.146	9.0%	2.663	3.8%	70.586	8.809	12.5%	
5A	24	43.411	45.752	2.341	5.1%	3.296	6.7%	49.048	5.637	11.5%	
5A	25	46.949	54.469	7.520	13.8%	2.297	4.0%	56.766	9.818	17.3%	
5A	26	36.456	35.610	−0.845	−2.4%	2.781	7.2%	38.391	1.936	5.0%	
5A	27	53.960	61.437	7.477	12.2%	1.105	1.8%	62.541	8.581	13.7%	SEM
5A	28	40.348	46.704	6.356	13.6%	6.090	11.5%	52.794	12.446	23.6%	
5A	29	56.735	61.137	4.402	7.2%	3.043	4.7%	64.180	7.445	11.6%	
5A	30	54.045	60.293	6.248	10.4%	2.224	3.6%	62.516	8.471	13.6%	
5B	31	67.413	74.704	7.291	9.8%	3.939	5.0%	78.643	11.230	14.3%	
5B	32	53.384	60.328	6.944	11.5%	4.791	7.4%	65.119	11.736	18.0%	
5B	33	69.521	76.813	7.292	9.5%	1.668	2.1%	78.481	8.960	11.4%	
5B	34	64.789	72.240	7.451	10.3%	1.094	1.5%	73.333	8.545	11.7%	
5B	35	49.358	53.013	3.655	6.9%	−0.757	−1.4%	52.256	2.898	5.5%	
5B	36	52.520	58.691	6.172	10.5%	2.122	3.5%	60.813	8.294	13.6%	
5B	37	62.623	67.124	4.501	6.7%	2.674	3.8%	69.798	7.175	10.3%	
5B	38	59.405	62.669	3.264	5.2%	2.915	4.4%	65.584	6.180	9.4%	
5B	39	55.286	55.542	0.256	0.5%	0.831	1.5%	56.373	1.087	1.9%	
5B	40	63.385	70.186	6.800	9.7%	4.872	6.5%	75.058	11.673	15.6%	SEM
	Min.	36.456		−0.845		−2.379			−0.281		
	Max.	96.998		8.821		6.706			13.580		
	mean	58.461		4.793		1.951			6.743		
	SE	1.5		0.3		0.3			0.5		

Table 4-7. Raw data of the weight and growth rate of *Hydrolithon samoense*.

Tank #	Sample ID	Initial mean weight (mg)	Mean weight after 4 weeks (mg)	Growth weight from 1 to 4 weeks (mg)	Growth rate from 1 to 4 weeks (mg)	Growth weight from 5 to 8 weeks (mg)	Growth rate from 5 to 8 weeks (mg)	Mean weight after 8 weeks (mg)	Grow1h weight from 5 to 8 weeks (mg)	Growth rate from 1 to 8 weeks (mg)	SEM photo
1A	1	119.444	122.278	2.834	2.3%	−1.378	−1.1%	120.899	1.455	1.2%	SEM
1A	7	161.563	163.946	2.383	1.5%	−0.248	−0.2%	163.698	2.136	1.3%	
1A	13	127.911	129.636	1.726	1.3%	−1.830	−1.4%	127.807	−0.104	−0.1%	
1A	19	104.872	107.777	2.905	2.7%	1.358	1.2%	109.135	4.263	3.9%	
1A	25	119.379	118.978	−0.401	−0.3%	0.190	0.2%	119.168	−0.211	−0.2%	
1A	31	85.106	84.827	−0.279	−0.3%	0.164	0.2%	84.991	−0.115	−0.1%	
1A	37	73.997	75.189	1.192	1.6%	3.101	4.0%	78.290	4.293	5.5%	
1A	43	88.016	88.742	0.725	0.8%	0.325	0.4%	89.066	1.050	1.2%	
1A	49	86.895	86.736	−0.159	−0.2%	−1.308	−1.5%	85.428	−1.467	−1.7%	
1A	55	56.191	55.209	−0.982	−1.8%	2.690	4.6%	57.899	1.708	2.9%	
1B	4	100.305	99.684	−0.622	−0.6%	0.869	0.9%	100.553	0.248	0.2%	
1B	10	143.232	146.366	3.135	2.1%	−0.618	−0.4%	145.748	2.517	1.7%	
1B	16	114.735	115.071	0.336	0.3%	1.465	1.3%	116.535	1.800	1.5%	
1B	22	119.119	121.503	2.385	2.0%	1.052	0.9%	122.555	3.436	2.8%	
1B	28	113.848	113.314	−0.535	−0.5%	1.953	1.7%	115.267	1.419	1.2%	
1B	34	65.375	66.257	0.882	1.3%	1.357	2.0%	67.614	2.239	3.3%	
1B	40	87.407	88.877	1.470	1.7%	1.277	1.4%	90.154	2.747	3.0%	
1B	46	74.808	75.046	0.238	0.3%	2.209	2.9%	77.255	2.447	3.2%	SEM
1B	52	72.654	73.294	0.640	0.9%	2.356	3.1%	75.650	2.996	4.0%	
1B	58	86.170	87.084	0.914	1.0%	0.979	1.1%	88.063	1.893	2.1%	
4A	2	204.770	206.196	1.426	0.7%	2.661	1.3%	208.858	4.088	2.0%	
4A	8	114.680	119.386	4.706	3.9%	2.674	2.2%	122.060	7.380	6.0%	
4A	14	125.615	126.485	0.870	0.7%	3.140	2.4%	129.625	4.010	3.1%	SEM
4A	20	117.380	118.119	0.739	0.6%	1.053	0.9%	119.172	1.792	1.5%	
4A	26	75.511	75.739	0.228	0.3%	3.210	4.1%	78.949	3.438	4.4%	
4A	32	70.361	72.240	1.880	2.6%	2.745	3.7%	74.986	4.625	6.2%	
4A	38	75.666	85.475	9.809	11.5%	1.971	2.3%	87.446	11.780	13.5%	
4A	44	94.654	93.776	−0.878	−0.9%	0.975	1.0%	94.752	0.098	0.1%	
4A	50	121.382	120.681	−0.701	−0.6%	2.136	1.7%	122.817	1.435	1.2%	
4A	56	64.073	65.593	1.520	2.3%	−0.618	−1.0%	64.975	0.902	1.4%	
4B	5	86.048	88.111	2.064	2.3%	3.154	3.5%	91.265	5.218	5.7%	
4B	11	87.236	87.615	0.379	0.4%	2.710	3.0%	90.325	3.089	3.4%	
4B	17	98.714	99.765	1.051	1.1%	4.110	4.0%	103.875	5.161	5.0%	
4B	23	115.763	115.966	0.203	0.2%	1.374	1.2%	117.340	1.577	1.3%	
4B	29	76.477	79.099	2.622	3.3%	3.862	4.7%	82.961	6.484	7.8%	
4B	35	82.442	84.330	1.888	2.2%	3.438	3.9%	87.768	5.326	6.1%	
4B	41	87.814	89.072	1.258	1.4%	3.112	3.4%	92.185	4.370	4.7%	
4B	47	104.810	108.319	3.509	3.2%	−1.022	−1.0%	107.298	2.488	2.3%	
4B	53	79.110	81.134	2.024	2.5%	1.309	1.6%	82.442	3.333	4.0%	
4B	59	78.475	79.421	0.945	1.2%	0.039	0.0%	79.459	0.984	1.2%	SEM
5A	3	83.004	83.235	0.231	0.3%	1.285	1.5%	84.520	1.516	1.8%	
5A	9	82.830	82.969	0.139	0.2%	1.548	1.8%	84.517	1.687	2.0%	
5A	15	73.567	73.100	−0.466	−0.6%	1.957	2.6%	75.057	1.490	2.0%	
5A	21	101.540	102.682	1.142	1.1%	1.143	1.1%	103.825	2.285	2.2%	
5A	27	106.352	106.157	−0.195	−0.2%	2.040	1.9%	108.197	1.845	1.7%	
5A	33	94.956	97.587	2.630	2.7%	−1.885	−2.0%	95.702	0.745	0.8%	
5A	39	108.986	108.764	−0.222	−0.2%	2.818	2.5%	111.582	2.596	2.3%	SEM
5A	45	96.087	95.619	−0.469	−0.5%	2.746	2.8%	98.365	2.277	2.3%	
5A	51	74.938	76.069	1.131	1.5%	0.003	0.0%	76.072	1.134	1.5%	
5A	57	87.547	86.715	−0.832	−1.0%	2.329	2.6%	89.044	1.497	1.7%	
5B	6	169.218	174.139	4.921	2.8%	4.455	2.5%	178.594	9.376	5.2%	
5B	12	73.190	73.808	0.618	0.8%	3.518	4.5%	77.327	4.137	5.3%	
5B	18	97.833	98.501	0.669	0.7%	4.184	4.1%	102.685	4.852	4.7%	
5B	24	92.776	94.280	1.504	1.6%	3.411	3.5%	97.691	4.915	5.0%	
5B	30	109.999	112.622	2.623	2.3%	−0.110	−0.1%	112.512	2.513	2.2%	
5B	36	79.404	82.780	3.376	4.1%	4.710	5.4%	87.490	8.086	9.2%	
5B	42	86.653	87.359	0.706	0.8%	2.798	3.1%	90.157	3.504	3.9%	
5B	48	94.054	94.519	0.466	0.5%	2.189	2.3%	96.709	2.655	2.7%	
5B	54	59.341	62.341	3.000	4.8%	1.765	2.8%	64.105	4.765	7.4%	
5B	60	52.348	55.307	2.959	5.4%	1.356	2.4%	56.663	4.315	7.6%	SEM
	Min.	52.348		−0.982		−1.885			−1.467		
	Max.	204.770		9.809		4.710			11.780		
	mean	96.444		1.304		1.671			2.975		
	SE	3.5		0.2		0.2			0.3		

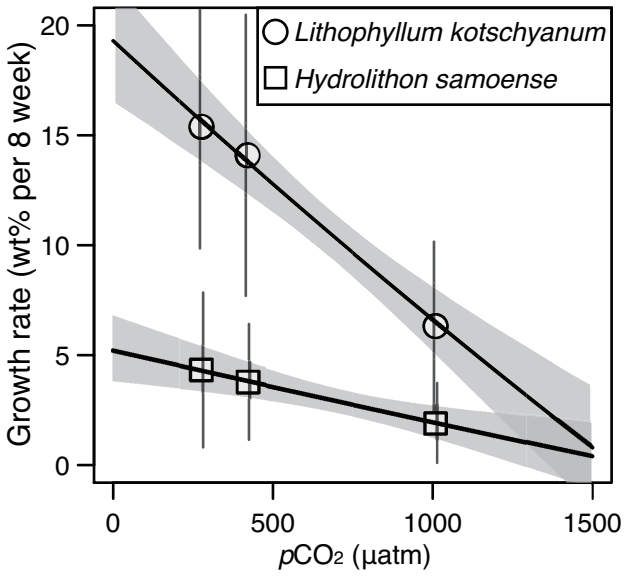

Fig. 4-2. Growth rate (mean ± standard deviation) of *Lithophyllum kotschyanum* and *Hydrolithon samoense*, shown on a percent scale. The regression curves and 95% confidence intervals are shown in solid lines and in gray bands, respectively. The statistical analysis was conducted on the basis of ratios: see Table 4-2 and 4-3.

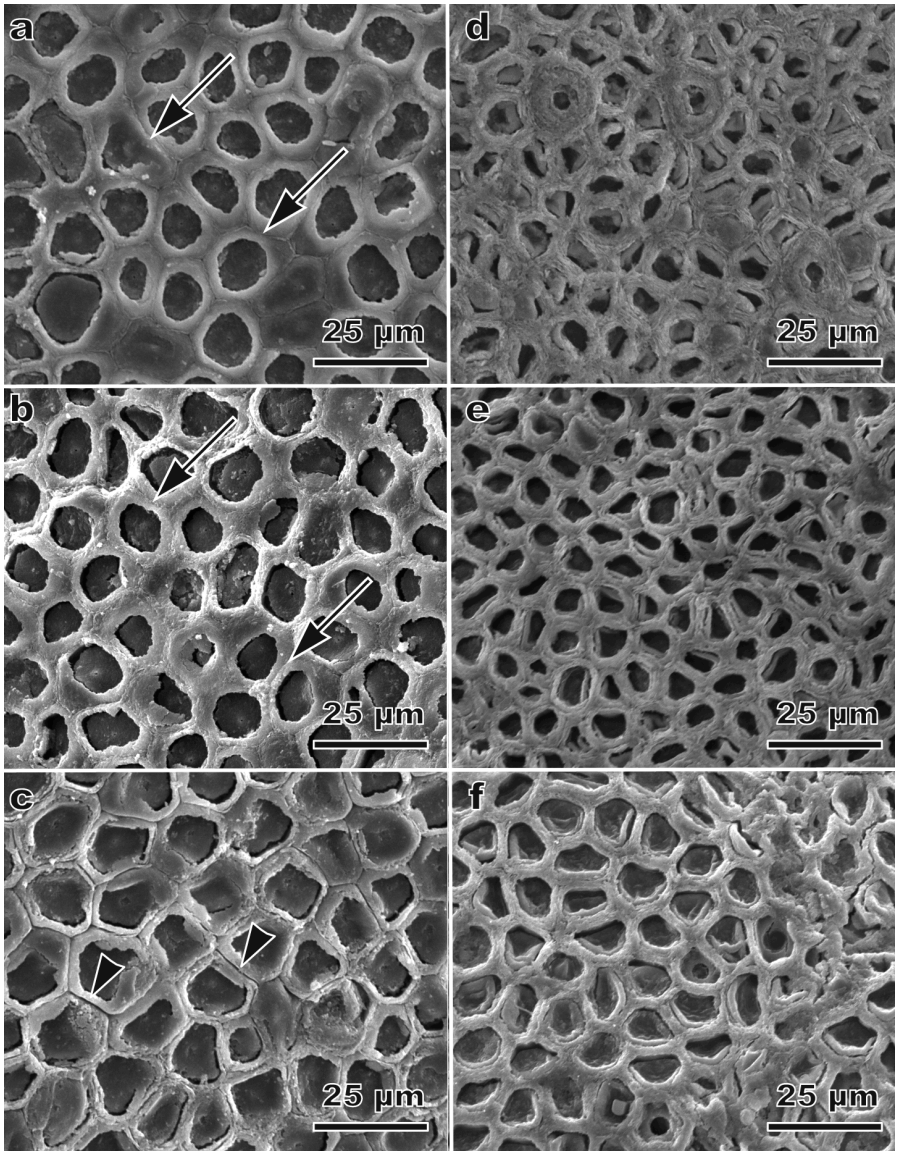

Figure 4-3. SEM micrographs of epithelial cells from the thallus surface of *Lithophyllum kotschyanum* (a, b, c) and *Hydrolithon samoense* (d, e, f) following 8 weeks exposure to pre-industrial (281 μatm, a, d), control (418 μatm, b, e) and high pCO_2 (1019 μatm, c, f). Arrows indicate boundaries (shallow grooves) between epithallial cells, and arrowheads indicate cracks (deep grooves) between epithallial cells.

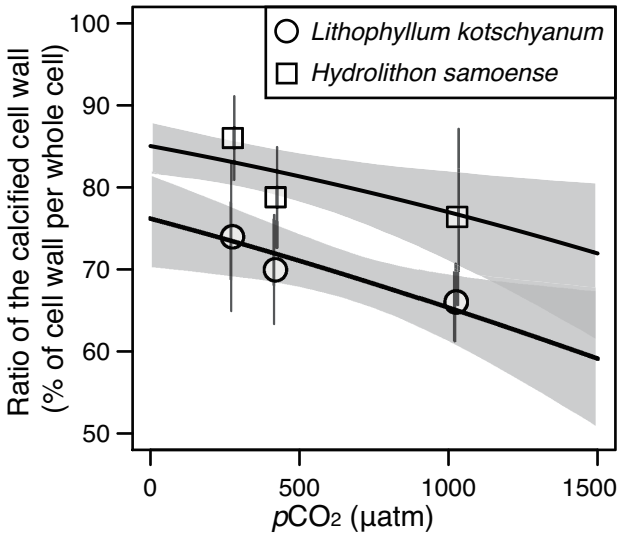

Figure 4-4. The ratio of the calcified cell wall (mean ± standard deviation) in *Lithophyllum kotschyanum* and *Hydrolithon samoense*, shown on a percent scale. The regression curves and 95% confidence intervals are shown in the solid lines and in gray bands, respectively. The statistical analysis was conducted on the basis of ratios: see Tables 4-4 and 4-5.

4.4. Discussion

This study confirmed that the species-level difference in acidification effects on CCA using genetically homogenous samples for the first time, and also indicates that elevated pCO_2 caused the reduction in the growth rates and the calcification of epithallial cell walls on *L. kotschyanum* and *H. samoense*. The growth rate of coralline species under high pCO_2 condition varied from positive to negative but often showed negative results on several species under around or greater than 1000 μatm (Koch et al.

2013). In my study, the growth of *L. kotschyanum* was strongly inhibited by elevated pCO_2 compared to that of *H. samoense*. The calcification of cell walls was also impaired by high pCO_2, which has been reported for *Corallina officinalis* Linnaeus (Hofmann et al. 2012) and *Lithothamnion glaciale* Kjellman (Burdett et al. 2012, Ragazzola et al. 2012). In my study, the decreasing trend in calcification of the epithallial cell walls was not different between examined species. However, cracks between epithallial cells were observed in *L. kotschyanum* under 1019 μatm as observed in Burdett et al. (2012), whereas they were hardly found in *H. samoense*. Moreover, calcification of epithallial cell walls in *L. kotschyanum* was lower than that of *H. samoense*. These differences between species may indicate that the susceptibility of *L. kotschyanum* to ocean acidification is higher than that of *H. samoense*.

It is unclear why the difference of susceptibility to high pCO_2 between species was observed in the growth rates. Most of coralline biomass is calcium carbonate and thus calcification is an important physiological process as well as photosynthesis. Although several calcification models of coralline algae have been proposed (Mori et al. 1996, McConnaughey and Whelan 1997, Comeau et al. 2013a, Koch et al. 2013), they are consistent with respect to creating favorable pH and carbonate ion concentration for calcification by ion transport related to CCMs utilizing bicarbonate to convert it to CO_2 for photosynthesis. The increasing in bicarbonate concentrations by ocean acidification dose not adversely affect coralline photosynthesis (Comeau et al. 2013a), therefore, negative responses of coralline growth to acidified conditions might be caused by increased dissolution due to the decreasing in carbonate ion concentration and lowering carbonate saturation state (Roleda et al. 2012, Egilsdottir et al. 2012, Comeau et al. 2013a). Therefore, the susceptibility of coralline algae under future ocean acidification

will be closely related to their carbonate. In my study, calcification between epithallial cells in *L. kotschyanum,* unlike that in *H. samoense*, was apparently reduced under high pCO_2 condition, despite the fact that the reduction in surface area (= calcification) of epithallial cell walls was not different between examined species. Additionally, high growth rate may also have solubility effects on coralline carbonate, because *L. kotschyanum* grew four-times faster than *H. samoense*. Moreover, coralline carbonate crystals differ between subfamilies (Fragoso et al. 2010), of *L. kotschyanum* and *H. samoense*, are the subfamilies Lithophylloideae and Mastophoroideae, respectively. Considering these factors, carbonate in *L. kotschyanum* might be more soluble than that in *H. samoense*. Nonetheless, further research on the relationship among the growth rate, phylogenetic position, and the solubility of carbonate is needed.

In terms of carbonate minerals, coralline algae precipitate high Mg-calcite, and they are comprised of 12.3-18.9 mol% $MgCO_3$ (Smith et al. 2012). Although the solubility of Mg-calcite at about 12-15 mol% $MgCO_3$ is larger than those at 0-20 mol% $MgCO_3$, the solubility could be organism specific rather than Mg content (Morse et al. 2006). In my study, *L. kotschyanum* (22.2 mol% $MgCO_3$) appear to be more soluble than H. samoense (17.7 mol% $MgCO_3$). Besides Mg-calcite, some samples of *P. onkodes* have been reported to have dolomite ($Mg0.5Ca0.5(CO_3)$), which is a magnesium-rich and stable carbonate. Dried dolomite-rich (17.3-18 mol% $MgCO_3$) *P. onkodes* have six times lower rates of dissolution than predominantly Mg-calcite one (16.3-17.5 mol% MgCO3) under high pCO_2 (less than 700 ppm) conditions (Nash et al. 2013). At least high latitude surface seawater will become undersaturated with respect to Mg-calcite phases containing 12 mol% and higher MgCO3 by the year 2100 (Andersson et al. 2008). Further research using more than one species at both mineralogical and

ecophysiological aspects are needed at several regions of the world.

The species-level susceptibility of coralline algae to ocean acidification may probably change interactions between coralline algae and other organisms and shuffle distributions of these species. Coralline algae offer inductive settlement cues for planktonic invertebrate larvae (Rodriguez et al. 1993, Diaz-Pulido et al. 2010). There are several investigations on coral larvae that their settlements (i.e. attachment and metamorphosis) are reduced as pCO_2 increases (e.g. Nakamura et al. 2011, Doropoulos et al. 2012). Although percentage metamorphosis of coral larvae (Acropora millepora) on one of my examined species *L. kotschyanum* (22.8±9.2%) is lower than those of *P. onkodes* (as *Hydrolithon onkodes* (Heydrich) Penrose et Woelkerling, more than about 80%) and *Mesophyllum* sp. (about 90%) (Heyward and Negri 1999). However, pCO_2 increases have also been demonstrated to affect the preferences of coral larvae for settlement substrate (species) (Doropoulos et al. 2012), and also change bacterial assemblages on coralline algae (Webster et al. 2013). Moreover, coralline algae inhabit the various depth ranges from the intertidal and subtidal zone to the deepest depths recorded for marine algae (e.g. Kleypas and Yates 2009). Coralline algae inhabiting intertidal rock pool are relatively robust to elevated pCO_2 within its natural range of variability (up to 1000μatm), probably because it may already have adapted to such levels of pCO_2 (Egilsdottir et al. 2012). *H. samoense*, examined in my study, exhibited a slower growth rate and higher tolerance to elevated pCO_2 than *L. kotschyanum*, which might be related to that *H. samoense* can grow at the intertidal zone where is emergent at low tide in Okinawa, Japan. To investigate how the species-level susceptibility to local and global environmental stresses affect community structures and ecosystem function, better understandings of species interactions and coralline distributional

ranges are needed.

4.5. Summary and Conclusion

In this study, in order to eliminate genetic influences, I used genetically homogenous samples of two crustose coralline species common to Pacific coral reefs, *Lithophyllum kotschyanum* Unger and *Hydrolithon samoense* (Foslie) Keats et Y. M. Chamberlain, and evaluated acidification effects under three pCO_2 levels (281 μatm representing conditions of the pre-Industrial Revolution; 418 μatm, present; 1019 μatm, the end of this century). The growth rate and the calcification of epithallial cell (thallus surface cell) walls of both species decreased with pCO_2 concentration. However, the growth of *L. kotschyanum* was strongly inhibited by elevated pCO_2 compared to that of *H. samoense*. Whereas the decrease trend in calcification of epithallial cell walls was not different between examined species, although calcification between epithallial cells in *L. kotschyanum* was apparently reduced under elevated pCO_2. These results might indicate that carbonate in coralline skeleton was closely related to the species-level susceptibility of coralline algae to ocean acidification.

5. General conclusion

In order to examine the effect of oceanic acidification on marine organisms, I investigated the calcification responses of coral reef calcifiers through the culturing experiments.

Large benthic foraminifera are important producers of carbonate in tropical and subtropical shallow-water areas. Also, they are important producers of organic matter. My results suggest that calcification rates of *B. sphaerulata* and *C. gaudichaudii* that have a hyaline test wall and belong to perforate species are increased with rising pCO_2 in seawater, whereas those of *A. kudakajimensis* that have a porcelaneous test wall and belong to imperforate species were decreased. In another culture experiment conducted in seawater in which bicarbonate ion concentrations were varied under a constant carbonate ion concentration, calcification was not significantly different between treatments in *Amphisorus hemprichii*, a species closely related to *A. kudakajimensis*, or in *C. gaudichaudii*. From these results, I concluded that carbonate ion and CO_2 were the carbonate species that most affected growth of *Amphisorus* and *Calcarina,* respectively. The cause of the observed contrasting calcification response to ocean acidification between two species may not be attributed to methodological differences for each species. They have another difference of endosymbionts between two groups: *A. hemprichii* is host to dinoflagellate endosymbionts, whereas *B. sphaerulata* and *C. gaudichaudii* are hosts to diatom endosymbionts. As one possible cause of the different response to ocean acidification, I speculated that the perforate species harboring diatom as their symbiont algae influences the strength of a CO_2 - fertilizing effect.

Although the relationship of calcification and photosynthesis is complex in symbiotic systems, I can utilize carbon isotope signature of their carbonate skeleton to

explore carbon metabolism. To investigate the factors leading to different calcification response to ocean acidification, I analyzed the stable oxygen and carbon isotope compositions of the two groups of foraminifer's tests: *A. hemprichii* (imperforate species), *B. sphaerulata* and *C. gaudichaudii* (perforate species) subjected to five different pCO_2 conditions for twelve weeks. Shell $\delta^{13}C$ of the present pCO_2 condition indicated that imperforate species precipitated their tests under almost isotopic equilibrium with respect to dissolved inorganic carbon in seawater, and that perforate species showed an evident negative shift, probably caused by more incorporation of ^{13}C-depleted metabolic carbon into their test compared to the imperforate species. I hypothesize that calcification sites of imperforate species are more permeable, and thus calcification of that species is more sensitive to seawater pH compared to perforate species. Carbon isotope signature of tests has the potential to reveal inter-species difference in ocean acidification tolerance of symbiotic foraminifers.

Coralline algae are one of largest calcifying macroalgal group, and play a role as important reef-building organisms and settlement or morphogenetic inducers for marine invertebrates. In this study, in order to eliminate genetic influences, I used genetically homogenous samples of two crustose coralline species common to Pacific coral reefs, *Lithophyllum kotschyanum* and *Hydrolithon samoense*, and evaluated acidification effects under three pCO_2 levels (pre-Industrial Revolution, present, and the end of this century). The growth rate and the calcification of epithallial cell (thallus surface cell) walls of both species decreased with pCO_2 concentration. However, the growth of *L. kotschyanum* was strongly inhibited by elevated pCO_2 compared to that of *H. samoense*. Whereas the decrease trend in calcification of epithallial cell walls was not different between examined species, although calcification between epithallial cells in *L.*

kotschyanum was apparently reduced under elevated pCO_2. These results might indicate that carbonate in coralline skeleton was closely related to the species-level susceptibility of coralline algae to ocean acidification.

My results suggest that ocean acidification should be a severe threat to reef calcifying organisms such as large benthic foraminifers and calcareous algae. Their calcification rates are certainly reduced in the acidified seawater despite a positive response of some foraminiferal taxa (e.g., perforate species such as *B. sphaerulata* and *C. gaudichaudii*). It would be caused by the differences of their symbiont algae (i.e., CO_2 - fertilizing effect) and calcification mechanism (i.e., permeable to outer seawater). Out results also propose that carbon isotope signature of tests has the potential to reveal inter-species difference in ocean acidification tolerance of symbiotic marine calcifiers.

6. Acknowledgements

This study would not have been possible without the supports of many people. First of all, I express the deepest gratitude to my supervisor, professor Hodaka Kawahata for improving my doctor thesis and giving me effective advice. I also would like to express much appreciation to Dr. Atsushi Suzuki of AIST for many supports of chemical procedure, helpful comments, valuable discussion and many supports for my research life, to Dr. Yukihiro Nojiri of NIES for enlightening discussion, continuous encouragement and his kind guidance throughout this study, and to Dr. Kazuhiko Sakai of TBRC sesoko station for teaching me how to perform experiments with AICAL and overall supports in my sesoko activity. I also express my hearty thanks to Dr. Mayuri Inoue and Dr. Azumi Kuroyanagi of AORI, and to Dr. Kazuhiko Fujita of University of the Ryukyus for a lot of helpful advice, valuable comments, and overall supports in my academic life. I extend my thanks to Dr. Takahiro Irie of AORI for appropriate advise of culture experiments and assistance of statistical analysis, to Dr. Hiroyuki Ushie for overall supports concerning cultural experiments and maintenance of instruments, to Dr. Akira Iguchi for devoted help of designing for experiments, to Ms. Hiromi Kinjo and Mr. Shun Ohki of TBRC sesoko station for a maintenance of AICAL, to Mr. Yoji Kanda of TBRC sesoko station for field assistance. As for isotope analysis at AIST, I express special thanks to Dr. Toyoho Ishimura for technical assistance. Ms. Haruka Takagi, Dr. Kozue Nishida and Ms. Erika Hayashi and Mr. Hisato Izumida also helped me in the laboratory. Finally, I wish to thank my family and friends for various supports in my doctor program. Without their encouragements, I could not have done this work. I appreciate all people helped me in my doctor's program.

7. References

Chapter 1

Akimoto, K., Tanaka, T., Hattori, M. and Hotta, H. 1990. Recent bethic foraminiferal assemblages around hydrothemral vents in the Okinawa Trough, Ryukyu Islands, Japan. Studies in Benthic Foraminifera, Benthos ’90, Sendai, 211-225, Tokai University.

Alegret, L. and Ortiz, S. 2006. Global extinction event in benthic foraminifers across the Paleocene/Eoceneat the Dababiya Stratotype section. Micropaleontology 52, 433−447.

Bijma, J., H. Spero and D. Lea (1999), Reassessing foraminiferal stable isotope geochemistry: impact of the oceanic carbonate system (experimental results), in Use of Proxies in Paleoceanography: Examples from the South Atlantic, edited by G. Fischer, and G. Wefer, Springer-Verlag, Berlin, Heidelberg, Germany, 489–512.

Crawley, A., Kline, D. I., Dunn, S., Anthony, K, and Dove, S. (2009). The effect of ocean acidification on symbiont photorespiration and productivity in Acropora formosa. Global Change Biology, 16, 851−863.

Doney, S. C., V. J. Fabry, R. A. Feely, and J. A. Kleypas (2009), Ocean Acidification: The Other CO2 Problem, Ann. Rev. Mar. Sci., 1, 169–192.

Engel, A., K. G. Schulz, U. Riebesell, R. Bellerby, B. Delille, and M. Schartau (2008), Effects of CO2 on particle size distribution and phytoplankton abundance during a mesocosm bloom experiment (PeECE II), Biogeosciences, 5, 509−521.

Fabry, V. J. (2008), Marine calcifiers in a high-CO2 ocean, Science 320, 1020–1022.

Fabry, V.J., Seibel, B.A., Feely, R.A., Orr, J.C., (2008). Impacts of ocean acidification on marine fauna and ecosystem processes. ICES J. Mar. Sci. 65, 414-432.

Feely R. A, C. L. Sabine, K. Lee, W. Berelson, J. Kleypas, V. J. Fabry, F. J. Millero (2004), Impact of anthropogenic CO_2 on the $CaCO_3$ system in the oceans, Science, 305, 362-366, doi: 10.1126/science.1097329.

Finger, K.L. and Lapps, J.H. 1981. Foraminiferal decimation and repopulation in an active volcanic caldera, Deception Island, Antarctica, Micropaleontology 27, 111-139.

Fujita, K., Y. Osawa, H. Kayanne, Y. Ide, and H. Yamano (2009), Distribution and sediment production of large benthic foraminifers on reef flats of the Majuro Atoll, Marshall Islands, Coral Reefs, 28, 29−45.

Fujita, K., M. Hikami, A. Suzuki, A. Kuroyanagi, K. Sakai, H. Kawahata, and Y. Nojiri (2011), Effects of ocean acidification on calcification of symbiont-bearing reef foraminifers , Biogeosciences, 8, 2089-2098.

Gattuso, J.-P., Frankignoulle, M., Bourge, I., Romaine, S., Buddemeier, R.W., (1998). Effect of calcium carbonate saturation of seawater on coral calcification. Glob. Planet. Change18, 37–46.

Gazeau, F., C. Quibler, J. M. Jansen, J-P. Gattuso, J. J. Middelburg, and C. H. R. Heip (2007), Impact of elevated CO2 on shellfish calcification, Geophysical Research Letters, 34: L07603. doi 10.1029/ 2006GL028554

Giusberti, L., Coccioni, R., Spovieri, M. and Tateo, F. 2009. Perturbation at the sea floor during the ... maximum: Evidence from benthic foraminifera at Contessa Road,

Italy. Marine Micropaleontology 70, 102-119.

Hönisch, B., A. Ridgwell, D. N. Schmidt, E. Thomas, S. J. Gibbs, A., Sluijs, R. Zeebe, L. Kump, R. C. Martindale, S. E. Greene et al. (2012). The geological record of ocean acidification. Science 335: 1058 −1063.

Hoegh-Guldberg, O., Mumby, P. J., Hooten, A. J., Steneck, R. S., Greenfield, P., Gomez, E., Harvell, C. D., Sale, P. F., Edwards, A. J., Caldeira, K., Knowlton, N., Eakin, C. M., Iglesias-Prieto, R., Muthiga, N., Bradbury, R. H., Dubi, A., and Hatziolos, M. E. (2007). Coral reefs under rapid climate change and ocean acidification. Science, 318, 1737−1742.

Hohenegger, J. (2006), The importance of symbiont-bearing benthic foraminifera for West Pacific carbonate beach environments, Marine Micropaleontology, 61, 4−39.

Iguchi, A., Ozaki, S., Nakamura, T., Inoue, M., Tanaka, Y., Suzuki, A., Kawahata, H. and Sakai, K. (2011) The effect of acidified seawater on coral calcification and symbiotic algae of a massive coral Porites australiensis. Marine Environmental Research, 73, 32-36.

Inoue,S., Kayanne, H., Yamamoto, S., Kurihara, H. (2013) Spatial community shift from hard to soft corals in acidified water. Nature Climate Change, 3, 683-687.

Jury, C. P., Whitehead, R. F., and Szmant, A. M. (2010). Effects of variations in carbonate chemistry on the calcification rates of Madracis auretenra (= Madracis mirabilis sensu Wells, 1973): bicarbonate concentrations best predict calcification rates. Global Change Biology, 16, 1632−1644.

Kaiho, K, Takeda, K, Petrizzo, M.R. and Zachos, J.C. 2006. Anomalous shifts in tropical Pacific planktonic and benthic foraminiferal test size during the

Paleocene-Eocene thermal maximum. Palaeogeography, Palaeoclimatology 237, 456-464.

Kleypas, J. A., Feely, R. A., Fabry, V. J., Langdon, C., Sabine, C. L., and Robbins, L. L. (2006). Impacts of ocean acidification on coral reefs and other marine calcifiers: a guide for future research. Report of a workshop held on 18-20 April 2005, St. Petersburg, FL, sponsored by NSF, NOAA, and the U.S. Geological Survey, 88 pp.

Kroeker K.J., R. L. Kordas, R. Crim, I. E. Hendriks, L. Ramajo, G. S. Singh, C. M. Duarte, and J-P. Gattuso (2013), Impacts of ocean acidification on marine organisms: quantifying sensitivities and interaction with warming, Glob. Change Biol., 19, 1884-1896, doi: 10.1111/gcb.12179.

Kuffner, I. B., A. J. Andersson, P. L. Jokiel, K. S. Rodgers, and F. T. Mackenzie (2008), Decreased abundance of crustose coralline algae due to ocean acidification, Nature Geosci., 1, 114–117.

Kuroyanagi, A., H. Kawahata, A. Suzuki, K. Fujita, and T. Irie (2009), Impacts of ocean acidification on large benthic foraminifers: Results from laboratory experiments, Marine Micropaleontology, 73, 190−195.

Lee, J. J. (1998), "Living sands" - larger foraminifera and their endosymbiotic algae, Symbiosis, 25, 71−100.

Marubini, F., Christine, A. E., Ferrier-Page's, A. E., Furla, P., and Allemand, D. (2008). Coral calcification responds to seawater acidification: a working hypothesis towards a physiological mechanism. Coral Reefs 27, 491−499.

Morse, J. W., A. J. Andersson, and F. T. Mackenzie (2006), Initial responses of carbonate-rich shelf sediments to rising atmospheric pCO_2 and "ocean acidification":

Role of high Mg-calcites, Geochim. Cosmochim. Acta, 70, 5814−5830.

Murray, J.W. 2008. Ecology and applications of benthic foraminifera, Cambridge University Press, U.K., pp. 440.

Orr, J. C., V. J. Fabry, O. Aumont, L. Bopp, S. C. Doney, R. A. Feely, A. Gnanadesikan, N. Gruber, A. Ishida, F. Joos, R. M. Key, K. Lindsay, E. Maier-Reimer, R. Matear, P. Monfray, A. Mouchet, R. G. Najjar, G.-K. Plattner, K. B. Rodgers, C. L. Sabine, J. L. Sarmiento, R. Schlitzer, R. D. Slater, I. J. Totterdell, M.-F. Weirig, Y. Yamanaka, and A. Yool (2005), Anthropogenic ocean acidification over the twenty-first century and its impact on calcifying organisms, Nature, 437, 681–686.

Petrizzo, M.R. 2007. The onset of the Paleocene-Eocene Thermal Maximum (PETM) at Sites 1209 and 1210 (Shatsky Rise, Pacific Ocean) as recorded by planktonic foraminifera. Marine Micropaleontology 63, 187-200.

Raffi, I., Backman, J. and Pälike, H. 2005. Changes in calcareous nannofossil assemblages across the Paleocene/Eocene transition from the paleo-equatorial Pacific Ocean, Palaeogeography, Palaeoclimatology, Palaeoecology, 226, 93 − 126.

Ries, J., Cohen, A. and McCorkle, D. A non-linear calcification response to CO_2 -induced ocean acidification by the coral Oculina. Coral Reefs 29, 661−674 (2010).

Rost, B., K.-U. Richter, U. Riebesell, and P. J. Hansen (2006) Inorganic carbon acquisition in red-tide dinoflagellates, Plant, Cell and Environment, 29, 810−822.

Solomon, S., D. Qin, M. Manning, Z. Chen, M. Marquis, K. B. Averyt, M. Tignor, and H. L. Miller (Eds.) (2007), Climate Change 2007: The Physical Science Basis. Contribution of Working Group I to the Fourth Assessment Report of the

Intergovernmental Panel on Climate Change, Cambridge Univ. Press, Cambridge.

Spero, H. J., J. Bijma, D. W. Lee, B. E. Bemis (1997), Effect of seawater carbonate concentration on foraminiferal carbon and oxygen isotopes, Nature 390, 497–500.

Tantawy, A.A.A.N. (2006). Calcareous nannofossils of the Paleocene-Eocene transition at Qena Region, central Nile Valley, Egypt. Micropaleontology 52, 193-222.

Todo, Y., Kitazato, H., Hashimoto, J. and Gooday, A.J. (2005) Simple Foraminifera Flourish at the Ocean's Deepest Point. Science, 307, 689 , DOI: 10.1126/science.1105407.

Wittmann, A. C, Pörtner, H.-O. (2013), Sensitivities of extant animal taxa to ocean acidification, Nat. Clim. Chang., 3, 995-1001, doi:10.1038/nclimate1982.

Wu, Y., K. Gao, and U. Riebesell (2010), CO2-induced seawater acidification affects physiological performance of the marine diatom Phaeodactylum tricornutum, Biogeosciences, 7, 2915−2923.

Zeebe, R. E., and A. Ridgwell. 2011. Past changes of ocean carbonate chemistry. Pp. 21－40 in Ocean Acidification, J.-P. Gattuso and L. Hansson, eds. Oxford University Press, New York.

Zili, L. and Zaghbib－Turki, D. 2010. Foraminiferal Biostratigraphy and Palaeoenvironmental Reconstruction of the Paleocene－Eocene Transition at the Kharrouba Section, Tunisia (Southern Tethys Margin). Turkish Journal Earth Science 19, 385-408

Zili, L., Zaghbib−Turki, D., Alegret, L., Arenillas, I. and Molina, E. 2009. Foraminiferal turnover across the Paleocene/Eocene boundary at the Zumaya section,

Spain: record of a bathyal gradual mass extinction. Revista mexicana de ciencias geológicas 26, 729-744.

Chapter 2

Badger, M. R., T. J. Andrews, S. M. Whitney, M. Ludwig, D. C. Yellowlees, W. Leggat, and G. D. Price (1998), The diversity and coevolution of Rubisco, plastids, pyrenoids, and chloroplast-based CO2-concentrating mechanisms in algae, Can. J. Botany, 76, 1052–1071.

Bentov, S., C. Brownlee and J. Erez (2009), The role of seawater endocytosis in the biomineralization process in calcareous foraminifera, P. Natl. Acad. Sci. USA, 106, 21500-21504, doi:10.1073/pnas.0906636106.

Bijma, J., H. Spero, and D. Lea (1999), Reassessing foraminiferal stable isotope geochemistry: impact of the oceanic carbonate system (experimental results), in Use of Proxies in Paleoceanography: Examples from the South Atlantic, edited by G. Fischer, and G. Wefer, Springer-Verlag, Berlin, Heidelberg, Germany, 489–512.

Bijma, J., B. Hönisch and R.E. Zeebe (2002), Impact of the ocean carbonate chemistry on living foraminiferal shell weight: Comment on "Carbonate ion concentration in glacial-age deep waters of the Caribbean Sea" by W. S. Broecker and E. Clark, Geochem. Geophys. Geosyst., 3(11), 1064, doi:10.1029/2002GC000388.

Dickson, A. G., and F. J. Millero (1987), A comparison of the equilibrium constants for the dissociation of carbonic acid in seawater media, Deep-Sea Res., 34, 1733–1743.

de Nooijer, L. J., T. Toyofuku and H. Kitazato (2009), Foraminifera promote calcification by elevating their intracellular pH, P. Natl. Acad. Sci. USA, 106,

15374–15378, doi:10.1073/pnas.0904306106.

Dissard, D., G. Nehrke, G.J. Reichart and J. Bijma (2010), Impact of seawater pCO2 on calcification and Mg/Ca and Sr/Ca ratios in benthic foraminifera calcite: results from culturing experiments with *Ammonia tepida*, Biogeosciences, 7, 81-93, doi:10.5194/bg-7-81 .

Doney, S. C., V. J. Fabry, R. A. Feely, and J. A. Kleypas (2009), Ocean Acidification: The Other CO2 Problem, Ann. Rev. Mar. Sci., 1, 169–192.

Engel, A., K. G. Schulz, U. Riebesell, R. Bellerby, B. Delille, and M. Schartau (2008), Effects of CO2 on particle size distribution and phytoplankton abundance during a mesocosm bloom experiment (PeECE II), *Biogeosciences*, *5*, 509–521.

Erez, J. (2003), The source of ions for biomineralization in foraminifera and their implications for paleoceanographic proxies, Rev. Mineral. Geochem., 54, 115–149, doi:10.2113/0540115.

Fabry, V. J. (2008), Marine calcifiers in a high-CO2 ocean, Science 320, 1020–1022.

Fujita, K., and H. Fujimura (2008), Organic and inorganic carbon production by algal symbiont-bearing foraminifera on northwest Pacific coral-reef flat, Journal of Foraminiferal Research, 38, 2, 117–126.

Fujita, K., Y. Osawa, H. Kayanne, Y. Ide, and H. Yamano (2009), Distribution and sediment production of large benthic foraminifers on reef flats of the Majuro Atoll, Marshall Islands, Coral Reefs, 28, 29–45.

Fujita, K., M. Hikami, A. Suzuki, A. Kuroyanagi, K. Sakai, H. Kawahata, and Y. Nojiri (2011), Effects of ocean acidification on calcification of symbiont-bearing reef foraminifers , Biogeosciences, 8, 2089-2098.

Gazeau, F., C. Quibler, J. M. Jansen, J-P. Gattuso, J. J. Middelburg, and C. H. R. Heip (2007), Impact of elevated CO2 on shellfish calcification, Geophysical Research Letters, 34: L07603. doi 10.1029/ 2006GL028554

Hoegh-Guldberg, O., P. J. Mumby, A. J. Hooten, R. S. Steneck, P. Greenfield, E. Gomez, C. D. Harvell, P. F. Sale, A. J. Edwards, K. Caldeira, N. Knowlton, C. M. Eakin, R. Iglesias-Prieto, N. Muthiga, R. H. Bradbury, A. Dubi, and M. E. Hatziolos (2007), Coral reefs under rapid climate change and ocean acidification, Science, 318, 1737–1742.

Hallock, P. (1999), Symbiont-bearing foraminifera, in: Modern Foraminifera, edited by: Sen Gupta, B.K., Kluwer Academic Publishers, Dordrecht, Netherlands, 123-139.

Hohenegger, J. (1994), Distribution of living larger Foraminifera NW of Sesoko-Jima, Okinawa, Japan, Mar. Ecol, 15, 291–334.

Hohenegger, J. (2006), The importance of symbiont-bearing benthic foraminifera for West Pacific carbonate beach environments, Marine Micropaleontology, 61, 4–39.

Iglesias-Rodriguez, M. D., E. T. Buitenhuis, J. A. Raven, O. Schofield, A. J. Poulton, S. Gibbs, P. R. Halloran, and H. J. W. de Baar (2008), Phytoplankton Calcification in a High-CO2 World, Science, 320, 336–340.

Irie, T., and B. Adams (2007), Sexual dimorphism in soft body weight in adult Monetaria annulus (Family Cypraeidae), Veliger 49, 209–211.

Kuffner, I. B., A. J. Andersson, P. L. Jokiel, K. S. Rodgers, and F. T. Mackenzie (2008), Decreased abundance of crustose coralline algae due to ocean acidification, Nature Geosci., 1, 114–117.

Kuroyanagi, A., H. Kawahata, A. Suzuki, K. Fujita, and T. Irie (2009), Impacts of

ocean acidification on large benthic foraminifers: Results from laboratory experiments, Marine Micropaleontology, 73, 190–195.

Lee, J. J., K. Sung, B. ter Kuile, E. Strauss, P. J. Lee, and W.W. Faber, Jr. (1991), Nutritional and related experiments on laboratory maintenance of three species of symbiont-bearing, large foraminifera, Mar. Biol., 109, 417–425.

Lee, J. J. (1998), "Living sands" - larger foraminifera and their endosymbiotic algae, Symbiosis, 25, 71–100.

Lombard, F., R.E. da Rocha, J. Bijma and J-P. Gattuso (2010), Effect of carbonate ion concentration and irradiance on calcification in planktonic foraminifera, Biogeosciences, 7, 247-255, doi:10.5194/bg-7-247.

Mehrbach, C., C. H. Culberson, J. E. Hawley, and R. M. Pytkowicz (1973), Measurement of the apparent dissociation constants of carbonic acid in seawater at atmospheric pressure, Limnol. Oceanogr., 18, 897–907.

Morse, J. W., A. J. Andersson, and F. T. Mackenzie (2006), Initial responses of carbonate-rich shelf sediments to rising atmospheric pCO_2 and "ocean acidification": Role of high Mg-calcites, Geochim. Cosmochim. Acta, 70, 5814–5830.

Orr, J. C., V. J. Fabry, O. Aumont, L. Bopp, S. C. Doney, R. A. Feely, A. Gnanadesikan, N. Gruber, A. Ishida, F. Joos, R. M. Key, K. Lindsay, E. Maier-Reimer, R. Matear, P. Monfray, A. Mouchet, R. G. Najjar, G.-K. Plattner, K. B. Rodgers, C. L. Sabine, J. L. Sarmiento, R. Schlitzer, R. D. Slater, I. J. Totterdell, M.-F. Weirig, Y. Yamanaka, and A. Yool (2005), Anthropogenic ocean acidification over the twenty-first century and its impact on calcifying organisms, Nature, 437, 681–686.

Pierrot, D., E. Lewis, and D. Wallace (2006), MS Excel Program developed for CO2 system calculations, ORNL/CDIAC-105a, Carbon Dioxide Information Analysis

Center, Oak Ridge National Laboratory, U.S. Department of Energy, Tennessee.

Raven, J., K. Caldeira, H. Elderfield, O. Hoegh-Guldberg, P. Liss, U. Riebesell, J. Shepherd, C. Turley, and A. Watson (2005), Ocean acidification due to increasing atmospheric carbon dioxide. Policy Document 12/05, Royal Society, London.

Ries, J. B., A. L. Cohen, and D. C. McCorkle (2009), Marine calcifiers exhibit mixed responses to CO2-induced ocean acidification, Geology, 37, 1131–1134.

Rost, B., K.-U. Richter, U. Riebesell, and P. J. Hansen (2006), Inorganic carbon acquisition in red-tide dinoflagellates, Plant, Cell and Environment, 29, 810–822.

Sabine, C. L., and R. A. Feely (2007), The oceanic sink for carbon dioxide, In Greenhouse Gas Sinks, edited by D. Reay, N. Hewitt, J. Grace, and K. Smith, CABI Publishing, Oxfordshire.

Röttger, R. and R. Kru¨ger (1990), Observations on the biology of Calcarinidae (Foraminiferida), Mar. Biol., 106, 419-425.

Sabine, C. L., R. A. Feely, N. Gruber, R. M. Key, K. Lee, J. L. Bullister, R. Wanninkhof, C. S. Wong, D. W. R. Wallace, B. Tilbrook, F. J. Millero, T. H. Peng, A. Kozyr, T. Ono, and A. F. Rios (2004), The oceanic sink for anthropogenic CO2, Science, 305, 367–371.

Sakai, K. and M. Nishihira (1981), Population study of the benthic foraminifer *Baculogypsina sphaerulata* on the Okinawan reef flat and preliminary estimation of its annual reproduction. Proc. Fourth Int. Coral Reef Symp., 2, 763-766.

Solomon, S., D. Qin, M. Manning, Z. Chen, M. Marquis, K. B. Averyt, M. Tignor, and H. L. Miller (Eds.) (2007), Climate Change 2007: The Physical Science Basis. Contribution of Working Group I to the Fourth Assessment Report of the Intergovernmental Panel on Climate Change, Cambridge Univ. Press, Cambridge.

Spero, H. J., J. Bijma, D. W. Lee, B. E. Bemis (1997), Effect of seawater carbonate concentration on foraminiferal carbon and oxygen isotopes, Nature 390, 497–500.

ter Kuile, B. and J. Erez (1991), Carbon Budgets for Two Species of Benthonic Symbiont-Bearing Foraminifera. Biol. Bull., 180, 489-495.

Wu, Y., K. Gao, and U. Riebesell (2010), CO2-induced seawater acidification affects physiological performance of the marine diatom Phaeodactylum tricornutum, Biogeosciences, 7, 2915–2923.

Chapter 3

Dias, B. B., M. B. Hart, C. W. Smart, and J. M. Hall-Spencer (2010). Modern seawater acidification: the response of foraminifera to high-CO_2 conditions in the Mediterranean Sea, J. Geol. Soc. London, 167, 843-846, doi:10.1144/0016-76492010-050.

Emiliani, C. (1966). Paleotemperature analysis of Caribbean cores P6304-8 and P6304-9 and a generalized temperature curve for the past 425,000 years, J. Geol., 74(2), 109-124.

Engel, A., K. G. Schulz, U. Riebesell, R. Bellerby, B. Delille, and M. Schartau (2008). Effects of CO_2 on particle size distribution and phytoplankton abundance during a mesocosm bloom experiment (PeECE II), Biogeosciences, 5, 509-521.

Erez, J. (1978). Vital effect on stable-isotope composition seen in foraminifera and coral skeletons, Nature, 273, 199-202, doi: 10.1038/273199a0.

Eres, J, and B. Luz (1983), Experimental paleotemperature equation for planktonic foraminifera. Geochim.Cosmochim. Acta, 47, 1025-1031

Feely R. A, C. L. Sabine, K. Lee, W. Berelson, J. Kleypas, V. J. Fabry, F. J. Millero (2004), Impact of anthropogenic CO_2 on the $CaCO_3$ system in the oceans, Science, 305, 362-366, doi: 10.1126/science.1097329.

Fujita, K., and H. Fujimura (2008), Organic and inorganic carbon production by algal symbiont-bearing foraminifera on northwest Pacific coral-reef flats, J. Foraminiferal Res., 38, 117-126, doi: 10.2113/gsjfr.38.2.117.

Fujita, K., M. Hikami, A. Suzuki, A. Kuroyanagi, and H. Kawahata (2011), Effects of ocean acidification on calcification of symbiont-bearing reef foraminifers, Biogeosciences, 8, 2089–2098, doi: 10.5194/bg-8-1809-2011.

Hikami, M., H. Ushie, T. Irie, K. Fujita, A. Kuroyanagi, K. Sakai, Y. Nojiri, A. Suzuki, and H. Kawahata (2011), Contrasting calcification responses to ocean acidification between two reef foraminifers harboring different algal symbionts, Geophys. Res. Lett., 38, L19601, doi: 10.1029/2011GL048501.

Hohenegger, J. (1994), Distribution of living larger foraminifera NW of Sesoko‐Jima, Okinawa, Japan, Mar. Ecol., 15, 291-334, DOI: 10.1111/j.1439-0485.1994.tb00059.x.

Iglesias-Rodriguez, M. D., P. R. Halloran, R. E. M. Rickaby, I. R.Hall, E. Colmenero-Hidalgo, J. R. Gittins, D. R. H. Green1, T. Tyrrell, S. J. Gibbs, P. von Dassow, E. Rehm, E. V. Armbrust, and K. P. Boessenkool (2008), Phytoplankton calcification in a high-CO_2 world, Science, 320, 336-340, doi: 10.1126/science.1154122.

Ishimura, T., U. Tsunogai, and T. Gamo (2004), Stable carbon and oxygen isotopic determination of sub‐microgram quantities of $CaCO_3$ to analyze individual foraminiferal shells, Rapid Commun. Mass Spectrom., 18, 2883-2888, doi:

10.1002/rcm.1701.

Ishimura, T., U. Tsunogai, and F. Nakagawa (2008), Grain-scale heterogeneities in the stable carbon and oxygen isotopic compositions of the international standard calcite materials (NBS 19, NBS 18, IAEA-CO-1, and IAEA-CO-8), Rapid Commun. Mass Spectrom., 22, 1925-1932, doi: 10.1002/rcm.3571.

Kato, A., M. Hikami, N. H. Kumagai, A. Suzuki, Y. Nojiri, and K. Sakai (2013), Negative effects of ocean acidification on two crustose coralline species using genetically homogeneous samples, Mar. Environ. Res., 94, 1-6, doi: 10.1016/j.marenvres.2013.10.010.

Kroeker K.J., R. L. Kordas, R. Crim, I. E. Hendriks, L. Ramajo, G. S. Singh, C. M. Duarte, and J-P. Gattuso (2013), Impacts of ocean acidification on marine organisms: quantifying sensitivities and interaction with warming, Glob. Change Biol., 19, 1884-1896, doi: 10.1111/gcb.12179.

ter Kuile, B. (1991), Mechanisms for calcification and carbon cycling in algal symbiont-bearing foraminifera, in Lee, J. J., and Anderson, O. R. (eds.), Biology of Foraminifera: Academic Press. London, p. 73–89.

ter Kuile, B., and J. Erez (1987), Uptake of inorganic carbon and internal carbon cycling in symbiont-bearing benthonic foraminifera, Mar. Biol., 94, 499-509, doi: 10.1007/BF00431396.

ter Kuile, B., and J. Erez (1988), The size and function of the internal inorganic carbon pool of the foraminifer Amphiseigina lobifera. Mar Biol., 99, 481-487.

ter Kuile, B. H., and J. Erez (1991), Carbon budgets for two species of benthonic symbiont-bearing foraminifera, Biol. Bull., 180, 489-495.

ter Kuile B, J. Erez, E., Padan (1989a), Competition for inorganic carbon between

photosynthesis and calcification in the symbiont-bearing foraminifer *Amphistegina lobifera*. Mar. Biol., 103, 253-259.

ter Kuile B, J. Erez, and E. Padan (1989b), Mechanisms for the uptake of inorganic carbon by two species of symbiont-bearing foraminifera. Mar. Biol., 103, 241-251.

Langer, M. R. (1995), Oxygen and carbon isotopic composition of Recent and larger and smaller foraminifera from the Madang Lagoon (Papua New Guinea). Mar. Micropaleontol., 26, 215-221, doi: 10.1016/0377-8398(95)00073-9.

Lee, J. J. (1998), "Living sands"— Larger foraminifera and their endosymbiotic algae, Symbiosis, 25, 71–100.

Lee, J. J. (2006), Algal symbiosis in larger foraminifera, Symbiosis, 42, 63-75.

McCulloch, M., J. Falter, J. Trotter, and P. Montagna (2012), Coral resilience to ocean acidification and global warming through pH up-regulation, Nat. Clim. Chang., 2, 623-633, doi: 10.1038/nclimate1473.

Meehl, G. A., and T. F. Stocker (2007), Global climate projections, in Climate Change 2007: The Physical Science Basis-Contribution of Working Group I to the Fourth Assessment Report of the Intergovernmental Panel on Climate Change, edited by S. Solomon et al., pp. 748-845, Cambridge Univ. Press, New York.

Mook, W. G. (1986), ^{13}C in atmospheric CO_2, Ned. J. Sea Res., 20, 211-223.

Ohki, S., T. Irie, M. Inoue, K. Shinmen, H. Kawahata, T. Nakamura, A. Kato, Y. Nojiri, A. Suzuki, K. Sakai, and R. von Woesik (2013), Calcification responses of symbiotic and aposymbiotic corals to near-future levels of ocean acidification, Biogeosciences, 10, 6807-6814, doi: 10.5194/bg-10-6807-2013.

Omata, T., A. Suzuki, T. Sato, K. Minoshima, E. Nomaru, A. Murakami, S.

Murayama, H. Kawahata, and T. Maruyama (2008), Effect of photosynthetic light dosage on carbon isotope composition in the coral skeleton: Long-term culture of Porites spp., J. Geophys. Res., 113, G02014. doi: 10.1029/2007JG000431.

Ries, J. B., A. L. Cohen, and D. C. McCorkle, (2009), Marine calcifiers exhibit mixed responses to CO_2-induced ocean acidification, Geology, 37, 1131-1134, doi: 10.1130/G30210A.1.

Romanek, C. S., E. L. Grossman, and J. W. Morse (1992), Carbon isotopic fractionation in synthetic aragonite and calcite: effects of temperature and precipitation rate, Geochim. Cosmochim. Acta, 56, 419-430, doi: 10.1016/0016-7037(92)90142-6.

Saraswati, P. K., K. Seto, and R. Nomura (2004), Oxygen and carbon isotopic variation in co-existing larger foraminifera from a reef flat at Akajima, Okinawa, Japan, Mar. Micropaleontol., 50, 339-349, doi: 10.1016/S0377-8398(03)00099-9.

Shackleton, N. J. (1967), Oxygen isotope analyses and Pleistocene temperatures re-assessed, Nature, 215, 15-17.

Spero, H. J., and M. J. DeNiro (1987), The influence of symbiont photosynthesis on the $\delta^{18}O$ and $\delta^{13}C$ values of planktonic foraminiferal shell calcite, Symbiosis, 4, 213-228.

Spero, H. J., J. Bijma, D. W. Lea, and B. E. Bemis (1997), Effect of seawater carbonate concentration on foraminiferal carbon and oxygen isotopes, Nature, 390, 497-500, doi: 10.1038/37333.

Spero, H.J. (1992), Do planktic foraminifera accurately record shifts in the carbon isotopic composition of seawater ΣCO_2, Mar. Micropaleontol, 19, 275-285. doi: 10.1016/0377-8398(92)90033-G, doi: 10.1016/0377-8398(92)90033-G.

Suzuki, A., M. K. Gagan , K. Fabricius, P. J. Isdale , I. Yukino, H. Kawahata

(2003), Skeletal isotope microprofiles of growth perturbations in Porites corals during the 1997–1998 mass bleaching event, Coral Reefs, 22, 357–369. doi: 10.1007/s00338-003-0323-4.

Tarutani, T., R. N. Clayton, and T. K. Mayeda (1969), The effect of polymorphism and magnesium substitution on oxygen isotope fractionation between calcium carbonate and water, Geochim. Cosmochim. Acta, 33, 987-996, doi: 10.1016/0016-7037(69)90108-2

Urey, H. C. (1947), The thermodynamic properties of isotopic substances, J. Chem. Soc., 562-581, doi: 10.1039/JR9470000562.

Wefer, G., and W. H. Berger (1980), Stable isotopes in benthic foraminifera: seasonal variation in large tropical species, Science, 209, 803-805, doi: 10.1126/science.209.4458.803.

Wefer, G., J. S. Killingley, and G. F. Lutze, (1981), Stable isotopes in recent larger foraminifera, Paleogeogr. Paleoclimatol. Paleoecol., 33, 253-270, doi: 10.1016/0031-0182(81)90042-0.

Wittmann, A. C, Pörtner, H.-O. (2013), Sensitivities of extant animal taxa to ocean acidification, Nat. Clim. Chang., 3, 995-1001, doi:10.1038/nclimate1982.

Wolf-Gladrow, D. A., and R. E. Zeebe, (2008), Isotope fractionation, in Encyclopedia of paleoclimatology and ancient environments, edited by V. Gornitz, pp. 479-481, Springer, Netherlands.

Wu, Y., K. Gao, and U. Riebesell, (2010), CO_2-induced seawater acidification affects physiological performance of the marine diatom Phaeodactylum tricornutum, Biogeosciences, 7, 2915–2923, doi: 10.5194/bg-7-3855-2010.

Chapter 4

Andersson, A. J., Mackenzie, F. T. and Bates, N. R. 2008. Life on the margin: implications of ocean acidification on Mg-calcite, high latitude and cold-water marine calcifiers. *Mar. Ecol. Prog. Ser.* 373:265-73.

Anthony, K. R. N., Kline, D. I., Diaz-Pulido, G., Dove, S. and Hoegh-Guldberg, O. 2008. Ocean acidification causes bleaching and productivity loss in coral reef builders. *Proc. Natl. Acad. Sci. USA* 105:17442-46.

Bilan, M. I. and Usov, A. I. 2001. Polysaccharides of calcareous algae and their effect on calcification process. *Russ. J. Bioorganic. Chem.* 27:4-20.

Burdett, H. L., Aloisio, E., Calosi, P., Findlay, H. S., Widdicombe, S., Hatton, A. D. and Kamenos, N. A. 2012. The effect of chronic and acute low pH on the intracellular DMSP production and epithelial cell morphology of red coralline algae. *Marine Biology Research* 8:756-63.

Comeau, S., Carpenter, R. C. and Edmunds, P. J. 2013a. Coral reef calcifiers buffer their response to ocean acidification using both bicarbonate and carbonate. *Proc. R. Soc. Lond. B* 280 (in press)

Comeau, S., Edmunds, P. J., Spindel, N. B. and Carpenter, R. C. 2013b. The responses of eight coral reef calcifiers to increasing partial pressure of CO_2 do not exhibit a tipping point. *Limnol. Oceanogr.* 58:388-98.

Cornwall, C. E., Hepburn, C. D., Pritchard, D., Currie, K. I., McGraw, C. M., Hunter, K. A. and Hurd, C. L. 2012. Carbon-use strategies in macroalgae: differential responses to lowered pH and implications for ocean acidification. *J. Phycol.* 48:137-44.

Diaz-Pulido, G., Anthony, K. R. N., Kline, D. I., Dove, S. and Hoegh-Guldberg, O. 2012. Interactions Between Ocean Acidification and Warming on the Mortality and

Dissolution of Coralline Algae. *J. Phycol*. 48:32-39.

Diaz-Pulido, G., Harii, S., McCook, L. J. and Hoegh-Guldberg, O. 2010. The impact of benthic algae on the settlement of a reef-building coral. *Coral Reefs* 29:203-08.

Dickson, A. G. and Millero, F. J. 1987. A comparison of the equilibrium constants for the dissociation of carbonic acid in seawater media. *Deep Sea Res*. 34:1733-43.

Dixon, K. R. and Saunders, G. W. 2013. DNA barcoding and phylogenetics of *Ramicrusta* and Incendia gen. nov., two early diverging lineages of the Peyssonneliaceae (Rhodophyta). *Phycologia* 52:82-108.

Dobson, A. J. 2002. *An introduction to generalized linear models*. Chapman and Hall. London, UK, 225 pp.

Doropoulos, C., Ward, S., Diaz-Pulido, G., Hoegh-Guldberg, O. and Mumby, P. J. 2012. Ocean acidification reduces coral recruitment by disrupting intimate larval-algal settlement interactions. *Ecol. Lett*. 15:338-46.

Egilsdottir, H., Noisette, F., Noël, L. M.-L. J., Olafsson, J. and Martin, S. 2012. Effects of pCO_2 on physiology and skeletal mineralogy in a tidal pool coralline alga *Corallina elongata*. *Mar. Biol*. (in press)

Fabry, V. J. 2008. Marine calcifiers in a high-CO_2 ocean. *Science* 320:1020-22.

Fujita, K., Hikami, M., Suzuki, A., Kuroyanagi, A., Sakai, K., Kawahata, H. and Nojiri, Y. 2011. Effects of ocean acidification on calcification of symbiont-bearing reef foraminifers. *Biogeosciences* 8:2089-98.

Harley, C. D. G., Anderson, K. M., Demes, K. W., Jorve, J. P., Kordas, R. L., Coyle, T. A. and Graham, M. H. 2012. Effects of Climate Change on Global Seaweed

Communities. *J. Phycol*. 48:1064-78.

Harvey, A. S., Phillips, L. E., Woelkerling, W. J. and Millar, A. J. K. 2006. The Corallinaceae, subfamily Mastophoroideae (Corallinales, Rhodophyta) in south-eastern Australia. *Aust. Syst. Bot*. 19:387-429.

Heyward, A. J. and Negri, A. P. 1999. Natural inducers for coral larval metamorphosis. *Coral Reefs* 18:273-79.

Hofmann, L. C., Yildiz, G., Hanelt, D. and Bischof, K. 2012. Physiological responses of the calcifying rhodophyte, *Corallina officinalis* (L.), to future CO_2 levels. *Mar. Biol*. 159:783-92.

Iguchi, A., Ozaki, S., Nakamura, T., Inoue, M., Tanaka, Y., Suzuki, A., Kawahata, H., et al. 2012. Effects of acidified seawater on coral calcification and symbiotic algae on the massive coral *Porites australiensis*. *Mar. Environ. Res*. 73:32-6.

IPCC 2007. *Working Group 1 Report,* The *Physical Science Basis*. Available at: http://www.ipcc.ch/publications_and_data/ar4/wg1/en/contents.html (last accessed 1 Feb 2013)

Jiang, J. 2007. *Linear and* generalized *linear mixed models and their applications*. Springer. New York, New York, USA, 257 pp.

Johansen, H. W. 1981. *Coralline Algae, A First Synthesis*. CRC Press, Boca Raton, FL, 239 pp.

Kato, A., Baba, M. and Suda, S. 2011. Revision of the Mastophoroideae (Corallinales, Rhodophyta) and polyphyly in nongeniculate species widely distributed on Pacific coral reefs. *J. Phycol*. 47:662-72.

Kato, A., Baba, M. and Suda, S. 2013. Taxonomic circumscription of heterogeneous species *Neogoniolithon brassica-florida* (Corallinales, Rhodophyta) in

Japan. *Phycol. Res.* 61:15-26.

Kleypas, J. A. and Yates, K. K. 2009. Coral Reefs and Ocean Acidification. *Oceanography* 22:108-17.

Langer, G., Nehrke, G., Probert, I., Ly, J. and Ziveri, P. 2009. Strain-specific responses of *Emiliania huxleyi* to changing seawater carbonate chemistry. *Biogeosciences* 6:2637-46.

Lee, D. and Carpenter, S. J. 2001. Isotopic disequilibrium in marine calcareous algae. *Chem. Geo.* 172:307-29.

Marconi, M., Giordano, M. and Raven, J. A. 2011. Impact of taxonomy, geography, and depth on $\delta^{13}C$ and $\delta^{15}N$ variation in a large collection of macroalgae. *J. Phycol.* 47:1023-35.

Marubini, F., Ferrier-Pages, C. and Cuif, J.-P. 2003. Suppression of skeletal growth in scleractinian corals by decreasing ambient carbonate-ion concentration: a cross-family comparison. *Proc. R. Soc. Lond. B* 270:179-84.

McConnaughey, T. A. and Whelan, J. F. 1997. Calcification generates protons for nutrient and bicarbonate uptake. *Earth-Sci. Rev.* 42:95-117.

Mehrbach, C., Culberson, C. H., Hawley, J. E. and Pytkowicz, R. M. 1973. Measurement of the apparent dissociation constants of carbonic acid in seawater at atmospheric pressure. *Limnol. Oceanogr.* 18: 897-907.

Mori, I. C., Sato, G. and Okazaki, M. 1996. Ca^{2+}-dependent ATPase associated with plasma membrane from a calcareous alga, *Serraticardia maxima* (Corallinaceae, Rhodophyta). *Phycol. Res.* 44:193-202.

Morse, J. W., Andersson, A. J. and Mackenzie, F. T. 2006. Initial responses of carbonate-rich shelf sediments to rising atmospheric pCO_2 and "ocean acidification":

Role of high Mg-calcites. *Geochim. Cosmochim. Acta* 70:5814-30.

Nakamura, M., Ohki, S., Suzuki, A. and Sakai, K. 2011. Coral larvae under ocean acidification: survival, metabolism, and metamorphosis. *PloS one* 6:e14521.

Nash, M. C., Opdyke, B. N., Troitzsch, U., Russell, B. D., Adey, W. H., Kato, A., Diaz-Pulido, G., et al. 2013. Dolomite-rich coralline algae in reefs resist dissolution in acidified conditions. *Nature Clim. Change* 3:268-72.

Nelson, W. A. 2009. Calcified macroalgae - critical to coastal ecosystems and vulnerable to change: a review. *Mar. Freshw. Res.* 60:787-801.

Okazaki, M., Pentecost, A., Tanaka, Y. and Miyata, M. 1986. A study of calcium carbonate deposition in the genus *Padina* (Phaeophyceae, Dictyotales). *Brit. Phycol. J.* 21:217-24.

Pierrot, D., Lewis, E. and Wallace, D. W. R. 2006. *CO2SYS DOS Program developed for CO2 system calculations. ORNL/CDIAC-105.* Carbon Dioxide Information Analysis Center, Oak Ridge National Laboratory, US Department of Energy, Oak Ridge, TN.

Porzio, L., Buia, M. C. and Hall-Spencer, J. M. 2011. Effects of ocean acidification on macroalgal communities. *J. Eex. Mar. Biol. Ecol.* 400:278-87.

Ragazzola, F., Foster, L. C., Form, A., Anderson, P. S. L., Hansteen, T. H. and Fietzke, J. 2012. Ocean acidification weakens the structural integrity of coralline algae. *Glob. Change Biol.* 18:2804-12.

Raven, J. A. and Hurd, C. L. 2012. Ecophysiology of photosynthesis in macroalgae. *Photosynth. res.* 113:105-25.

R Development Core Team 2012. *R: A language and environment for statistical computing*. R Foundation for Statistical Computing, Vienna, Austria.

Ries, J. B., Cohen, A. L. and McCorkle, D. C. 2009. Marine calcifiers exhibit mixed responses to CO_2-induced ocean acidification. *Geology* 37:1131-34.

Rodriguez, S. R., Ojeda, F. P. and Inestrosa, N. C. 1993. Settlement of benthic marine invertebrates. *Mar. Ecol. Prog. Ser.* 97:193-207.

Roleda, M. Y., Boyd, P. W. and Hurd, C. L. 2012. Before ocean acidification: calcifier chemistry lessons. *J. Phycol.* 48:840-3.

Semesi, I. S., Kangwe, J. and Björk, M. 2009. Alterations in seawater pH and CO_2 affect calcification and photosynthesis in the tropical coralline alga, *Hydrolithon* sp. (Rhodophyta). *Estuar. Coast. Shelf S.* 84:337-41.

Smith, A. M., Sutherland, J. E., Kregting, L., Farr, T. J. and Winter, D. J. 2012. Phylomineralogy of the Coralline red algae: Correlation of skeletal mineralogy with molecular phylogeny. *Phytochemistry* 81:97-108.

Webster, N. S., Uthicke, S., Botté, E. S., Flores, F. and Negri, A. P. 2013. Ocean acidification reduces induction of coral settlement by crustose coralline algae. *Glob. Change Biol.* 19:303-15.

Woelkerling, W. J. 1988. *The Coralline Red Algae: An Analysis of the Genera and Subfamilies of Nongeniculate Corallinaceae*. British Museum (Natural History) and Oxford University Press, London and Oxford, 268 pp.

Yoshida, T. and Baba, M. 1998. Corallinales. *In* Yoshida, T. (Ed.) *Marine Algae of Japan*. Uchida Rokakuho Publishing Co., Tokyo, pp. 525-627 (in Japanese).